THE A $^2\Pi$ - X $^2\Sigma^+$ ELECTRONIC SPECTRUM OF ZnD

by

ALAN WILLIAM TAYLOR
B.Sc., University of Victoria, 1978

A THESIS SUBMITTED IN PARTIAL FULFILLMENT
OF THE REQUIREMENTS FOR THE DEGREE OF
MASTER OF SCIENCE
in the Department
of
Chemistry

We accept this thesis as conforming
to the required standard

[redacted]
W. J. Balfour
[redacted]
R. M. Clements
[redacted]
G. R. Branton
[redacted]
T. W. Dingle

UNIVERSITY OF VICTORIA

October 1980

Supervisor: Professor Walter Joseph Balfour

ABSTRACT

The band spectrum of ZnD in the region 350 - 500 nm has been recorded in emission with a Jarrell - Ash 70-000 series, 3.4 meter Ebert Spectrograph. The electronic transition involved is the A $^2\Pi$ (near case (a)) - X $^2\Sigma^+$ (case (b)) system. The following bands have been analyzed: 0-0, 0-1, 0-2, 1-0, 1-1, 1-2, 1-3, 2-1, 2-2, and 2-3. The 3-2 band is also present, as is probably the 2-4 band and possibly the 3-3 band, but these have not been fully investigated.

The principal molecular constants for the X $^2\Sigma^+$ state of ^{64}ZnD are as follows (in cm^{-1}, except where noted): $B_v = 3.399_0 - 0.096\ 3_7(v + 1/2) - 0.004\ 97_1(v + 1/2)^2$; $D_v = 1.15_6 \times 10^{-4} + 0.006\ 4_4 \times 10^{-4}(v + 1/2)$; $r_e = 0.159\ 3_7$ nm; $\gamma_0 = 0.122_4$, $\gamma_1 = 0.112_8$, $\gamma_2 = 0.106_5$, $\gamma_3 = 0.098_7$; $G(v) = -0.38_6 + 1\ 141.5_4(v + 1/2) - 24.2_9(v + 1/2)^2 - 0.96_2(v + 1/2)^3$; $k_e = 149.91_7$ $N \cdot m^{-1}$.

The formula of Mulliken and Christy, with the Almy and Horsfall centrifugal distortion term, has been used to obtain the rotational constants of the A $^2\Pi$ state of ^{64}ZnD. The principal constants follow: $B_v = 3.777_2 - 0.086_8(v + 1/2)$; $D_0 = 1.14_3 \times 10^{-4}$, $D_1 = 1.13_2 \times 10^{-4}$, $D_2 = 1.14_4 \times 10^{-4}$; $r_e = 0.151\ 1_9$ nm; $A_0 = 343.28_6$,

$A_1 = 342.55_5$, $A_2 = 342.03_5$; $p_0 = 0.149_0$, $p_1 = 0.135$, $p_2 = 0.110_4$; $q_0 = 0.001\,5_3$, $q_1 = 0.002_6$, $q_2 = 0.002_9$; $G(v) = 0.1_8 + 1\,361.48_7(v + 1/2) - 20.69_3(v + 1/2)^2$; $k_e = 213.25_3$ N·m^{-1}. Effective constants for the individual substates have also been calculated.

The origin of the band system, ν_e, is $23\,280.54_7$ cm^{-1} (with Y_{oo} included with the electronic energy, rather than with the vibrational energy). RKR potential energy curves and Franck - Condon factors have been calculated.

Comparison has been made with the spectrum of ZnH. Lines due to the three isotopic molecules ^{64}ZnD, ^{66}ZnD, and ^{68}ZnD have been resolved in a number of bands, and this isotopic splitting has also been briefly discussed.

[redacted]

(Dr. W. J. Balfour)

[redacted]

(Dr. R. M. Clements)

[redacted]

(Dr. G. R. Branton)

[redacted]

(Dr. T. W. Dingle)

TABLE OF CONTENTS

Page

LIST OF TABLES

LIST OF FIGURES

Figure Page

ACKNOWLEDGEMENT

First and foremost, I sincerely wish to thank Dr. Walter J. Balfour for suggesting this project, for guiding and teaching me, for many useful comments and suggestions, for helping to measure the spectrum, for patience, and for providing a large work - space area.

I wish to thank my parents for support, for encouragement, and for help with the finishing stages of this manuscript.

An especial thanks is given to Kathy Beveridge for her darkroom work, for laboriously transferring line measurements onto prints of the spectrum, and for translation work (German to English).

The assistance of Ken Pollitt and Ron Cox in making zinc electrodes and doing other mechanical work, often on short notice, is gratefully acknowledged, as is the electronics expertise provided by Terry Davies and Terry Wiley and the glasswork done by Dave Searle and Arnold Eisenberg.

I also thank Dr. Paul West for allowing me to use his high voltage power supply.

Financial assistance from the National Research Council and Natural Sciences and Engineering Research Council of Canada in the form of Postgraduate Scholarships, and from the University of Victoria Faculty of Graduate Studies in the form of a travel grant, is gratefully acknowledged.

CHAPTER I

INTRODUCTION

A general, theoretical background, necessary for an understanding of the electronic spectrum of zinc monohydride or zinc monodeuteride is presented in the first of two major sections of this chapter. Following this, in section I.B, the scope of the present study is discussed and related to previous studies of these molecules.

I.A. Energy Levels and Spectra

Zinc monohydride, ZnH, can be compared with BeH (and the isoelectronic BH^+), MgH (and AlH^+), CaH, SrH, BaH, CdH, and HgH.† All these molecules have $^2\Sigma^+$ ground states and $^2\Pi_r$ first excited states, and most, if not all, have $^2\Sigma^+$ second excited states.

According to Mulliken,[1],[2] hydrides are expected to closely approximate their united atoms. The electron configurations of the above molecules can be obtained by considering the configurations of the corresponding united atoms. For example, the united atom corresponding to ZnH is gallium, the ground state electron configuration of which is

$$\ldots 4s^2\ 3d^{10}\ 4p^1\ \ ^2P.$$

---

† In this section, ZnD is not distinguished from ZnH, and both isotopic molecules are being referred to. Similarly for the other molecules.

This gives rise to the two molecular electron configurations

$...(4s\sigma)^2\ (3d\sigma)^2\ (3d\pi)^4\ (3d\delta)^4\ (4p\sigma)^1\ \ ^2\Sigma^+$ (ground state)

$...(4s\sigma)^2\ (3d\sigma)^2\ (3d\pi)^4\ (3d\delta)^4\ (4p\pi)^1\ \ ^2\Pi$ (first excited state).

The electron configurations dominating[†] the ground and first two excited states obtained in this manner are presented in Table I.[ʃ] The terms thus predicted, in general, agree with those found experimentally (though see the footnotes to Table I).

However, this agreement may be partly fortuitous. By comparison with the corresponding halides (which show similar optical spectra to the hydrides) and backed up by ESR data,[11] Klynning and Martin[12] have very recently shown that some of the states, including the ground states, of MgH, CaH, SrH, and BaH are predominantly ionic. Instead of comparing the electronic states of these hydrides with those of the united atoms, the comparison should be made with the metal ions (e.g. Ca^+ for CaH) or the corresponding isoelectronic neutral metals (e.g. K). Furthermore, the $B'\ ^2\Sigma^+$ state of MgH should be compared with the $D\ ^2\Sigma^+$ states of CaH, SrH, and BaH, rather than with the $B\ ^2\Sigma^+$

[†] To determine the electron configuration of a given state more accurately, allowance has to be made for contributions from other electron configurations.

[ʃ] For further details of this procedure, the reader is referred to Herzberg,[3] pp. 322-348.

TABLE I. Dominant electron configurations and term types of the lowest states of the ZnH-like group of diatomic hydrides.[a]

Molecule	Ground state (X)		Notes	First excited state (A)		Notes	Second excited state (B)		Notes
BeH	K $(2s\sigma)^2$ $(2p\sigma)^1$	$^2\Sigma^+$		$(2s\sigma)^2$ $(2p\pi)^1$	$^2\Pi_r$		$(2s\sigma)^2$ $(3s\sigma)^1$	$^2\Sigma^+$	(b)
BH^+	K $(2s\sigma)^2$ $(2p\sigma)^1$	$^2\Sigma^+$		$(2s\sigma)^2$ $(2p\pi)^1$	$^2\Pi_r$		[$(2s\sigma)^1$ $(2p\sigma)^2$	$^2\Sigma^+$]	
MgH	KL $(3s\sigma)^2$ $(3p\sigma)^1$	$^2\Sigma^+$		$(3s\sigma)^2$ $(3p\pi)^1$	$^2\Pi_r$		$(3s\sigma)^2$ $(4s\sigma)^1$	$^2\Sigma^+$	(c)
AlH^+	KL $(3s\sigma)^2$ $(3p\sigma)^1$	$^2\Sigma^+$		$(3s\sigma)^2$ $(3p\pi)^1$	$^2\Pi_r$		[$(3s\sigma)^1$ $(3p\sigma)^2$	$^2\Sigma^+$]	
CaH	KLM_{sp} $(4s\sigma)^2$ $(3d\sigma)^1$	$^2\Sigma^+$		$(4s\sigma)^2$ $(3d\pi)^1$	$^2\Pi_r$	(d)	$(4s\sigma)^2$ $(3d\delta)^1$	$^2\Delta$	(d)
SrH	$KLMN_{sp}$ $(5s\sigma)^2$ $(4d\sigma)^1$	$^2\Sigma^+$		$(5s\sigma)^2$ $(4d\pi)^1$	$^2\Pi_r$		$(5s\sigma)^2$ $(5p\sigma)^1$	$^2\Sigma^+$	
BaH	$KLMN_{spd}O_{sp}$ $(6s\sigma)^2$ $(5d\sigma)^1$	$^2\Sigma^+$		$(6s\sigma)^2$ $(5d\pi)^1$	$^2\Pi_r$		$(6s\sigma)^2$ $(5d\delta)^1$	$^2\Delta$	(e)
ZnH	KLM $(4s\sigma)^2$ $(4p\sigma)^1$	$^2\Sigma^+$		$(4s\sigma)^2$ $(4p\pi)^1$	$^2\Pi_r$		$(4s\sigma)^2$ $(5s\sigma)^1$	$^2\Sigma^+$	(f)
CdH	$KLMN_{spd}$ $(5s\sigma)^2$ $(5p\sigma)^1$	$^2\Sigma^+$		$(5s\sigma)^2$ $(5p\pi)^1$	$^2\Pi_r$		$(5s\sigma)^2$ $(6s\sigma)^1$	$^2\Sigma^+$	(f)
HgH	$KLMNO_{spd}$ $(6s\sigma)^2$ $(6p\sigma)^1$	$^2\Sigma^+$		$(6s\sigma)^2$ $(6p\pi)^1$	$^2\Pi_r$		$(6s\sigma)^2$ $(7s\sigma)^1$	$^2\Sigma^+$	(f)

(a) Obtained from the united atoms. These are also the observed configurations and terms, except where noted. The states in brackets have not been observed. K, L, M, and N denote closed shells: M_{sp} denotes the closed subshells 3s and 3p of the M shell, and so on. The closed shells and subshells have not been repeated for the excited states. (An identical table is given by Herzberg[3] but only for the ground and first excited states.)

(b) BeH: $(2s\sigma)^2$ $(3p\pi)^1$ $^2\Pi$ has been the observed second excited state recorded in the literature up until the present.[4] However, the predicted low-lying $^2\Sigma^+$ state has recently been observed by Colin.[5]

footnotes continued on next page...

Footnotes to Table I continued

(c) MgH: According to Mulliken and Christy[2] and Mulliken:[1] $(3s\sigma)^2\ (4p\pi)^1\ {}^2\Pi$. However, experimentally the second excited state, designated B', is a $^2\Sigma^+$ term.[6]

(d) CaH: The observed second excited state is a $^2\Sigma^+$ term,[2],[1],[4] and the electron configurations of this and the first excited state according to Mulliken and Christy[2] and Mulliken[1] are

A: $(4s\sigma)^2\ (4p\pi)^1\ {}^2\Pi_r$

B: $(4s\sigma)^2\ (4p\sigma)^1\ {}^2\Sigma^+$.

These configurations were derived by a more advanced consideration than that used in obtaining the present table: calculations were performed assuming a relation of pure precession and a good fit was obtained with L = 1. However, this may have been merely fortuitous. Recent calculations by Berg and Klynning[7] have not resulted in theoretical values in agreement with experimental ones when using a pure precession relation involving L = 1 (or 2). Mulliken and Christy mention some evidence for a ... $3d\pi$ state. Berg and Klynning suspect a $^2\Delta$ state may be present but have yet to confirm this. However, even if a $^2\Delta$ state is found, the electron configurations may not be as predicted in the table: by analogy with BaH, the situation may be more complicated (cf. footnote (e); see also the discussion in the text regarding the possibility of ionic states).

(e) BaH: Although the observed "B" state is a $^2\Sigma^+$ term, it is now known (based on indirect evidence) that there is, indeed, a $^2\Delta$ state (labelled H) having approximately the right energy.[4],[8] However, the situation may still not be as predicted by the simple united atom approach. (continued)

footnotes continued on next page...

Footnotes to Table I continued

(e) (cont.) Veseth[9] has shown that the observed A $^2\Pi$ and B $^2\Sigma^+$ states are related to each other in the manner of pure precession, with L = 2 (the first such case discovered). This implies that the outermost electron of these two states must be a d - electron and that the configurations must be the same for the two states, other than that one has a $d\pi$ and the other a $d\sigma$ outer electron. This uses up the configuration predicted in the table for the ground state. Veseth invokes a configuration involving an outer 4f electron to account for the ground state.

In summary, Veseth's configurations are

$(6s\sigma)^2\ (4f\sigma)^1$ X $^2\Sigma^+$

$(6s\sigma)^2\ (5d\delta)^1$ H $^2\Delta$

$(6s\sigma)^2\ (5d\pi)^1$ A $^2\Pi$

$(6s\sigma)^2\ (5d\sigma)^1$ B $^2\Sigma^+$.

(f) According to Mulliken and Christy[2] and Mulliken:[1]

ZnH $(4s\sigma)^1\ (4p\sigma)^2$ $^2\Sigma^+$

CdH $(5s\sigma)^1\ (5p\sigma)^2$ $^2\Sigma^+$

HgH $(6s\sigma)^1\ (6p\sigma)^2$ $^2\Sigma^+$.

Bengtsson and Hulthén[10] also list the same electron configurations as Mulliken and Christy, but they put a question mark after each.

states. And, while the M—H bonds are here covalent, the A $^2\Pi$ states of BeH and MgH should be compared with the E $^2\Pi$ states of CaH, SrH, and BaH, rather than with the A $^2\Pi$ states. Klynning and Martin did not discuss ZnH, CdH, and HgH. It may be that some of the states of these molecules also have a degree of ionic character, though (at least for the ground states) less so than the former molecules. Knight and Weltner[13] have shown with ESR measurements that the ground states of ZnH, CdH, and HgH are more covalent than the Mg, Ca, Sr, and Ba monohydrides, with HgH being the most covalent.

Following convention, the terms are designated X, A, B, ..., where X denotes the ground state and A, B, ... denote excited states of the same multiplicity as the ground state, normally in order of increasing energy.

The X $^2\Sigma^+$ and A $^2\Pi$ states of ZnH may be related to each other approximately in the manner of "pure precession." Van Vleck's[14] hypothesis of pure precession refers to the situation in which two states (in this case, Σ and Π) have the same orbital angular momentum, $\vec{L}$, which precesses uniformly about the internuclear axis at two different angles to that axis. That is, the two states act as if they had identical electron configurations except that one state has $\Lambda = 0$ (the Σ state) and the other has $\Lambda = 1$ (the Π state), where Λ is the quantum number corresponding to the projection of $\vec{L}$ along the internuclear axis. As shown by Mulliken and Christy,[2] the pure precession

relation is often a reasonable approximation for hydrides.†

The most important effects of interaction between the $^2\Pi$ and $^2\Sigma$ states are Λ - type doubling in the $^2\Pi$ state and spin - rotation splitting in the $^2\Sigma$ state.

Potential energy curves derived from elementary Heitler - London theory are shown dotted in Fig. 1. However, states of the same species will mutually interact in such a manner that the potential curves repel each other and so avoid crossing. The resulting curves are shown as solid curves in the figure. Such figures have been given by Herzberg[3] for the lowest three states of BeH and by Balfour and Lindgren[15] for the lowest three states of MgH. According to Klynning and Martin,[12] the ground - state Heitler - London curve for MgH correlates with the $Mg^+(^2S) + H^-(^1S)$ states of the separated ions, rather than with the $Mg(^3P) + H(^2S)$ states of the neutral atoms. The $^2\Pi$ and the repulsive $^2\Sigma^+$ states are still as drawn in Fig. 1. Klynning and Martin show potential energy curves for CaH and BaH, also. The situation in ZnH is probably similar to that shown in Fig. 1. Whether, in the absence of perturbation by the repulsive $^2\Sigma^+$ state, the ground $^2\Sigma^+$ state would correlate with the $^2S + {}^1S$ states of the ions or with the $^3P + {}^2S$ states of the neutral atoms is not known for ZnH. RKR potential energy curves for ZnH will be discussed later (section III.D.4; Fig. 24).

---

† However, this may have to be re-studied in the light of the work of Klynning and Martin discussed previously.

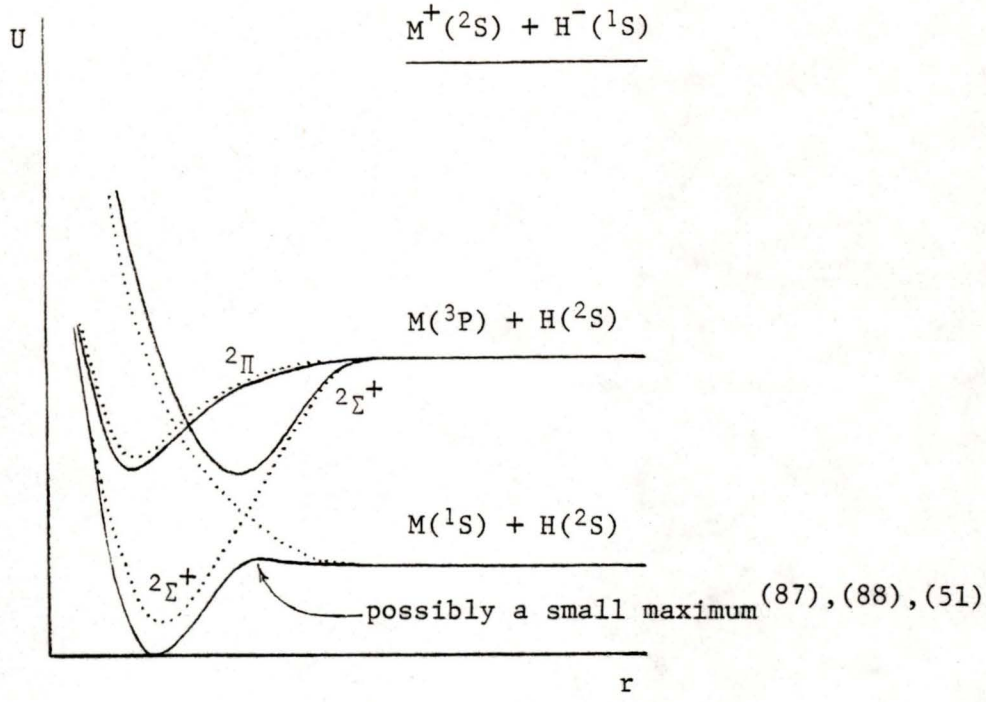

FIGURE 1. Potential curves (schematic) for molecules such as BeH, MgH, and ZnH. The dotted curves are those determined from elementary Heitler - London theory; the solid line curves are the actual curves, which allow for the mutual interaction of the states. For BaH, the separated atom states should be $^3D + ^2S$, rather than $^3P + ^2S$. According to Klynning and Martin,[12] the $^2\Pi$ and upper $^2\Sigma^+$ solid curves are for the A and B (or B') states, respectively, of BeH and MgH, but for the E and D states of CaH, SrH, and BaH. Also, according to Klynning and Martin, the E $^2\Pi$ states of CaH, SrH, and BaH correlate with the excited ^1P state of the metal, rather than with the ^3P state. Also, the lower, dotted $^2\Sigma^+$ curve and the upper, solid $^2\Sigma^+$ curve should correlate with the ground $^2S + ^1S$ states of the ions, at least for MgH and CaH and probably for SrH, and with the first excited $^2D + ^1S$ states of the ions for BaH.

Rotational perturbations between the close - lying A $^2\Pi$ and B $^2\Sigma^+$ states in this series of molecules would be expected, especially in the region where the potential curves cross, and have been observed.† It would also be expected that interaction with the B $^2\Sigma^+$ state would prevent the hypothesis of a relation of pure precession between the X $^2\Sigma^+$ and A $^2\Pi$ states from being completely good, though as discussed later (section I.A.2) such interaction is small.

(In this section, the symbol "ZnH" has been used in the general sense to denote any isotope of zinc and any isotope of hydrogen. From this point on, ZnH will refer specifically to Zn^1H, and ZnD will be used to indicate Zn^2H. Because of the large relative mass difference between the ^1H and ^2H isotopes, there are considerable differences in the spectra of ZnH and ZnD (though there are definite relationships between the two, as discussed in section III.E). Since the splitting of the spectral lines due to different isotopes of zinc is very small, the symbols ZnH and ZnD still refer to any isotope of zinc in the general discussions. However, all numerical data refer specifically to the

---

† See e.g. ref. (16) for perturbations in Zn^1H. Note that the A $^2\Pi$ state (not the E $^2\Pi$ state) is being referred to here, even in CaH, SrH, and BaH, since it was for this state (together with the ground state) that Mulliken and Christy[2] proposed the relation of pure precession (though as noted in Table I, any experimental agreement with this relation may be coincidental in CaH, SrH, and BaH).

^{64}Zn isotope, since this has the greatest natural abundance and the measurements were made on the corresponding most intense ^{64}ZnH or ^{64}ZnD spectral lines.)

I.A.1. Rotational energy expressions for the $^2\Sigma^+$ states[†]

The $^2\Sigma$ states belong to Hund's coupling case (b),[ʃ] and the rotational term values are given by the expressions[(2),(3)]

$$F_1(N) = B_v^*N(N+1) - D_vN^2(N+1)^2 + \frac{\gamma_v}{2}N + 0 + \ldots \qquad \ldots(1a)$$

$$F_2(N) = B_v^*N(N+1) - D_vN^2(N+1)^2 - \frac{\gamma_v}{2}(N+1) + 0 \ldots . \qquad \ldots(1b)$$

The subscripts 1 and 2 distinguish the components having $J = N + 1/2$ (F_1) and $J = N - 1/2$ (F_2). In the e,f nomenclature for labelling parity doublets, as recommended by Brown *et al.*,[(17)] the F_1 levels are e levels and the F_2 levels are f levels. The subscript v's denote the v^{th} vibrational level. The rotational B_v constant is starred to indicate that it differs from the constant as usually

---

[†] All "energies" in this thesis are expressed in units of cm^{-1}. These "energies," F, are related to the proper energies, E, as follows:

$$F = \frac{E}{hc} .$$

[ʃ] Hund's coupling cases (a) - (e) and various subclasses describe the various ways in which the electronic and rotational angular momenta can couple together. Descriptions of the coupling cases can be found in any standard reference work on diatomic spectroscopy, such as references (1), (3), (18), and (19).

defined, as follows:

$$B_v^* = B_v - C_3 \qquad \ldots(2)$$

This difference, and the O term in equation (1) arise from interaction with $^2\Pi$ states, as shown by Van Vleck.[14] Mulliken and Christy[2] give expressions for C_3 and O. The D_v term represents centrifugal distortion. Higher order centrifugal distortion terms have been neglected. γ_v is the spin - rotation coupling constant.

I.A.2. Rotational energy expressions for the $^2\Pi$ state

$^2\Pi$ states can belong to Hund's coupling case (a), to case (b), or, most commonly, to an intermediate situation between these limiting cases, often approaching case (a) for small rotation and gradually undergoing a transition to case (b) with increasing rotation. The general formulas for the rotational terms for the intermediate situation (i.e. allowing for any degree of spin uncoupling), including the limiting cases (a) and (b), are, for a $^2\Pi$ state[3] †

$$F_1(J) = B_v[(J + \tfrac{1}{2})^2 - 1 - \tfrac{1}{2}X_v] - D_v[J^2(J+1)^2 - \tfrac{1}{2}J(J+1) + \tfrac{13}{16}] \qquad \ldots(3a)$$

$$F_2(J) = B_v[(J + \tfrac{1}{2})^2 - 1 + \tfrac{1}{2}X_v] - D_v[J^2(J+1)^2 - \tfrac{1}{2}J(J+1) + \tfrac{13}{16}], \qquad \ldots(3b)$$

---

† For simplifications to these formulas in the limiting cases (a) and (b), see Herzberg,[3] p. 233, and also equation (50) later in this thesis.

where

$$X_v = \sqrt{Y_v(Y_v - 4) + 4(J + \tfrac{1}{2})^2} \quad \text{(the positive square root)} \qquad \ldots(4)$$

$$Y_v = \frac{A_v}{B_v} . \qquad \ldots(5)$$

The first term is the well - known Hill and Van Vleck[20] formula. The second term accounts for the centrifugal distortion. As shown by Almy and Horsfall,[21] in the intermediate situation, the dependence on D_v is more complicated than the usual $-D_v J^2(J+1)^2$ (case (a)) or $-D_v N^2(N+1)^2$ (case (b)). A yet much more complicated expression for the centrifugal distortion given more recently by Veseth[22] has not been employed here. Terms involving γ_v (the same as in equations (1a) and (1b) or the more advanced formulas derived by Kovács[23] and by Veseth[22]) have been omitted, since they are mainly of importance for near case (b) situations (very small A_v or very large J (N)). A_v is the spin - orbit coupling constant. The $^2\Pi$ state is defined as a regular or inverted doublet depending on whether A is positive or negative. (The A $^2\Pi$ states of all the hydrides in Table I, including ZnH and ZnD, are regular doublets--indicated by the subscript r on the term symbols.)

The ratio A_v/B_v ($=Y_v$) is an indicator of the closeness to case (a) or case (b). The larger $|Y_v|$ is, the closer the vibronic state is to case (a). (Case (a) is characterized by large spin - orbit coupling.) Case (b) is

approximated when $|Y_v|$ is small, and pure case (b) pertains when $Y_v = 0$ or $+4$ (the particular values which make the $Y_v(Y_v - 4)$ term in the expression for X_v disappear).

In regular case (a), the energy levels, F_1 and F_2, correspond to the substates that are called $^2\Pi_{1/2}$ and $^2\Pi_{3/2}$, respectively, where the subscripts 1/2 and 3/2 give the value of $\Lambda + \Sigma$. Actually, each substate is a mixture of $^2\Pi_{1/2}$ and $^2\Pi_{3/2}$, but as $|Y_v|$ increases, the amount of mixing decreases and the pure substates are approached.[24] In ZnH and ZnD, Y_v is large, so the substates will be referred to in this thesis as if they were the pure substates.

The Hill and Van Vleck formula does not allow for any uncoupling of the orbital angular momentum, $\vec{L}$, from the internuclear axis. This $\vec{L}$ - uncoupling (incipient formation of Hund's case (d) due to interaction with $^2\Sigma$ (or $^2\Delta$) states) is important and cannot be neglected; it results in Λ - type doubling. To account for this, additional terms have to be added, as given by the Mulliken and Christy[2] formula (which is based on the work of Van Vleck[14]):

$$F_1(J) = B_v[(J + \tfrac{1}{2})^2 - 1 - \tfrac{1}{2}X_v] + \tfrac{1}{2}[o + \tfrac{1}{2}p^* + q^*(J + \tfrac{1}{2})^2]$$

$$- \frac{1}{2X_v}[(2 - Y_v)(o + \tfrac{1}{2}p^* + q^*) + (p^* + 2q^*)(J - \tfrac{1}{2})(J + \tfrac{3}{2})]$$

$$\pm \tfrac{1}{2}(J + \tfrac{1}{2})[(-1 + \frac{2 - Y_v}{X_v})(\tfrac{1}{2}p + q) + \frac{2q}{X_v}(J - \tfrac{1}{2})(J + \tfrac{3}{2})]$$

$$- D_v[J^2(J + 1)^2 - \tfrac{1}{2}J(J + 1) + \tfrac{13}{16}] + \ldots \qquad \ldots(6a)$$

$$F_2(J) = B_v[(J + \tfrac{1}{2})^2 - 1 + \tfrac{1}{2}X_v] + \tfrac{1}{2}[o + \tfrac{1}{2}p^* + q^*(J + \tfrac{1}{2})^2]$$

$$+ \frac{1}{2X_v}[(2 - Y_v)(o + \tfrac{1}{2}p^* + q^*) + (p^* + 2q^*)(J - \tfrac{1}{2})(J + \tfrac{3}{2})]$$

$$\mp \tfrac{1}{2}(J + \tfrac{1}{2})[(1 + \frac{2 - Y_v}{X_v})(\tfrac{1}{2}p + q) + \frac{2q}{X_v}(J - \tfrac{1}{2})(J + \tfrac{3}{2})]$$

$$- D_v[J^2(J + 1)^2 - \tfrac{1}{2}J(J + 1) + \tfrac{13}{16}] + \ldots , \qquad \ldots(6b)$$

where the spin - rotation coupling terms have again been omitted, and the centrifugal distortion term of Almy and Horsfall has been added to the formula of Mulliken and Christy. The term preceded by the $\pm$ or $\mp$ sign represents the Λ - type doubling, which is symmetrical about a mean position. This mean position itself differs from the pure Hill and Van Vleck energy, as reflected by the remaining terms. These latter terms, involving o, p*, and q*, arise from interaction with $^2\Sigma$ states and are in addition to the Λ - doubling term (which also arises from interaction with the $^2\Sigma$ states). The upper sign of $\pm$ or $\mp$ refers to F_e levels and the lower sign to F_f levels, where the Λ - type doublet levels have been labelled according to the recommendations of Brown et al.[17]† The quantities o, p,

---

† The correspondence between the e,f nomenclature and the former c,d nomenclature of Mulliken[1] for a regular $^2\Pi$ state is as follows:[17]

F_1: e = d
f = c

F_2: e = c
f = d.

q, p*, and q* are small parameters which are defined in the paper by Mulliken and Christy. The method by which p and q are evaluated will be discussed later (section III.B.5). In the absence of $^2\Sigma^-$ states, p* = p and q* = q.† An approximate value for o can be obtained from the expression given by Veseth:[22]

$$o = \frac{Y_v}{8} p^* . \qquad \ldots(7)$$

The derivation of equation (6) involved an approximation which is good only if $|A| << |\nu_{\Pi,\Sigma}|$, where $\nu_{\Pi,\Sigma}$ is the energy separation (in cm^{-1}) of the $^2\Pi$ state and an interacting $^2\Sigma$ state.ʃ Dousmanis, Sanders and Townes[25] have extended equation (6) to include the next higher order (second order). Their equation, rather than equation (6), should be employed if $|A|$ is not $<< |\nu_{\Pi,\Sigma}|$. For the A $^2\Pi$ and X $^2\Sigma^+$ states of ZnH

---

† $p^* = p + 2a_2$ and $q^* = q + 2C_2$, where a_2 and C_2 involve summations of matrix elements over $^2\Sigma^-$ states. (Complete expressions are given by Mulliken and Christy.[2]) In the absence of $^2\Sigma^-$ states, these summations will equal zero. MgH is the only one of the series of hydrides in Table I known to have a $^2\Sigma^-$ state and it is at much higher energy than the $^2\Pi$ state, so any interaction would probably be small.

ʃ Unlike the ν_o values defined later in this thesis, the $\nu_{\Pi,\Sigma}$ values are to be obtained by <u>vertical</u> projection from the v^{th} level of the $^2\Pi$ state to the point of intersection with the potential energy curve of the $^2\Sigma$ state, as described by Mulliken and Christy.[2] The sign of $\nu_{\Pi,\Sigma}$ is positive when the $^2\Pi$ state is above the $^2\Sigma$ state and negative for the reverse situation.

and ZnD, $\nu_{\Pi,\Sigma}$ lies in the range 22 000 - 23 000 cm^{-1}. and A is ≃340 cm^{-1}, so the approximation in equation (6) should be good for interaction between these states. In fact, Dufayard and Nedelec[26] have calculated the ratio of the second order terms of Dousmanis et al. to the first order terms (equation (6)) and found this ratio to be only 0.8% and 1.1% for the v' = 0 levels of the $^2\Pi_{1/2}$ substates of ZnH and ZnD, respectively, and 2.6% and 2.8%, again respectively, for the $^2\Pi_{3/2}$ (v' = 0) substates. The second order terms of Dousmanis et al. have been neglected in the present work.

The B $^2\Sigma^+$ state of ZnH is of very similar energy to the A $^2\Pi$ state and presumably is also in ZnD (though not yet observed), so |A| is not << $|\nu_{\Pi,\Sigma}|$. However, the B state is believed not to interact with the A state as much as the X state does. If Mulliken and Christy[2] are correct, the relation between the X and A states is approximately that of pure precession and the interaction should be strong, whereas no such relation exists between the A and B states. The interaction may also be small for pseudo Franck - Condon reasons--the respective potential curves have very different r_e values. From rotational perturbations and Franck - Condon factors, Dufayard and Nedelec[26] have calculated that the effect of the B state on the Λ - doubling of the A $^2\Pi$ v = 0 level of ZnH is about a thousand times smaller than the observed Λ - doubling. While it may be somewhat larger for the other vibrational levels, the effect

of the B $^2\Sigma^+$ state was neglected in the present work.

Equation (6) does not take into account interaction of the $^2\Pi$ state with $^2\Delta$ states. Further terms would have to be added if such interaction occurred. However, no $^2\Delta$ states are known in ZnH. If any do exist, it is assumed that the interaction is negligible.

I.A.3. Experimental constants as Dunham series coefficients

The experimentally - determined constants that have been called ω_e, B_e, α_e, etc. in this thesis (following convention and for convenience), apart from sign correspond to the coefficients $Y_{\ell m}$ of the Dunham[27] double power series for the terms of the vibrating rotator:

$$T_{vJ} = \sum_{\ell m} Y_{\ell m}(v + \tfrac{1}{2})^{\ell} J^m(J + 1)^m \qquad ...(8a)$$

or $$T_{vN} = \sum_{\ell m} Y_{\ell m}(v + \tfrac{1}{2})^{\ell} N^m(N + 1)^m . \qquad ...(8b)$$

Note, however, that for the $^2\Pi$ state, intermediate between cases (a) and (b), while the vibrational terms follow the Dunham formula, the rotational terms are not exactly of this form.

The relationship between the Y's and the usual spectroscopic notation is as follows:

$$\begin{aligned} & Y_{10} = \omega_e \quad Y_{20} = -\omega_e x_e \quad Y_{30} = \omega_e y_e \quad Y_{40} = \omega_e z_e \\ Y_{01} = B_e \quad & Y_{11} = \alpha_e \quad Y_{21} = \gamma_e \\ Y_{02} = -D_e \quad & Y_{12} = -\beta_e \\ Y_{03} = H_e & \end{aligned} \qquad ...(9)$$

These relationships have been assumed to be exact equalities,

and as a consequence, the usual formulas for these constants (e.g. $B_e = \frac{h}{8\pi^2 c I_e}$) are only approximate, as shown by Dunham. The approximations involve neglect of terms in $\frac{B_e^2}{\omega_e^2}$, which are largest for light molecules such as H_2 and the lighter hydrides. Further comments on this approximation will be made later (section III.D).

I.A.4. Branches and intensities in a $^2\Pi - {}^2\Sigma^+$ band

As a result of the selection rules

$$\Delta J = 0, \pm 1 \qquad \ldots(10)$$

and $+ \leftrightarrow -, \quad + \not\leftrightarrow +, \quad - \not\leftrightarrow -$ $\qquad \ldots(11)$

there are twelve possible branches in a $^2\Pi - {}^2\Sigma$ band: R_1, Q_1, P_1, R_2, Q_2, P_2, $^QR_{12}$, $^PQ_{12}$, $^OP_{12}$, $^SR_{21}$, $^RQ_{21}$, and $^QP_{21}$. The transitions to which these branches correspond are shown in the energy level diagram in Fig. 2, in which the $^2\Pi$ state is drawn for a situation intermediate between cases (a) and (b), but closer to (a) than to (b). Unless the state belongs to case (b), the branches are arranged in two sub-bands, as can be seen from the figure. Each sub-band consists of three main branches (R_1, Q_1, P_1 or R_2, Q_2, P_2), in which $\Delta J = \Delta N$, and three satellite branches, in which $\Delta J \neq \Delta N$. When $\Delta J \neq \Delta N$, the ΔN values are denoted by the superscripts S, R, Q, P, or O, which stand for $\Delta N = N' - N'' = +2, +1, 0, -1,$ or -2, respectively. In pure case (a), these superscripts are omitted.

Intensity factors (which when multiplied by a Boltzmann

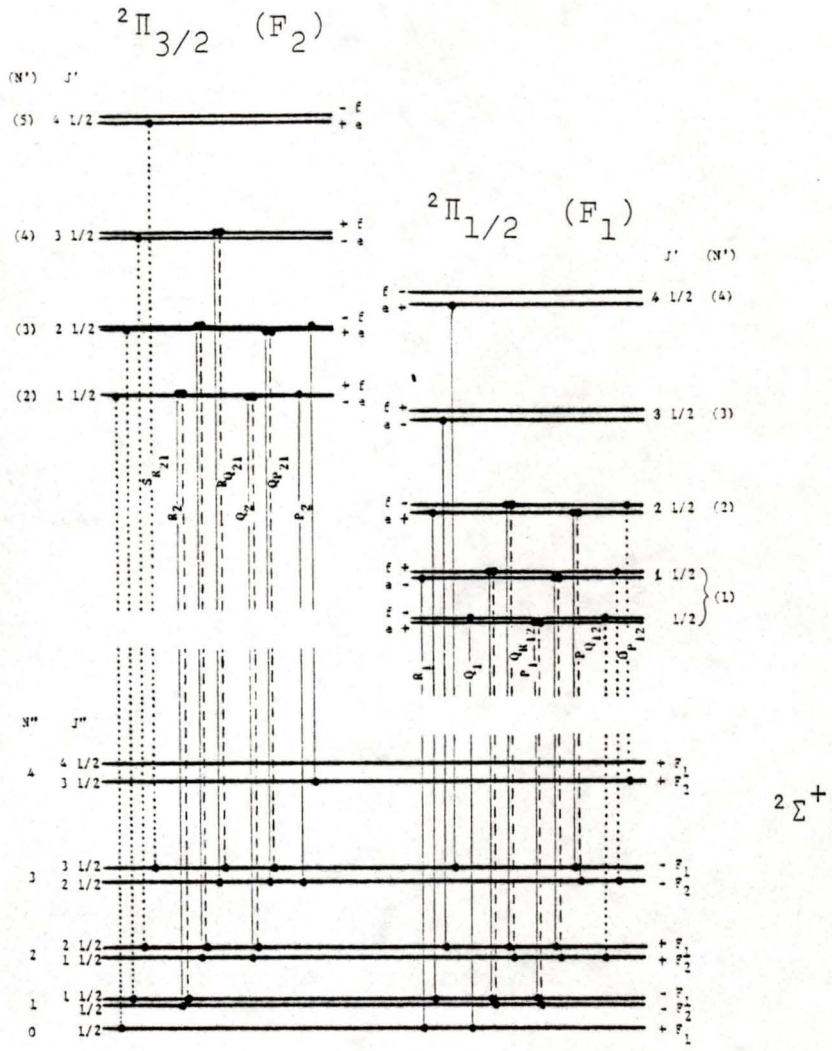

FIGURE 2. Energy level diagram for the first lines of a $^2\Pi_r - {}^2\Sigma^+$ band. The $^2\Pi$ state is drawn for a situation intermediate between Hund's coupling cases (a) and (b), but closer to (a) than to (b). In Zn^1H and Zn^2H, the spin - orbit splitting in the upper state is considerably larger than shown, while the spin - rotation splitting in the lower state and the Λ - doublet splitting in the upper state are smaller than shown. The main branches ($\Delta J = \Delta N$) are drawn as solid lines, while the satellite branches ($\Delta J \neq \Delta N$) are dashed ($\Delta N = 0, \pm 1$) or dotted ($\Delta N = \pm 2$). [Modified from ref. (3).]

factor and by a constant yield the intensities of the spectral lines) have been determined by Mulliken[28] for when the $^2\Pi$ state is pure case (b). Hill and Van Vleck[20] obtained formulas for the intermediate case (a-b) situation in terms of the parameter Y_v, and Earls[29] reduced these to a comparatively simple form. No matter what stage the $^2\Pi$ state represents in the range between pure case (a) and pure case (b), the six main branches are strong, with the Q_1 and Q_2 branches being roughly as strong as each other and approximately twice as intense as the other four. In pure case (a), the satellite branches are also intense; in each sub-band, the two Q branches are about equally strong and roughly twice as intense as the two P and two R branches, which are also about equally strong as one another. In pure case (b), the two satellite branches $^OP_{12}$ and $^SR_{21}$ are absent altogether because of the additional selection rule $\Delta N = 0, \pm 1$, which applies since the X $^2\Sigma$ state also belongs to case (b). The other four satellite branches are allowed, but decrease in intensity rapidly as N increases. For intermediate case (a-b) situations, the intensities of the satellite branches depend on the value of Y_v ($= A_v/B_v$), that is, on how close to case (a) or to case (b) the state is.

In the present study, the intensities of the lines were not studied explicitly. But the above qualitative description[30] was of use in identifying the branches.

I.B. Historical Survey

The spectrum of ZnH was first measured by Howson in 1912,[31] then by Hagenbach and Schumacher in 1919.[32] During the early 1920's, Hulthén[33],[34] again observed molecular lines (due to ZnH) in the spectrum of atomic zinc and measured and classified them into two bands. The spectrum observed by these early investigators was actually first identified as being due to the zinc hydride molecule by Kratzer in 1923[35] and is now known to be the 0-0 band of the $A\ ^2\Pi - X\ ^2\Sigma^+$ system. This system was further discussed by Mulliken[36] in the late 1920's. Volkringer again observed ZnH lines as an impurity in the spectrum of atomic zinc in 1929.[37] The $B\ ^2\Sigma^+ - X\ ^2\Sigma^+$ system was first reported by Hulthén,[38] who apparently observed the 4-0 band. Fukuda (1931)[39] rephotographed the spectrum and extended the analysis to include the 0-1 and 1-0 bands of the $A\ ^2\Pi - X\ ^2\Sigma^+$ system in addition to the 0-0 band. He also observed and analyzed the 4-0, 4-1, 6-0, 6-1, and 8-0 bands of the $B\ ^2\Sigma^+ - X\ ^2\Sigma^+$ system. However, many of his line measurements were inaccurate and in some cases his vibrational and rotational numberings were wrong.[16]

During the time period referred to in the previous paragraph, the understanding of quantum mechanics, and consequently its application to spectroscopy, was improving and the nomenclature of spectroscopy was undergoing changes. ZnH was one of the molecules particularly instructive in the development of the theory of the spectra of diatomic

molecules (see e.g. Mulliken[36],[40],[2]).

The work on ZnH culminated in the studies of Stenvinkel[16],[41],[42] and of Fujioka and Tanaka,[43] both published at about the same time (1936 - 37). The most extensive work on ZnH was performed by Stenvinkel and published as his doctoral dissertation in 1936.[16] He improved upon the analysis of Fukuda and analyzed many new bands. He employed the new nomenclature essentially as it is used today. Fujioka and Tanaka analyzed only the 0-0 band of the $A\ ^2\Pi - X\ ^2\Sigma^+$ system. Their analysis was in good agreement with that of Stenvinkel. They also photographed and analyzed the $A\ ^2\Pi - X\ ^2\Sigma^+$ 0-0 band of ZnD for the first time.

No further work was done on the molecule (other than in certain specialized studies referred to in the following paragraph) until 1962, when Khan reported[44] a new system for both ZnH and ZnD, the $C\ ^2\Sigma^+ - X\ ^2\Sigma^+$ system, observed in absorption. (The previous studies were in emission.) Rafi and Khan also rephotographed the $A\ ^2\Pi - X\ ^2\Sigma^+$ 0-0 band in emission and purportedly extended the analysis to higher J values in an error - ridden paper published in 1976.[45]

In addition to the foregoing general studies, ZnH has been the object of several relatively specialized studies. The Zeeman effect in ZnH (first reported on by Hulthén[34]) was studied by Watson and Perkins[46] and by Watson.[47] Bender[48] observed the spectrum as a result of an optical

resonance phenomenon. Mrozowski[49] observed a nuclear isotope shift of the lines in the A $^2\Pi$ - X $^2\Sigma^+$ 0-0 band. Knight and Weltner[13] trapped ZnH molecules in a matrix of solid argon and measured the ESR spectrum of the ground $^2\Sigma^+$ state. ZnH has been observed with strong intensity in flame emission studies of $Zn(CH_3)_2$ or $Zn(C_2H_5)_2$ by Egerton and Rudrakanchana[50] and by Lee and Zare.[51] Dufayard and Nedelec[26] selectively excited each A $^2\Pi$, v' = 0 rotational level of ZnH and ZnD by means of a pulsed dye laser, then studied the lifetimes, Λ - doubling, and hyperfine structure.

ZnH has been used as an example in a number of theoretical studies: Λ - doubling (Mulliken and Christy[2]), potential energy functions (Hulbert and Hirschfelder;[52] Lippincott, Steele, and Caldwell;[53] Wojtczak;[54] and Mirajkar[55]), bond lengths (Politzer[56]), spin - orbit coupling (Ishiguro and Kobori[57] and Veseth[22]), bond - charge model for vibrating diatomic molecules (Simons and Parr[58]), effect of centrifugal distortion on Λ - doubling and spin - splitting (Veseth[59]), and mean amplitudes of vibration and molecular polarizabilities (Pandey et al.[60]).

Spectroscopic studies of ZnH are also of possible significance to astronomy. Stenvinkel, Svensson, and Olsson[42] compared their laboratory - determined wavelengths for the lines of the six most intense branches of the A $^2\Pi$ - X $^2\Sigma^+$ 0-0 band with the nearest coinciding lines in a table of solar spectrum lines[61] and could come to no

definite conclusion as to whether ZnH existed in the sun. Recently (1976), Wojslaw and Peery[62] claim to have identified some of the branches of the A $^2\Pi_{1/2}$ - X $^2\Sigma^+$ 0-0 and 1-0 bands of ZnH in the spectrum of 19 Piscium (N0; C7, 3).

I.B.1. Present work

As preliminary work in the current project, the emission spectrum of ZnH was again photographed in the 370 - 520 nm region. The following bands of the A $^2\Pi \rightarrow$ X $^2\Sigma^+$ system were measured: 0-0, 0-1, 1-0, 1-1, 1-2, 2-1, 2-2, and 2-3. The wavelengths agree with those of Stenvinkel[16],[42] to 0.006 nm or better, and, for the 0-0 band, to within 0.002 nm with those of Fujioka and Tanaka.[43] Agreement with the measurements of Fukuda[39] was much poorer (often differences of 0.06 nm), presumably due to the low resolution of his spectrograph. In addition, his rotational assignments are not all correct. Stenvinkel[16] also pointed out these problems with Fukuda's work. The B $^2\Sigma^+ \rightarrow$ X $^2\Sigma^+$ system of ZnH is considerably weaker in intensity than the A $^2\Pi \rightarrow$ X $^2\Sigma^+$ system. The 0-4 and 0-5 bands of the B $^2\Sigma^+ \rightarrow$ X $^2\Sigma^+$ system were partially analyzed, but not measured. A number of other, weaker bands are present but have not been analyzed or measured.

It was initially hoped to extend the analysis of some of the branches of ZnH to higher rotational values than attained by previous workers. However, the intensities of

the spectra were not sufficient to allow for this. To obtain greater intensities, exposure times of impractical length would have been required, and this was not pursued further.

Instead, the present project was devoted primarily to a study of ZnD. Stenvinkel did not study ZnD. The only experimental studies of the A $^2\Pi$ - X $^2\Sigma^+$ system have been of the 0-0 band (Fujioka and Tanaka[43] and Dufayard and Nedelec[26]). Dufayard and Nedelec employed the 0-1 band in their study but only reported data on the v' = 0 level. The other bands of this system were not analyzed prior to the present work, and hence no values have previously been reported for the equilibrium rotational constants (B_e, α_e, D_e, β_e, etc.) nor equilibrium vibrational constants (ω_e, $\omega_e x_e$, etc.) of either the X $^2\Sigma^+$ or A $^2\Pi$ states, nor for the electronic term, T_e, of the A $^2\Pi$ state. Precise estimates of these ZnD parameters should provide valuable data with which to test further important theoretical relationships. The B $^2\Sigma^+$ - X $^2\Sigma^+$ system of ZnD has never been reported, a statement which still holds since if bands of this system were present in the spectral regions studied in this thesis, they were amongst the weaker bands not yet analyzed. Other (possibly stronger) B - X bands may occur at shorter wavelengths.

CHAPTER II

EXPERIMENTAL METHODS

The spectra of ZnH and ZnD have been observed in emission in the present work using the gas discharge cell designed at the University of Victoria by Cartwright[63] (Figs. 3 and 4). The tips of both electrodes were made of zinc (99.995% pure).

At first, a DC power supply was tried which provided voltage variable between 0 and 120 V and current 0 - 15 A. A ballast resistance was placed in series with the cell. It was found necessary to cool the ballast resistor (air - cooled by means of a fan). Various source voltages, ballast resistances (0 - 150 Ω), electrode shapes (Fig. 5), and gaps between the electrodes were tried. Most success was obtained with electrodes shaped as in Fig. 5d, with a source voltage of 120 V and a ballast resistance of 150 Ω.

The arc or discharge would not strike spontaneously. At first a Tesla coil† was used. Later, the arc was struck by touching the electrodes together then pulling them apart. Once the arc was struck, the width of the electrode gap appeared to make no difference to the running of the arc, over the range <0.5 mm - 15 mm.

Gas was allowed to flush continuously through the

---

† Edwards High - frequency Tester.

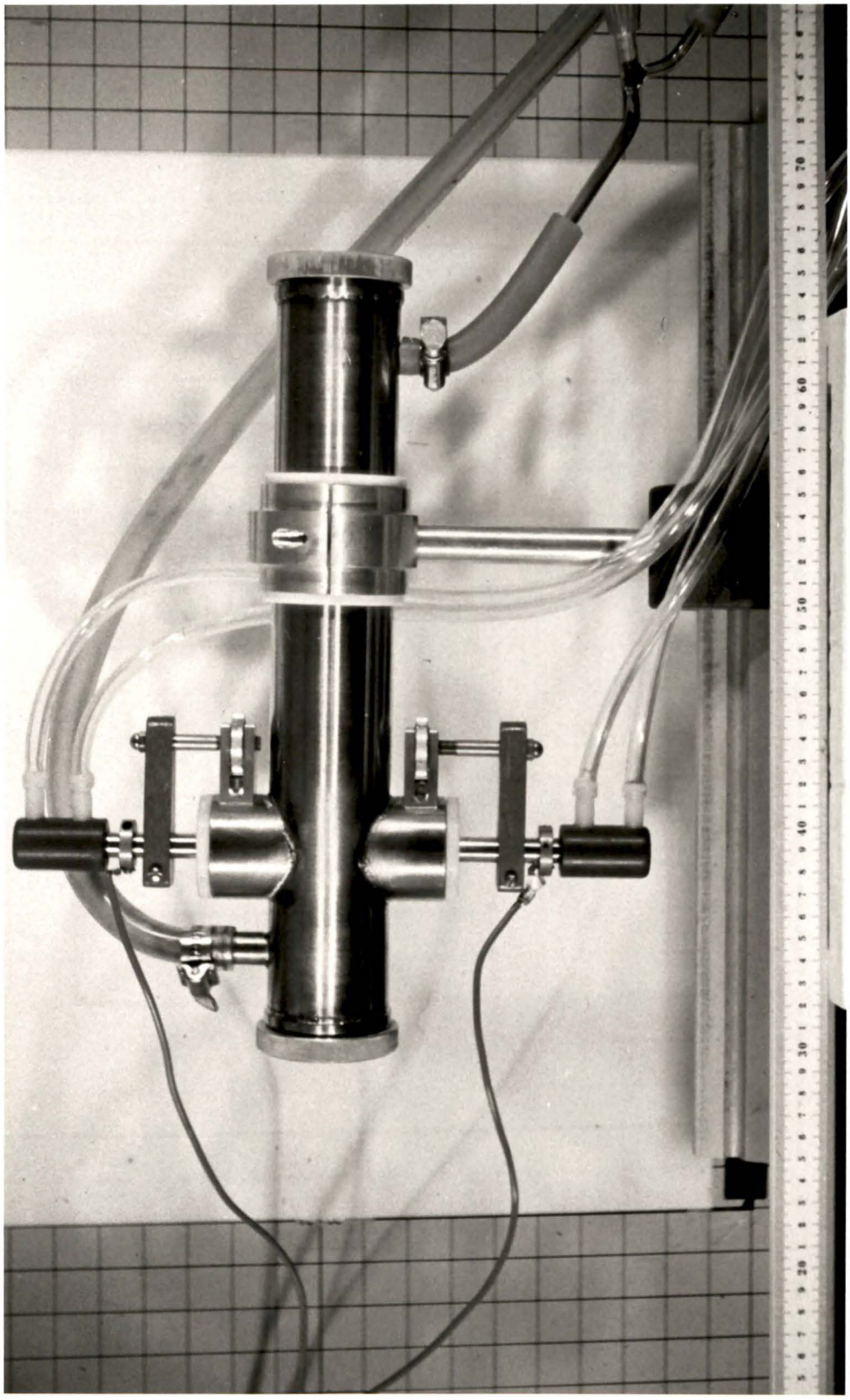

FIGURE 3. The emission cell.

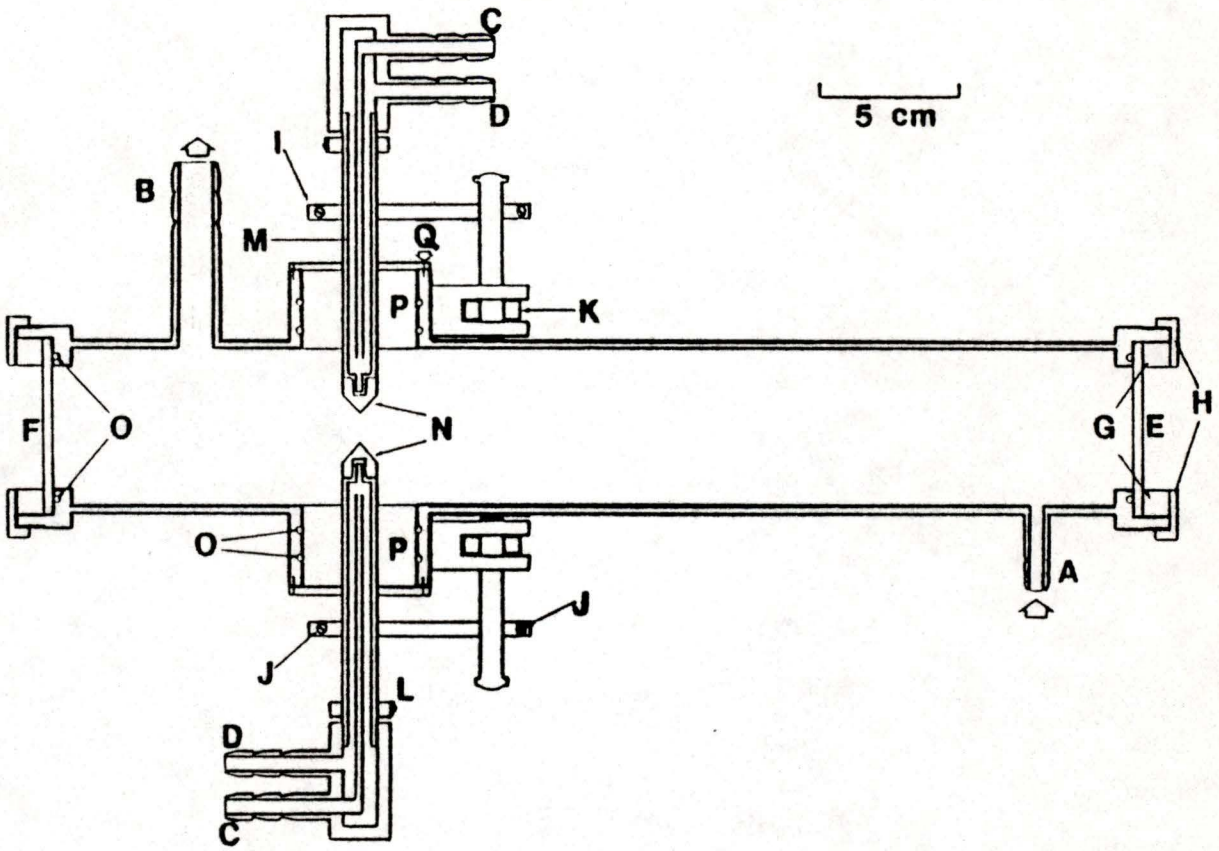

FIGURE 4. Emission cell in vertical cross section.[63] A: gas inlet. B: gas outlet. C: water inlet. D: water outlet. E: main viewing window. F: subsidiary viewing window. G: Teflon square - section O - ring. H: screw - on O - ring to lock Teflon ring. I: electrode clamp. J: lock nut. K: electrode adjusting screw. L: electrode electrical connector. M: water inlet pipe. N: exchangeable electrode tip. O: rubber O - ring. P: Teflon collar. Q: Teflon screw.

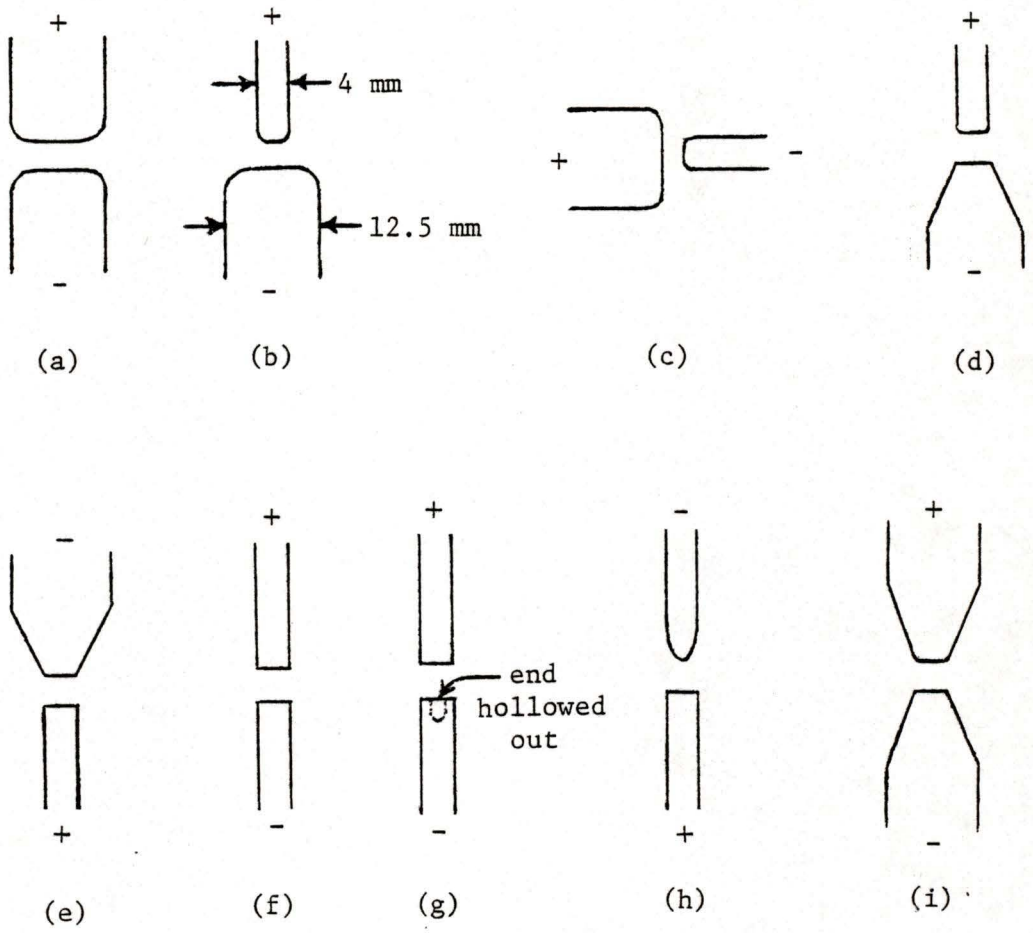

FIGURE 5. The electrode configurations tried with the DC power source. Various other irregular shapes were tried as a result of the electrodes melting. The polarities were also reversed relative to those shown.

cell to avoid buildup of impurities and coating of the cell windows. At first an atmosphere of Linde O_2 - free argon was used. It was found that the spectrum of ZnH was obtained without adding any hydrogen! The hydrogen presumably came from H_2O present in the Ar or a hydrogen source occluded in the zinc electrodes. Subsequently Linde Prepurified Ar (<5 ppm H_2O) was employed, but the spectrum of ZnH was still obtained. Passing the Ar through a liquid nitrogen - cooled trap† made no noticeable difference. Two molecular sieve traps (5 Å, 8 - 12 mesh; 3 Å, 14 - 30 mesh), through which the Ar was passed, did reduce the intensity of the spectrum but not completely eliminate it.

Generally pressures of <100 mm Hg were used. With increasing pressure the arc ran more steadily, but collision broadening of the spectral lines became noticeable, with consequent loss of isotopic structure.

A major problem with the power supply first used was that if any hydrogen∫ were added, even small amounts (unless the total pressures were high (approaching 1 atm.)), the arc would be immediately quenched. Hence, the spectra of ZnH were obtained with no added H_2, using the hydrogen from the

---

† ~1 m long, spiralled, 6 mm inside diameter.

∫ Linde O_2 - free grade.

impurities. The deuteride was successfully obtained by passing the Ar through a cell containing D_2O (Fig. 6); however, it was very difficult to maintain the arc running steadily.

A transformer† passed through a diode, providing up to 3200 V DC, was next tried as the power source. Unfortunately, the current had to be limited with a 100 kΩ resistor. Due to the low current density, no arc was obtained--just a glow discharge with, at most, some sparking. (An atmosphere of He was also tried, with no more success than with Ar.)

Finally, a large high - voltage power supply (Fig. 7) was obtained, which provided a supply voltage of up to 2000 V, with a current of up to 0.75 A, AC. A large ballast resistance (186 Ω cold resistance)ʃ was connected in series with the lamp. This provided a steady arc or discharge, which was struck spontaneously upon turning up the voltage. The arc could be run with any concentration of H_2 in Ar, or even with pure H_2. After again trying most of the electrode shapes in Fig. 5, the best configuration was found to be that shown in Fig. 8. The spectrum of ZnD could now be obtained by using D_2 gas, rather than D_2O.

The majority of the spectra have been taken with an Ar pressure of about 200 mm Hg. A pressure of 10 - 20 mm Hg

---

† Primary 90 V, secondary 6400 V.

ʃ Twenty 100 W light bulbs connected in series.

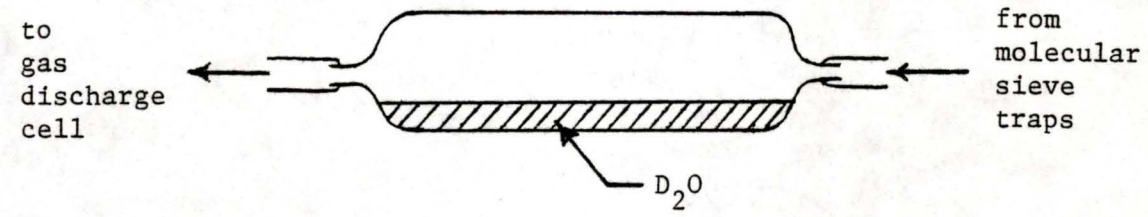

FIGURE 6. Apparatus used to obtain ZnD when using the original (DC) power supply.

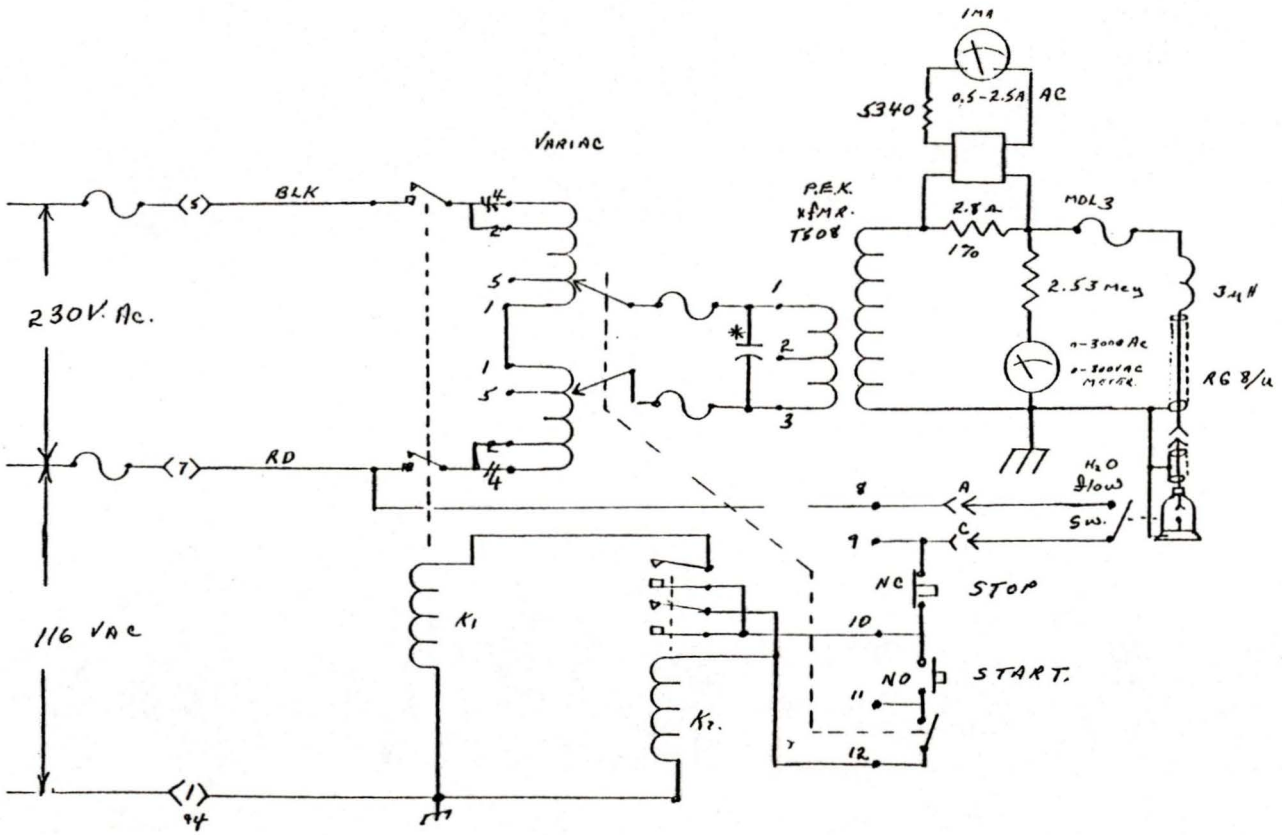

FIGURE 7. Circuit diagram of the high voltage AC power supply. (Courtesy of Chemistry Instruments Shop, University of Victoria.)

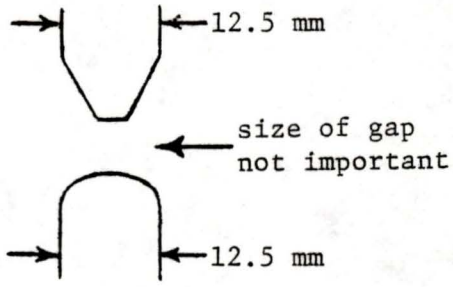

FIGURE 8. The best electrode configuration found with the high voltage power supply.

of H_2 or D_2 was added every approximately three minutes, then allowed to be pumped out. This resulted in greater spectral intensity than either letting the H_2 bleed in continuously or not adding any H_2 and relying on the impurities as the source of hydrogen.

Atomic zinc lines are, of course, present in the spectra. Also, some impurities have, at times, been observed, including atomic Fe, Cr I, Al I, and molecular N_2^+ (first negative system, B $^2\Sigma_u^+$ - X $^2\Sigma_g^+$ at 427.8 nm (0-1 band) and 470.9 nm (0-2)), N_2 (second positive system, C $^3\Pi_u$ - B $^3\Pi_g$ at 357.7 nm (0-1) and 380.5 nm (0-2)), CN (B $^2\Sigma$ - X $^2\Sigma$ 0-0 band at 388.3 nm), OH (A $^2\Sigma^+$ - X $^2\Pi$ 0-0 band at 306.4 nm), and AlO (B $^2\Sigma^+$ - X $^2\Sigma^+$ 1-0 band at 464.8 nm, 2-1 band at 467.2 nm, 3-2 band at 469.4 nm, 0-0 band at 484.2 nm, and 1-1 band at 486.6 nm). The N_2 and N_2^+ could be eliminated by fixing leaks in the vacuum system. Interference by the spectrum of CN below 388.3 nm was more of a problem. One spectrum in this region was obtained that did not show any CN, but all others, previous and subsequent, did. One other problem is that sometimes ZnH bands were present in the spectra of ZnD, the hydrogen having come from an impurity(ies), as mentioned before. However, ZnH - free spectra of ZnD have been obtained.

The spectra have been recorded on a Jarrell - Ash 70-000 series, 3.4 meter Ebert Spectrograph, with slit widths of 20 - 30 μm in the 2nd order of an 1180 g/mm grating, reciprocal dispersion 0.11 nm/mm, with order -

sorting by means of Corning glass filters; and, at higher resolution, in the 13^{th} order of a 300 g/mm grating, reciprocal dispersion 0.31 nm/mm, with order - sorting by means of narrow band - pass interference filters. The spectra were photographed on Ilford HP5 film, with exposure times of 15 minutes to 13 hours. The films were developed for four minutes at 17°C in Kodak D19 developer, fixed in a general purpose hardening fixer, and rinsed for 20 - 30 minutes in running water.

Calibration was with a neon - filled iron hollow cathode lamp and the wavelength table of Crosswhite.(64) The spectra have been measured on a Grants Instruments Co. oscilloscope - setting comparator. The standard deviation in the 1722 line frequencies (wavenumbers) used to calculate the term values of ZnD is ± 0.104 cm^{-1}. The absolute frequencies of most of the lines are estimated to be accurate to better than ± 0.1 cm^{-1}; a few lines are of lower accuracy due to blending of lines or random errors. The 284 lines of the $A\ ^2\Pi - X\ ^2\Sigma^+$ 0-0 band of ZnD have a standard deviation of ± 0.070 cm^{-1}.

CHAPTER III

ANALYSIS OF THE A $^2\Pi \rightarrow$ X $^2\Sigma^+$ SYSTEM OF ZnD

III.A. Overview of the Spectrum

The emission spectrum of ZnD has been photographed in the wavelength region 346 - 505 nm. The following violet - degraded bands of the A $^2\Pi \rightarrow$ X $^2\Sigma^+$ system have been measured and analyzed: 0-0, 0-1, 0-2, 1-0, 1-1, 1-2, 1-3, 2-1, 2-2, and 2-3. The 0-3 band is present but too faint to analyze. A CN impurity band occurs in the region where the 2-0 band would be if present. There is what appears to be a violet - degraded head at 387.429 nm, which may or may not be the 2-0 A $^2\Pi_{1/2}$ - X $^2\Sigma^+$ sub-band predicted to be at 387.435 nm, but there is no obvious head at the predicted position for the A $^2\Pi_{3/2}$ - X $^2\Sigma^+$ sub-band (382.622 nm). The 3-2 band is present, and the 2-4 band is believed to be also, as is possibly the 3-3 band, but these have not yet been fully investigated. Bands of the B $^2\Sigma^+ \rightarrow$ X $^2\Sigma^+$ system have not been identified, but it is possible that some of the as yet unidentified lines belong to this system.

A graphical version of a Deslandres table was found useful during the analysis for keeping track of the bands and predicting the positions of other bands (see Fig. 9).

The spectrum of ZnD is reproduced in Fig. 10. An enlarged, higher - resolution view of part of the 0-0 band is presented in Fig. 11. The structure of a typical band in the A $^2\Pi$ - X $^2\Sigma^+$ system can be seen from the

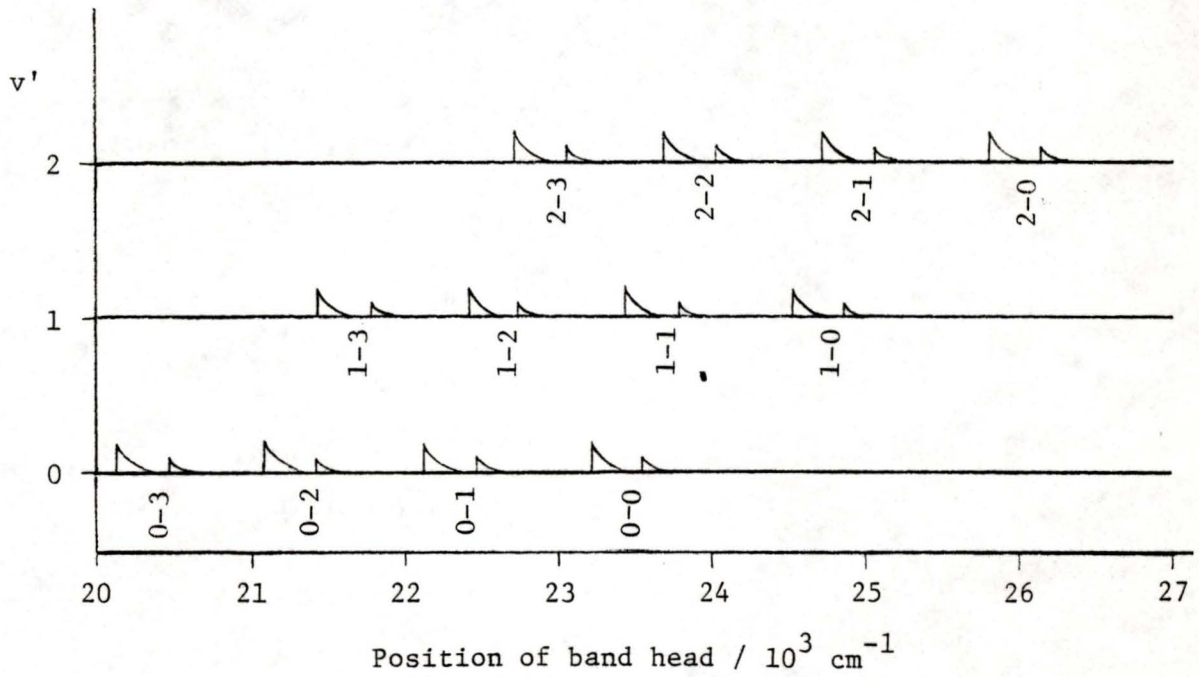

FIGURE 9. Graphical presentation of a Deslandres table. The positions of the $^2\Pi_{1/2} - {}^2\Sigma^+$ $^PQ_{12}$ ($\curlywedge$) and $^2\Pi_{3/2} - {}^2\Sigma^+$ Q_2 ($\curlyvee$) heads of ZnD are shown. The positions of other bands can be predicted by extrapolation or interpolation. Note that if all the bands are projected onto the v' = 0 line, the spectrum is obtained—the graph is just a blow - up of the spectrum.

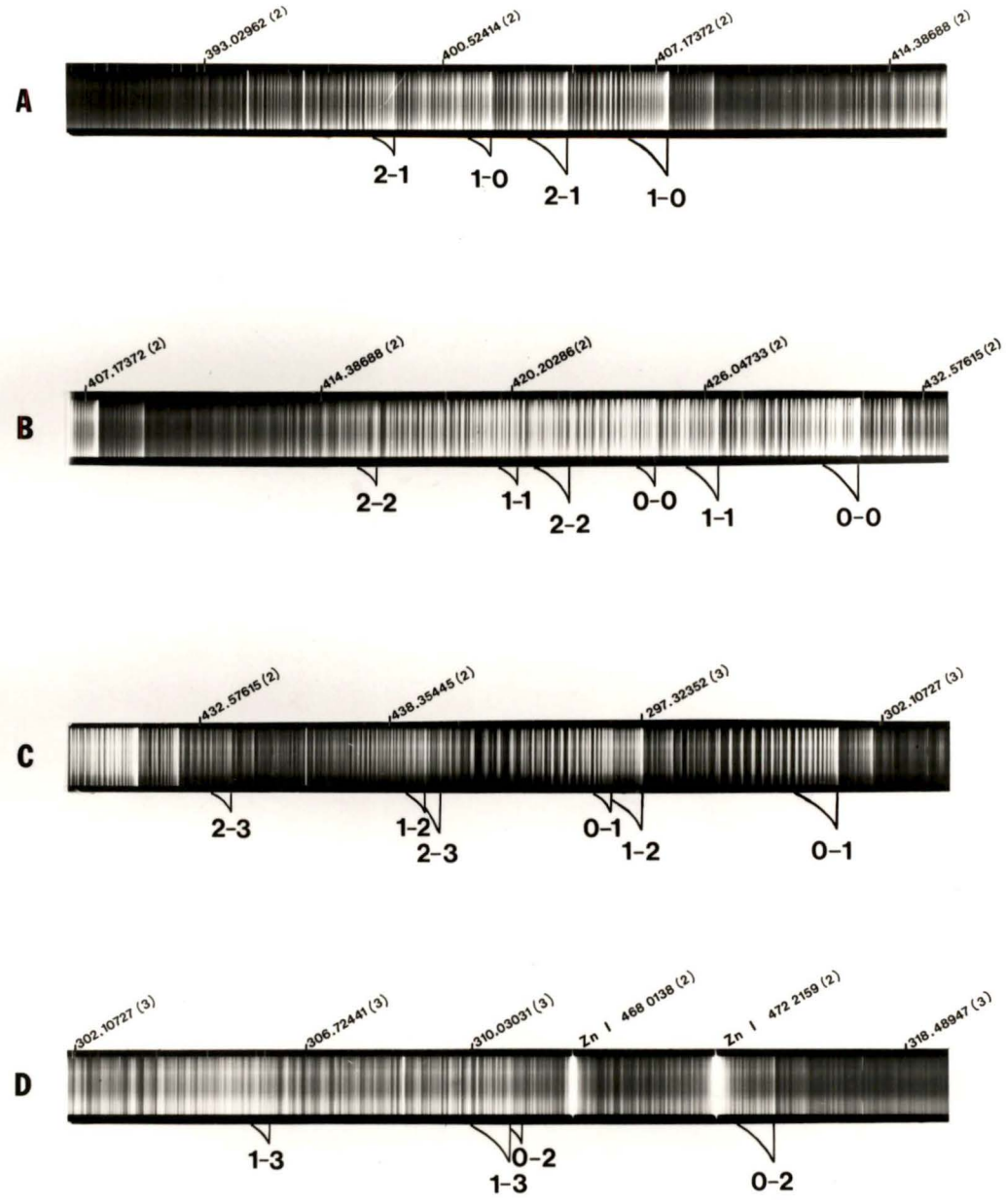

FIGURE 10. The emission spectrum of ZnD, recorded on Ilford HP5 film in the 2nd order of an 1180 g/mm grating. Fe/Ne reference line positions (air wavelengths) in nm, with orders in parentheses. Because of the different slit widths and exposure times, the intensities of the different regions cannot be compared. Molecular spectrum in 2nd order.

$\searrow\!\!\!\!\searrow = {}^2\Pi_{1/2} - {}^2\Sigma^+ \; {}^pQ_{12}$ head; $\searrow = {}^2\Pi_{3/2} - {}^2\Sigma^+ \; Q_2$ head.

	Slit width	Exposure time
A,B	20 μm	5 h, 25 m
C	20 μm	3 h
D	30 μm	11 h, 45 m

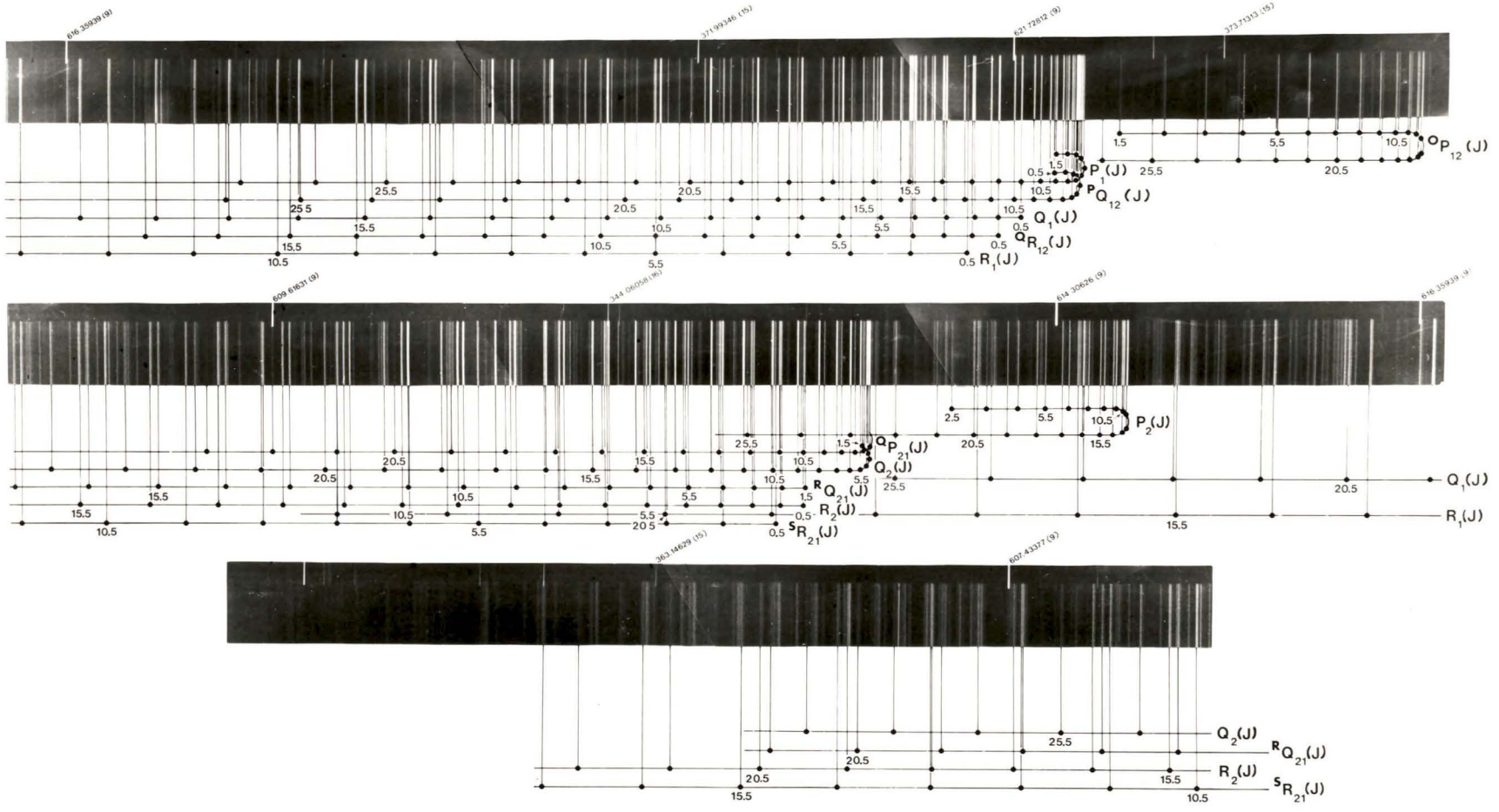

FIGURE 11. The $A^2\Pi - X^2\Sigma^+$ 0-0 band of ZnD: rotational analysis. Fe/Ne refererence line positions (air wavelengths) in nm, with orders in parentheses. Molecular spectrum in 13^{th} order.

rotational analysis below the spectrum in Fig. 11 and from the Fortrat diagram in Fig. 12.

The spectral lines were identified (assigned to branches and J values determined) using the usual methods described by Herzberg.[3] Considerable use was made of combination differences, both to check the analysis (by the constancy of the combination differences calculated from different lines or different bands) and to predict positions of lines not yet identified. The term value program (see below) calculated the differences between the calculated line positions (obtained from the term values) and the observed line positions, and these differences were useful for checking the line positions. This program was also useful for predicting the positions of new lines (provided the corresponding term values were already known from previously identified lines).

The analysis of the 0-0 band was, in general, in good agreement with that of Fujioka and Tanaka.[43] The individual line positions were mostly within ±0.5 cm^{-1} of those of Fujioka and Tanaka. However, a number of the lines with low J values have been reassigned.

The line positions are listed in Table II.

Term values were calculated using a computer program based on the least - squares method described by Aslund.[65] A consequence of the parity selection rule (equation (11)) is that two interleaving, but non - interconnecting, sets of term values are obtained. Since they are not connected

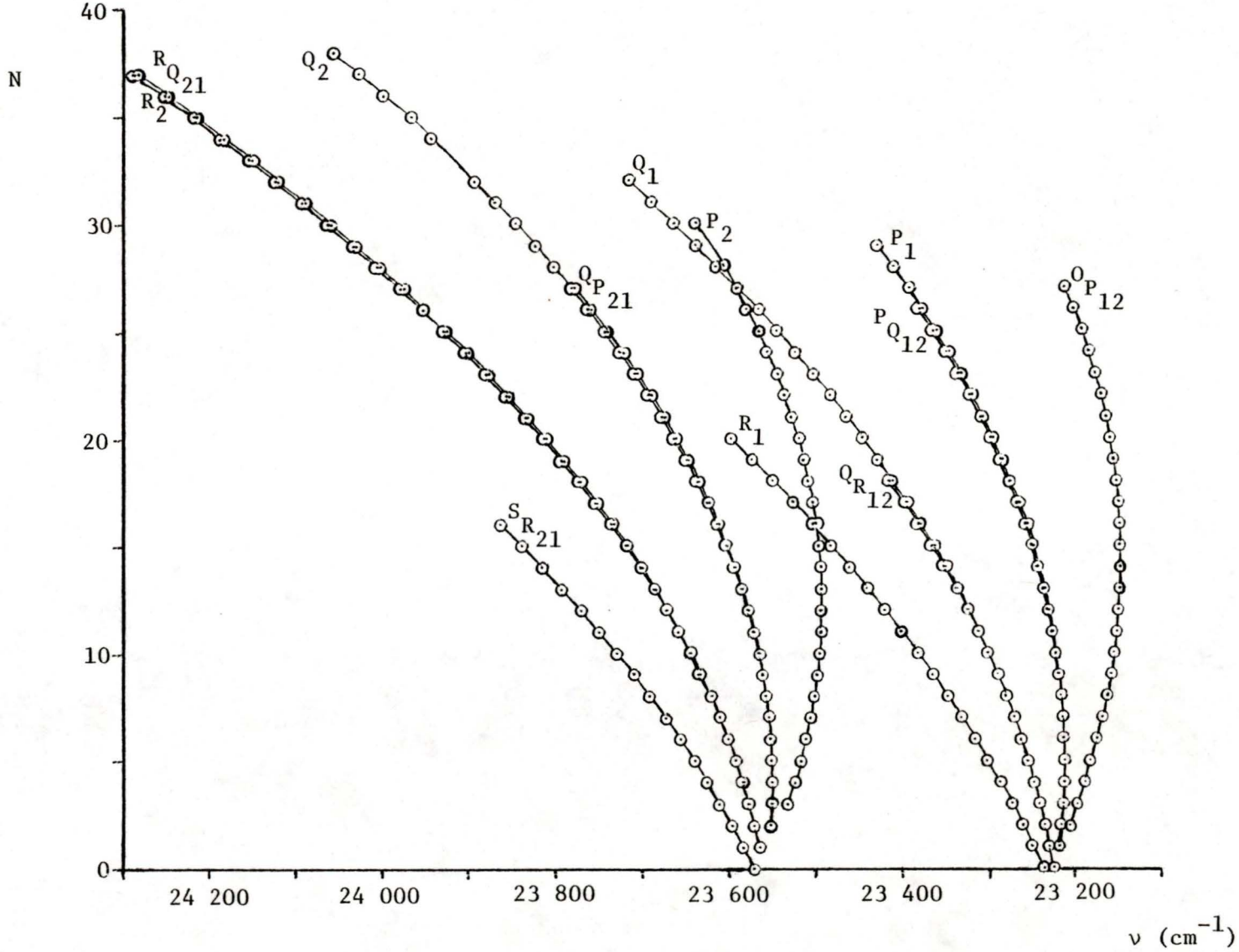

FIGURE 12. Fortrat diagram of the A $^2\Pi$ - X $^2\Sigma^+$ 0-0 band of ZnD.

TABLE II. (Following pages). Line positions (in cm^{-1}) of the A $^2\Pi$ - X $^2\Sigma^+$ system of ^{64}ZnD.

TABLE II: 0-0 band.

N	R_1	Q_1	P_1	R_2	Q_2	P_2
0.0	23235.38	23224.47[a]				
1.0	23247.05	23229.00	23217.60[b]	23563.30		
2.0	23259.29	23234.02	23215.20	23568.76	23549.89	(c)
3.0	23272.23	23239.76	23213.29	23575.16	23548.75	23525.35
4.0	23285.92	23246.20	23212.30	23582.38	23548.40	23522.34
5.0	23300.24	23253.31	23211.95	23590.46	23549.02	23516.10
6.0	23315.23	23261.11	23212.30	23599.38	23550.43	23509.33
7.0	23330.89	23269.59	23213.29	23609.16	23552.71	23503.30
8.0	23347.21	23278.75	23215.02	23619.76	23555.84	23496.47
9.0	23364.21	23288.66	23217.44	23631.20	23559.84	23490.01
10.0	23381.87	23299.19	23220.57	23643.49	23564.70	23483.43
11.0	23400.18	23310.45	23224.47	23656.63	23570.41	23491.77
12.0	23419.17	23322.38	23229.00	23670.58	23577.02	23491.07
13.0	23438.81	23335.00	23234.36	23685.26	23584.43	23491.37
14.0	23459.13	23348.34	23240.42	23700.86	23592.73	23499.15
15.0	23480.13	23362.37	23247.26	23717.23	23601.59	23494.37
16.0	23501.77	23377.11	23254.81	23734.45	23611.92	23490.20
17.0	23524.08	23392.57	23263.09	23752.57	23622.83	23500.24
18.0	23547.06	23408.73	23272.23	23771.45	23634.57	23509.31
19.0	23570.73	23425.61	23282.10	23791.20	23647.26	23513.33
20.0	23595.10	23443.23	23292.75	23811.71	23660.77	23517.39
21.0		23461.56	23304.16	23832.97	23675.16	23524.04
22.0		23480.63	23316.45	23855.10	23690.33	23533.15
23.0		23500.46	23329.47	23877.80	23706.45	23542.44
24.0		23521.02	23343.35	23901.60	23723.51	23552.71
25.0		23542.44	23357.94	23925.96	23741.36	23563.93
26.0		23563.93	23373.39	23951.52	23760.17	23576.15
27.0		23587.20	23389.75	23977.82	23779.97	23588.36
28.0		23610.39	23407.07	24004.83	23800.33	23603.23
29.0		23635.35	23425.22	24032.77	23821.95	
30.0		23660.59		24061.54	23843.90	23638.35
31.0		23686.58		24091.02	23867.36	
32.0		23713.50		24121.34	23891.43	
33.0				24152.56		
34.0				24185.07	23942.03	
35.0				24217.15	23969.53	
36.0				24251.31	23996.95	
37.0				24285.96	24025.41	
38.0					24054.77	

Notes: (a) This is the $Q_{f1}(\frac{1}{2})$ of Schadee (89).

(b) This is the $P_{f1}(\frac{3}{2})$ of Schadee.

(c) Our $P_2(2)$, not measured, is the $Q_{f2}(\frac{1}{2})$ of Schadee.

TABLE II (cont.): 0-0 band.

N	$Q_{R_{12}}$	$P_{Q_{12}}$	$O_{P_{12}}$	$S_{R_{21}}$	$R_{Q_{21}}$	$Q_{P_{21}}$
0.0				23569.79		
1.0	23229.30	23217.41(d)		23581.83	23562.99	
2.0	23234.36	23215.50	23204.67	23594.83	23564.44	23542.59
3.0	23240.31	23213.37	23195.80	23608.63	23574.69	23543.40
4.0	23246.77	23212.23	23187.64	23623.25	23581.85	23547.88
5.0	23254.02	23212.63	23180.18	23638.70	23589.75	23548.40
6.0	23261.94	23213.03	23173.44	23654.98	23598.54	23549.59
7.0	23270.55	23214.23	23167.38	23672.15	23608.19	23551.75
8.0	23279.85	23216.03	23162.06	23690.01	23618.66	23554.79
9.0	23289.84	23218.64	23157.45	23709.19	23629.99	23558.62
10.0	23300.55	23221.91	23153.58	23728.15	23642.18	23563.30
11.0	23311.91	23225.92	23150.46	23748.48	23655.11	23568.90
12.0	23323.98	23230.62	23148.12	23769.57	23669.00	23575.38
13.0	23336.73	23236.07	23146.46	23791.48	23683.56	23582.68
14.0	23350.16	23242.25	23145.57	23814.13	23699.04	23590.88
15.0	23364.21	23249.13	23145.57	23837.66	23715.33	23599.95
16.0	23379.19	23256.86	23146.23	23861.88	23732.46	23609.83
17.0	23394.75	23265.29	23147.70		23750.43	23620.67
18.0	23411.00	23274.45	23149.96		23769.25	23632.31
19.0		23284.43	23153.06		23788.76	23644.93
20.0		23295.21	23156.92		23808.99	23658.26
21.0		23306.76	23161.77		23830.44	23672.15
22.0		23319.11	23167.38		23852.06	23687.03
23.0		23332.25	23173.69		23875.01	23703.54
24.0		23346.23	23181.04		23898.53	23720.37
25.0		23361.03	23189.20		23923.15	23738.14
26.0		23376.95	23198.23			23756.60
27.0			23208.17		23974.63	23776.33
28.0					24001.45	
29.0					24029.40	
30.0					24058.29	
31.0					24087.53	
32.0					24118.20	
33.0					24149.02	
34.0					24180.86	
35.0					24213.67	
36.0					24247.50	
37.0					24282.96	

Note: (d) This is the $P_{f2}(3/2)$ of Schadee.

TABLE II (cont.): 0-1 band.

N	R_1	Q_1	P_1	R_2	Q_2	P_2
0.0		22134.57				
1.0	22157.60	22139.14	22128.02	22473.53		
2.0	22170.09	22144.68	22125.98	22479.64	22460.61	
3.0	22183.63	22151.13	22124.61	22486.53	22460.12	22441.48
4.0	22198.15	22158.42	22124.61	22494.67	22460.61	22434.15
5.0	22213.59	22166.67	22125.28	22503.87	22462.24	22428.27
6.0	22229.87	22175.81	22126.70	22514.07	22464.91	22423.69
7.0	22246.96	22185.79	22129.42	22525.10	22468.72	22419.76
8.0	22265.11	22196.64	22132.87	22537.64	22473.53	22417.15
9.0	22284.03	22208.55	22137.24		22479.64	22415.66
10.0	22303.85	22221.24	22142.61	22565.46	22486.53	22415.25
11.0	22324.60	22234.89	22148.87	22580.91	22494.67	22416.01
12.0	22346.20	22249.32	22156.11	22597.43	22503.87	22417.68
13.0	22368.72	22265.11	22164.30	22615.05	22514.07	22420.63
14.0	22392.06	22281.37	22173.43	22633.59		22424.77
15.0	22416.25	22298.60	22183.63	22653.44	22538.02	22430.02
16.0	22441.47	22316.86	22194.62	22674.20		22436.34
17.0	22467.56	22336.07	22206.70	22695.91	22566.14	22443.79
18.0	22494.67	22356.18	22219.75	22718.76	22581.93	22452.56
19.0	22522.45	22377.30	22233.88	22742.70	22598.79	22462.24
20.0	22551.24	22399.35	22248.95	22767.37	22616.73	
21.0	22580.91	22422.34	22265.11	22793.52	22635.74	22485.47
22.0	22611.49	22446.40	22282.13	22820.37	22655.85	
23.0	22643.00	22471.15	22300.43	22848.46	22677.15	
24.0	22675.63	22497.29	22319.67	22877.78	22699.47	22528.56
25.0		22524.30	22340.07	22908.04	22723.16	22545.65
26.0		22552.06	22361.52	22939.11	22747.98	
27.0		22581.21	22383.85	22971.68	22773.67	22583.04
28.0		22611.49	22407.69	23005.32	22800.61	22603.70
29.0		22642.51	22432.58		22828.72	22625.36
30.0		22674.50	22458.50		22858.02	22648.59
31.0		22707.99			22888.18	
32.0					22920.28	22698.10
33.0		22852.59			22953.36	
34.0					22987.54	22752.53

TABLE II (cont.): 0-1 band.

N	$Q_{R_{12}}$	$P_{Q_{12}}$	$O_{P_{12}}$	$S_{R_{21}}$	$R_{Q_{21}}$	$Q_{P_{21}}$
0.0				22580.11		
1.0				22491.97		
2.0	22145.30		22115.38	22505.51	22479.15	
3.0	22151.53	22125.28	22107.09	22520.01	22486.08	
4.0	22158.92	22124.96	22099.76	22535.45	22493.96	22460.12
5.0	22167.25	22125.98	22093.46	22552.06	22503.05	22461.54
6.0	22176.43	22127.81	22087.97	22569.58	22513.03	22464.27
7.0	22186.96	22130.26	22083.42	22588.13	22524.30	22467.56
8.0		22133.86	22079.82	22607.86	22536.39	22472.59
9.0	22209.54	22138.33	22077.12	22628.48	22549.80	22478.45
10.0	22222.33	22143.88	22075.53	22650.19	22564.13	22485.47
11.0	22236.14	22150.31	22074.35	22672.88	22579.57	22493.54
12.0		22157.60	22075.53	22696.65	22595.95	22502.42
13.0	22266.54	22165.87	22076.11	22721.34	22613.60	22512.66
14.0	22282.94	22175.12	22078.23	22747.10	22632.12	
15.0	22300.43	22185.37	22081.57	22773.67	22651.59	
16.0	22318.78		22085.77	22801.39	22672.24	
17.0	22338.11	22208.55	22090.94	22830.20	22693.87	
18.0	22358.33	22221.70	22097.29	22859.91	22716.70	
19.0	22379.51	22236.14	22104.53	22890.58	22740.40	
20.0	22401.59	22251.28	22112.90	22922.23	22765.08	
21.0	22424.77	22267.40	22122.29	22955.02	22791.13	
22.0	22448.86				22817.99	
23.0		22303.03			22845.88	
24.0		22322.46			22875.02	
25.0		22342.82			22904.98	
26.0					22936.43	
27.0					22968.63	
28.0					23002.18	

TABLE II (cont.): 0-2 band.

N	R_1	Q_1	P_1	R_2	Q_2	P_2
0.0	21112.93	21102.03				
1.0	21124.88	21106.94				
2.0	21138.27	21112.93	21094.27		21428.93	
3.0	21152.43	21120.02			21428.93	21410.16
4.0		21128.26		21464.33	21430.39	21404.30
5.0	21184.48	21137.61	21096.15	21474.55	21433.13	
6.0	21202.21	21148.10	21099.21	21486.20	21437.24	
7.0	21220.97	21159.76	21103.37	21498.97	21442.62	21393.61
8.0	21240.86		21108.68		21449.32	21392.91
9.0	21261.85	21186.41	21115.13	21528.68	21457.47	21393.61
10.0	21284.04	21201.47	21122.86	21545.60	21466.72	21395.43
11.0	21307.34	21217.65	21131.69	21563.55	21477.44	21398.86
12.0	21331.65	21234.97	21141.69	21582.89	21489.38	21403.38
13.0		21253.54	21152.99	21603.59	21502.61	21409.39
14.0	21383.96	21273.21		21625.45	21517.34	21416.78
15.0		21294.09	21179.01	21648.69	21533.32	21425.50
16.0		21316.12	21193.95		21550.62	21435.62
17.0		21339.37	21210.01		21569.45	21447.20
18.0	21502.08		21227.37	21726.28	21589.42	
19.0	21534.66	21389.48	21245.98	21754.60	21610.76	
20.0	21568.26	21416.26	21265.95		21633.51	
21.0		21444.45	21287.19		21657.74	
22.0	21639.09	21473.88	21309.67		21683.20	
23.0		21504.35	21333.49		21710.06	
24.0		21536.26			21738.65	
25.0					21768.22	

TABLE II (cont.): 0-2 band.

N	$^{Q}R_{12}$	$^{P}Q_{12}$	$^{O}P_{12}$	$^{S}R_{21}$	$^{R}Q_{21}$	$^{Q}P_{21}$
0.0				21447.20		
1.0				21459.98	21440.91	
2.0			21083.48	21473.88	21447.40	
3.0		21094.27	21075.92	21488.87	21455.11	21428.93
4.0		21094.97	21069.54	21505.08	21465.82	21430.39
5.0	21138.27	21096.83	21064.36	21522.96	21473.86	21432.66
6.0	21148.37	21099.96	21060.36	21541.62	21485.45	21436.42
7.0	21160.56	21104.23	21057.39	21562.26	21498.20	21441.65
8.0		21109.56	21055.67		21512.41	21448.33
9.0		21116.23	21055.06		21527.71	21456.28
10.0	21202.85	21124.03	21055.67		21544.30	21465.49
11.0	21218.78	21132.98	21057.39		21562.26	21476.05
12.0	21236.34	21143.13	21060.36		21581.60	21488.01
13.0	21254.91	21154.43	21064.73		21602.03	21501.25
14.0	21274.82		21070.29		21623.83	21515.70
15.0	21295.76	21180.64	21076.99		21646.96	21531.77
16.0	21317.90	21195.76	21084.98		21671.36	21548.81
17.0	21341.32	21212.00				21567.56
18.0		21229.52				
19.0		21248.14				
20.0		21268.10				
21.0		21289.40				
22.0		21311.95				
23.0		21336.00				

TABLE II (cont.): 1-0 band.

N	R_1	Q_1	P_1	R_2	Q_2	P_2
0.0	24555.22	24544.42				
1.0	24566.67	24548.82		24882.76		
2.0	24578.19	24553.63		24887.93		
3.0	24590.44	24558.57		24893.33		24849.45
4.0	24603.19	24564.37		24900.19	24867.02	24841.40
5.0	24616.53	24570.53	24530.05	24906.71	24867.02	24833.00
6.0	24630.07	24577.26	24529.45	24914.92	24867.02	24826.32
7.0	24644.37	24584.42	24529.45	24923.47	24868.20	24820.05
8.0	24659.37	24592.17	24530.05	24932.89	24869.98	24814.88
9.0	24674.32	24600.47	24530.58	24942.18	24872.60	
10.0	24690.11	24609.23	24532.27	24952.80	24875.68	
11.0	24706.23	24618.48	24534.45	24963.90	24879.52	24802.34
12.0	24722.97	24628.42	24537.46	24975.57	24884.19	24800.06
13.0	24740.24	24638.69	24540.60	24988.14	24889.39	24798.40
14.0	24757.91	24649.48	24544.42	25000.96	24895.47	24796.98
15.0	24776.14	24661.02	24548.82	25014.71	24902.25	24796.98
16.0	24794.94	24672.98	24553.63	25029.13	24909.24	24796.93
17.0	24814.18	24685.44	24559.18	25044.07	24917.39	
18.0	24833.86	24698.42	24565.30		24926.23	
19.0		24712.06	24572.24	25076.13	24935.56	
20.0		24726.40	24579.57	25092.43	24945.65	
21.0		24741.00	24587.60	25110.60	24956.32	
22.0		24756.33	24596.18	25128.72	24967.78	
23.0		24772.11	24605.49	25147.37	24979.94	
24.0		24788.62	24615.53		24993.20	
25.0		24805.38	24625.98		25006.74	
26.0		24823.14			25022.30	
27.0		24841.40				
28.0		24860.14				
29.0		24879.52				
30.0		24899.70				
31.0		24920.44				

TABLE II (cont.): 1-0 band.

N	$^{Q}R_{12}$	$^{P}Q_{12}$	$^{O}P_{12}$	$^{S}R_{21}$	$^{R}Q_{21}$	$^{Q}P_{21}$
0.0				24889.39		
1.0				24901.16	24832.76	
2.0		24535.26	24524.82	24913.16	24887.93	
3.0		24533.10	24515.78	24926.23	24892.59	
4.0		24531.66	24507.09	24940.17		
5.0	24571.25	24530.58	24499.01	24954.34	24905.92	
6.0	24578.19	24530.58	24491.51	24969.24	24914.07	
7.0	24585.26	24530.58	24484.55	24984.89	24922.50	
8.0	24593.27	24530.58	24478.06	25000.96	24931.63	24869.23
9.0	24601.79	24531.66	24472.22	25017.98	24941.29	24871.56
10.0	24610.62	24533.67	24466.95		24951.53	24874.59
11.0	24620.00	24536.14	24462.15	25053.73	24962.59	24878.10
12.0	24630.07	24538.93	24458.12		24974.00	24882.76
13.0	24640.36	24542.29	24454.48		24986.50	24887.93
14.0	24651.15	24546.19	24451.57		24999.48	
15.0	24662.92	24550.74	24449.16		25012.82	
16.0	24675.06	24555.74	24447.38		25026.89	
17.0	24687.63	24561.46	24446.36		25041.97	
18.0	24700.77	24567.75	24445.76		25057.48	
19.0	24714.56	24574.60	24445.76		25073.60	
20.0	24728.74	24582.09			25089.96	
21.0		24590.44				

TABLE II (cont.): 1-1 band.

N	R_1	Q_1	P_1	R_2	Q_2	P_2
0.0		23454.52				
1.0	23476.93	23458.92				
2.0	23488.79	23464.17	23445.71			
3.0	23501.93	23470.10	23444.17	23804.94	23779.22	
4.0	23515.49	23476.49	23443.48		23779.22	
5.0	23529.80	23483.90	23443.48	23820.25	23779.97	23740.43
6.0	23544.66	23491.95	23444.01	23829.59	23781.73	23741.18
7.0	23560.02	23500.48	23445.48	23839.40	23784.33	23736.64
8.0	23576.96	23509.99	23447.89	23850.67	23787.94	23732.84
9.0	23594.04	23520.23	23450.48	23862.08	23792.37	23729.94
10.0	23612.17	23531.29	23454.52	23874.65	23797.72	23728.15
11.0	23630.78	23542.99	23459.13	23888.02	23803.98	23727.18
12.0	23649.92	23555.45		23902.37	23811.06	23727.18
13.0	23670.35	23568.57	23470.50	23917.67	23819.34	23728.04
14.0	23690.85	23582.55	23477.23	23933.52	23828.44	23729.94
15.0	23712.42	23597.13	23484.99	23950.79	23838.27	23732.84
16.0		23612.63	23493.46	23968.73	23849.08	23736.64
17.0	23757.63	23629.06	23502.81	23987.32	23860.76	23741.36
18.0	23781.57	23645.96	23512.79	24006.92	23873.45	23747.07
19.0	23805.71	23663.80	23523.80	24027.33		23753.61
20.0	23831.03	23682.45	23535.62	24048.73		23761.49
21.0	23856.89	23701.71	23548.40	24071.09		
22.0	23883.68	23722.06	23561.80	24094.08		
23.0		23743.02		24118.20		
24.0		23764.82		24143.25		
25.0				24168.90		
26.0		23811.26		24195.65		
27.0		23835.45		24223.14		
28.0				24251.31		
29.0				24281.07		
30.0				24311.39		
31.0						

TABLE II (cont.): 1-1 band.

N	$^{Q}R_{12}$	$^{P}Q_{12}$	$^{O}P_{12}$	$^{S}R_{21}$	$^{R}Q_{21}$	$^{Q}P_{21}$
0.0				23799.27		
1.0				23811.31	23792.89	
2.0				23824.11	23798.38	
3.0				23838.38	23804.11	
4.0	23477.04		23419.17	23852.32	23811.71	
5.0	23484.49	23444.01	23412.50	23867.56	23819.84	23779.22
6.0	23492.72	23445.00	23406.06	23883.68	23828.64	23781.02
7.0	23501.45	23446.50	23400.87	23901.14	23838.65	23783.40
8.0	23511.15	23448.72	23395.89	23918.88		23786.81
9.0	23521.51	23451.85	23392.23	23937.76		23791.48
10.0	23532.49	23455.71	23388.87	23957.28		23796.50
11.0	23544.41	23460.42	23386.43	23977.82		23802.50
12.0	23556.92	23465.71	23385.04	23999.13		23809.74
13.0		23472.02	23384.29	24021.39		23817.77
14.0		23479.06	23384.29	24044.50		23826.52
15.0		23486.74	23385.04	24068.53		23836.52
16.0		23495.50	23386.43	24092.81		23846.97
17.0			23389.75	24118.20		
18.0				24144.30		23871.03
19.0		23526.01	23397.46	24172.01		23884.73
20.0		23538.03	23402.86	24200.09		
21.0			23408.53			23914.19
22.0			23415.84	24258.42		
23.0		23579.13	23423.86			
24.0		23594.80	23432.91	24320.16		
25.0						
26.0		23628.66				

TABLE II (cont.): 1-2 band.

N	R_1	Q_1	P_1	R_2	Q_2	P_2
0.0	22432.58					
1.0	22444.46	22426.90		22760.92		
2.0	22457.16	22432.58		22766.81	22748.58	
3.0	22470.99	22439.04		22773.67	22747.98	
4.0	22485.47	22446.40		22782.00	22748.58	
5.0	22500.83	22454.93	22414.30	22791.13	22751.04	
6.0	22517.24	22464.27		22801.84	22754.05	22713.49
7.0	22534.62	22474.57	22419.76	22813.54	22758.22	22710.37
8.0	22552.85	22486.08	22423.69	22826.42	22763.82	22708.55
9.0	22572.20	22498.32	22428.78	22839.80	22770.63	22707.99
10.0	22592.60	22511.59	22434.91	22854.97	22777.99	22708.55
11.0	22613.60	22525.80	22441.97	22871.00	22786.84	22710.03
12.0	22635.74	22541.12	22450.15	22888.18	22796.91	22712.59
13.0	22658.84	22557.37	22459.26	22906.42	22807.96	22716.70
14.0	22682.86	22574.59	22469.34	22925.74	22820.37	22721.91
15.0	22707.99	22592.76	22480.50	22946.34	22833.74	22728.38
16.0	22733.95	22612.07	22493.01	22967.89	22848.23	22735.98
17.0	22760.92	22632.32	22506.23	22990.69	22864.17	22744.83
18.0	22789.04	22653.61	22520.69	23014.58	22881.10	
19.0	22817.99	22676.00	22536.39	23039.57	22899.25	
20.0	22847.99	22699.47	22552.85	23065.48	22918.58	
21.0	22879.01	22723.94	22570.64	23093.01	22939.11	22792.37
22.0	22911.01	22749.34	22589.52	23121.66	22960.85	22807.03
23.0	22944.11	22776.10	22609.60	23151.59	22983.81	22823.88
24.0	22978.27	22803.78	22630.86	23182.77	23008.00	22841.56
25.0		22832.54	22653.44		23033.50	22860.34
26.0	23050.12	22862.98	22677.15		23060.02	
27.0	23087.84	22893.78	22701.67		23088.24	22902.33
28.0		22926.38			23117.46	
29.0		22960.05				22949.71
30.0		22994.86				22975.59

TABLE II (cont.): 1-2 band.

N	$^{Q}R_{12}$	$^{P}Q_{12}$	$^{O}P_{12}$	$^{S}R_{21}$	$^{R}Q_{21}$	$^{Q}P_{21}$
0.0				22766.81		
1.0				22779.01		
2.0			22403.68	22792.37		
3.0			22395.90	22806.55		
4.0			22389.13	22822.13	22781.64	
5.0			22383.30	22838.89	22790.82	
6.0	22464.91		22378.46	22856.24	22801.39	
7.0	22475.41	22420.63	22374.61	22875.02	22812.69	22757.59
8.0	22487.02	22424.77	22371.86	22894.81	22825.31	22762.82
9.0	22499.33	22430.02	22369.74	22915.79	22838.89	22769.25
10.0	22512.66	22436.15			22853.76	22776.83
11.0	22527.11	22443.31		22960.95	22869.71	22785.64
12.0	22542.52	22451.48	22370.57	22985.02	22886.74	22795.47
13.0	22558.85	22460.61	22372.86	23010.21	22904.98	22806.55
14.0	22576.18	22471.15	22376.34	23036.45	22924.20	22818.64
15.0	22594.56	22482.39	22380.92	23063.83	22944.59	22832.19
16.0	22613.86	22494.67	22386.27	23092.29	22966.13	
17.0	22634.08	22508.15	22393.02	23121.66	22988.76	22862.35
18.0	22655.35	22522.78	22400.76		23012.62	22879.01
19.0	22678.07	22538.32	22409.89		23037.49	22897.18
20.0	22701.67	22555.11				22916.30
21.0	22726.25	22572.94				22936.73
22.0		22592.00			23119.13	22958.50
23.0		22612.07				
24.0		22633.59				
25.0		22655.85				
26.0		22679.56				
27.0		22704.47				
28.0		22730.72				

TABLE II (cont.): 1-3 band.

N	R_1	Q_1	P_1	R_2	Q_2	P_2
0.0		21453.73				
1.0	21476.03	21458.11				
2.0		21463.82		21797.78	21779.63	
3.0	21502.01	21470.44		21805.11	21779.63	21761.01
4.0	21518.08	21479.06	21446.01	21814.53	21781.44	
5.0	21534.66	21488.87	21448.33	21825.35		
6.0	21552.52	21499.79	21452.07	21837.39	21789.35	21749.02
7.0	21571.90	21511.90	21456.90	21850.88	21795.44	21747.99
8.0		21525.25	21462.91	21865.54	21802.57	21747.99
9.0		21539.82	21470.44	21881.23	21811.82	21749.40
10.0	21636.54	21555.69	21479.06	21898.92	21821.94	
11.0	21660.49	21572.73	21488.87	21917.71	21833.58	21756.73
12.0	21685.75	21591.12	21500.11	21938.15	21846.70	21762.46
13.0	21712.46	21610.76	21512.51	21959.70	21861.19	21769.96
14.0	21740.10	21631.61	21526.31	21982.47	21876.99	21778.74
15.0	21769.17	21653.70	21541.62	22007.26	21894.76	21789.36
16.0	21799.26	21677.21	21557.95	22033.01	21913.33	21800.79
17.0	21830.54	21702.14	21575.96	22060.54		
18.0	21863.34	21728.13	21595.01		21955.24	
19.0	21897.69	21755.49	21615.48		21978.30	
20.0		21734.49	21637.58		22003.13	
21.0	21969.64	21814.53	21661.08		22029.56	
22.0	22007.63	21846.03	21685.75			
23.0	22046.96	21879.04	21712.46			
24.0		21913.33				
25.0		21949.21				
26.0		21986.65				
27.0		22025.56				
28.0		22066.03				

TABLE II (cont.): 1-3 band.

N	$^{Q}R_{12}$	$^{P}Q_{12}$	$^{O}P_{12}$	$^{S}R_{21}$	$^{R}Q_{21}$	$^{Q}P_{21}$
1.0	21458.11					
2.0	21463.32	21445.14	21434.36	21823.12	21797.75	
3.0	21470.65	21445.14	21427.35	21838.58		
4.0	21479.59	21446.36	21421.69	21854.95	21814.17	
5.0	21489.38	21449.00	21417.29	21872.43	21824.80	
6.0	21500.53	21452.60	21413.77		21836.41	
7.0	21512.99	21457.47	21411.72	21912.12	21849.94	
8.0	21526.31	21463.32	21411.01	21934.37	21864.54	
9.0	21540.93	21471.23	21411.72		21880.54	21810.78
10.0	21556.60	21480.08	21413.09		21897.69	
11.0	21573.75	21490.06	21416.26	22007.63	21916.69	21832.16
12.0		21501.25	21420.53	22035.10	21936.69	21845.28
13.0	21611.97	21513.92	21426.21	22063.71	21958.48	
14.0		21527.71	21433.13		21981.21	21875.55
15.0	21655.33	21543.15	21441.65		22005.83	
16.0	21678.74	21559.69	21450.98		22031.35	
17.0	21704.01	21577.64				
18.0	21729.89	21596.87				21953.44
19.0		21617.65				
20.0		21639.79				22001.13

TABLE II (cont.): 2-1 band.

N	R_1	Q_1	P_1	R_2	Q_2	P_2
0.0						
1.0				25071.90		
2.0	24766.93	24742.76		25077.01	25058.92	
3.0	24779.24	24747.89		25082.48	25057.48	
4.0	24791.81	24753.53		25089.38	25056.79	
5.0	24805.04	24759.91		25096.35	25056.79	
6.0	24818.83	24766.93		25104.40		
7.0	24833.00	24774.37		25112.98	25058.92	
8.0	24848.00	24782.39		25122.44	25061.33	25007.65
9.0	24863.29	24790.92		25132.32	25064.09	25003.35
10.0		24800.06	24725.29	25142.94	25067.90	25000.22
11.0		24809.80	24728.18	25154.56	25072.28	24997.37
12.0		24820.08	24731.62	25166.66	25077.42	24995.04
13.0	24930.48	24831.07	24735.56	25179.41	25083.25	24994.36
14.0	24948.62	24842.47	24740.24	25192.99	25089.96	
15.0	24967.26	24854.41	24745.36	25207.13	25097.28	24994.36
16.0			24751.28	25222.19	25105.36	24995.04
17.0		24880.41		25237.67	25114.12	
18.0		24894.29	24764.95	25253.92	25123.75	
19.0		24908.77	24772.80	25271.12	25134.06	
20.0		24923.55	24781.23	25288.65	25145.10	
21.0		24939.44	24790.26	25307.22	25157.02	
22.0		24955.81		25326.38	25169.55	
23.0		24972.74		25346.19	25182.94	
24.0		24990.26		25366.49	25197.24	
25.0		25008.59		25387.59	25211.93	
26.0		25027.63		25409.45	25227.70	
27.0		25047.31		25432.27	25243.98	
28.0		25067.34		25456.45		
29.0					25278.62	
30.0					25297.61	
31.0						
32.0						
33.0					25358.59	

TABLE II (cont.): 2-1 band.

N	$^{Q}R_{12}$	$^{P}Q_{12}$	$^{O}P_{12}$	$^{S}R_{21}$	$^{R}Q_{21}$	$^{Q}P_{21}$
0.0				25078.43		
1.0				25089.96	25071.90	
2.0				25101.97	25076.47	
3.0				25114.12	25082.01	
4.0			24697.85	25128.16	25088.66	
5.0			24690.11		25095.76	
6.0			24683.22	25157.02	25103.55	
7.0	24775.14		24676.80	25172.96	25112.07	
8.0	24783.35	24722.97	24671.34	25189.36	25121.35	25060.39
9.0	24791.81	24724.64	24665.70	25206.39	25131.26	25063.23
10.0	24801.42		24661.02	25223.78	25141.80	25066.72
11.0		24729.58	24657.38	25242.17	25153.30	25071.16
12.0	24821.68	24733.04	24653.75	25261.51	25165.23	25076.13
13.0		24737.16	24651.15	25280.66	25177.90	25082.01
14.0	24844.21	24741.73	24649.06	25300.81	25191.29	25088.66
15.0	24856.37	24747.22	24648.08	25321.71	25205.46	25095.76
16.0		24753.10	24647.05	25343.54	25220.32	25103.55
17.0		24759.28	24646.50	25365.61		25112.07
18.0		24766.93			25251.75	25121.55
19.0		24775.14		25411.99	25268.76	
20.0		24783.35				25142.94
21.0					25304.82	25154.56
22.0					25323.36	25166.86
23.0					25343.40	25180.07
24.0					25363.43	25194.44

TABLE II (cont.): 2-2 band.[a]

N	R_1	Q_1	P_1	R_2	Q_2	P_2
0.0	23710.89					
1.0						
2.0		23710.89	23692.14			
3.0	23746.25		23691.70			
4.0			23691.70	24058.58		
5.0		23731.19	23691.70	24067.32	24027.33	
6.0		23739.27	23692.93	24076.28		23990.59
7.0	23807.13	23743.28	23695.00	24086.08	24032.77	
8.0		23758.29	23697.70	24098.00	24037.00	
9.0				24110.03	24042.29	
10.0				24123.30	24048.21	23980.04
11.0	23878.58	23792.94			24055.04	23980.04
12.0		23805.71		24152.07	24063.43	23981.93
13.0		23819.60		24167.90	24071.84	23983.10
14.0		23834.53	23732.32		24082.03	
15.0	23962.78	23850.19	23741.10		24092.31	23989.70
16.0		23866.68			24104.43	23954.79
17.0		23883.68			24117.52	24000.37
18.0			23772.59		24131.15	
19.0		23921.16	23785.02		24145.03	24016.40
20.0		23940.71			24162.11	24025.41
21.0		23961.32				24035.97
22.0		23983.10				
23.0						24060.13

(a) Many of the lines in this band are missing, because they are overlapped by the more intense 0-0 and 1-1 lines.

TABLE II (cont.): 2-2 band.(a)

N	$^{Q}R_{12}$	$^{P}Q_{12}$	$^{O}P_{12}$	$^{S}R_{21}$	$^{R}Q_{21}$	$^{Q}P_{21}$
2.0					24044.50	
3.0		23691.70			24051.21	
4.0		23691.70			24058.88	
5.0		23692.15			24066.68	
6.0	23740.38	23693.55			24075.92	
7.0		23695.59			24086.11	24032.06
8.0		23698.85			24097.21	24035.97
9.0		23702.43			24109.00	
10.0					24122.21	
11.0	23793.95	23712.42			24135.93	
12.0	23807.13	23718.45			24150.64	
13.0					24166.44	24070.26
14.0	23836.32	23734.02				24080.52
15.0	23851.68	23742.80				24091.02
16.0		23752.36				
17.0		23762.68				
18.0		23774.67				

(a) Many of the lines in this band are missing, because they are overlapped by the more intense 0-0 and 1-1 lines.

TABLE II (cont.): 2-3 band.

N	R_1	Q_1	P_1	R_2	Q_2	P_2
0.0	22742.70	22732.97				
1.0	22754.05	22736.98				
2.0	22766.29	22742.00	22723.16	23075.79	23057.95	
3.0	22779.63	22748.58	22723.16	23082.81	23057.95	
4.0	22794.32	22756.28	22723.94	23091.52	23059.35	
5.0	22810.01	22765.08	22725.70	23101.20	23061.79	23029.37
6.0	22826.42	22774.32	22728.38	23111.97	23065.48	23025.71
7.0	22844.35	22785.04	22732.16	23124.01	23070.34	23023.66
8.0	22862.93	22797.51	22736.98	23137.29	23076.56	23022.79
9.0	22882.92	22810.55	22742.70	23151.59	23083.67	23022.79
10.0	22903.73	22824.61	22749.98	23167.32	23092.29	23024.57
11.0	22925.74	22839.80	22758.22	23184.09	23102.04	23027.13
12.0	22948.53	22855.93	22767.37	23202.09	23113.07	23031.05
13.0	22972.55	22873.07			23125.30	23036.45
14.0	22997.63	22891.51	22779.04		23138.78	23042.99
15.0	23023.85	22911.01	22801.84			23050.83
16.0	23050.82	22931.64	22815.68		23169.60	23060.32
17.0	23079.70	22953.36	22830.68		23187.04	
18.0	23108.92	22976.29	22846.83		23205.51	23082.48
19.0		23000.35	22864.17			23095.32
20.0		23025.71	22882.92			23110.12
21.0		23052.11	22902.99			23126.60
22.0		23079.70				23144.41
23.0		23108.70				23163.61
24.0						23184.09
25.0						23206.50

TABLE II (cont.): 2-3 band.

N	$Q_{R_{12}}$	$P_{Q_{12}}$	$O_{P_{12}}$	$S_{R_{21}}$	$R_{Q_{21}}$	$Q_{P_{21}}$
0.0				23076.36		
1.0	22736.93			23088.24		
2.0	22742.00		22713.86		23075.79	23057.95
3.0			22706.53	23115.09	23052.81	23057.95
4.0	22756.69	22724.44	22700.26	23130.67	23091.11	23058.77
5.0		22726.25	22695.22		23100.78	23061.27
6.0	22775.62	22729.03	22691.04	23165.10	23111.28	23064.83
7.0	22786.70	22732.97	22688.04	23184.09	23123.30	23069.40
8.0	22798.46	22737.92	22686.12	23204.60	23136.36	
9.0	22811.54	22743.92	22685.44			
10.0	22825.53	22751.04	22685.44		23166.32	
11.0	22840.90	22759.28	22686.93		23182.77	
12.0	22857.16	22768.65	22689.50		23200.82	
13.0	22874.60	22779.01	22693.24			
14.0	22893.00	22790.82	22698.10			
15.0	22912.53	22803.46	22704.12			
16.0	22933.33	22817.43	22711.22			
17.0	22955.02	22832.54	22719.81			
18.0	22978.04					
19.0	23002.18	22866.30				
20.0		22885.08				
21.0		22904.98				
22.0		22926.38				

to each other and have no common reference point, the two sets can be arbitrarily shifted relative to each other. In order to remove this arbitrariness--i.e. to find the actual relative positions of the two sets of energy levels in the molecule--the term values have to be fitted to a model of the energy levels in the molecule. This was done as follows. The members of each of the two sets in the $^2\Sigma^+$, v" = 0 state were fitted to the appropriate one of the formulas

$$F_1(N) = B_0^*N(N+1) - D_0N\ (N+1) + \frac{\gamma_0}{2} N \qquad ...(12a)$$

$$F_2(N) = B_0^*N(N+1) - D_0N\ (N+1) - \frac{\gamma_0}{2} (N+1) \qquad ...(12b)$$

(cf. equation (1)) using the method of least squares. (The values of B_0, D_0, and γ_0 had been determined prior to this by the methods to be described later, since these did not depend on the relative positions of the two sets of term values.) Despite this least - squares best - fitting method, the errors in differences between terms belonging to the different sets were considerably larger than those in differences between terms belonging to the same set. This is a problem typical of this method of establishing the term values. For example, analysis of the term values determined by Berg and Klynning[7] for the A $^2\Pi$ and X $^2\Sigma^+$ states of CaH showed the same problem. This problem has been discussed by Albritton et al.[66] A better placement of the two sets of term values relative to each other could probably have been achieved by fitting

all the term values to the appropriate energy formulas, rather than just the $^2\Sigma^+$, v" = 0 terms. Aslund[67] formerly used a more sophisticated least - squares fitting method than that employed here to adjust the two sets of terms relative to each other. A new method of evaluating the term values, devised by Aslund,[68] is claimed to avoid this problem.

The term values are listed in Table III.

The molecular constants were evaluated primarily by the traditional, graphical methods, using combination differences.[30],[3] These combination differences were evaluated from the term values, rather than from the spectral line positions. This method had the advantage that, for each constant to be determined, only one set of combination differences had to be calculated for each vibronic state, rather than evaluating several sets (one from each of the different ways in which each combination difference could be calculated from the spectral lines) then averaging. In the method employed, the averaging was done previously, during the determination of the term values.

III.B. Rotational Analysis

III.B.1. Rotational constants of the X $^2\Sigma^+$ state

The usual procedure for the evaluation of the rotational constants of the X $^2\Sigma^+$ state would be to calculate the

TABLE III. (A) Term values (in cm^{-1}) for the X $^2\Sigma^+$ state of ^{64}ZnD.

	v" = 0		v" = 1		v" = 2		v" = 3	
N	F_1	F_2	F_1	F_2	F_1	F_2	F_1	F_2
0.0	0.00		1089.93		2122.51		3090.71	
1.0	6.67	6.57	1096.30	1096.26	2128.69	2128.56	3097.24	3097.26
2.0	20.16	19.88	1109.45	1109.03	2141.21	2140.94	3110.03	3110.01
3.0	40.38	39.88	1128.94	1128.46	2159.88	2159.60	3128.23	3128.06
4.0	67.15	66.56	1154.94	1154.42	2184.93	2184.58	3152.38	3151.91
5.0	100.70	100.02	1187.36	1186.71	2216.31	2215.84	3182.30	3181.69
6.0	140.84	140.01	1226.26	1225.36	2253.85	2253.06	3218.46	3217.73
7.0	187.65	186.72	1271.56	1270.63	2297.51	2296.71	3260.22	3259.37
8.0	241.00	239.96	1323.19	1322.16	2347.35	2346.35	3308.11	3307.13
9.0	301.06	299.89	1381.30	1380.16	2403.35	2402.22	3361.75	3360.76
10.0	367.64	366.31	1445.65	1444.44	2465.34	2464.16	3421.22	3420.18
11.0	440.75	439.29	1516.33	1515.00	2533.51	2532.22	3486.56	3485.39
12.0	520.41	518.82	1593.41	1591.96	2607.77	2606.35	3557.72	3556.45
13.0	606.51	604.82	1676.54	1675.08	2687.94	2686.49	3634.48	3633.17
14.0	699.04	697.28	1766.10	1764.50	2774.13	2772.48	3717.11	3715.66
15.0	798.00	796.07	1861.76	1859.97	2866.23	2864.53	3805.14	3803.61
16.0	903.32	901.26	1963.54	1961.64	2964.25	2962.45	3899.07	3897.39
17.0	1014.94	1012.77	2071.40	2069.48	3068.05	3066.15	3998.26	3996.47
18.0	1132.83	1130.51	2185.35	2183.21	3177.67	3175.62	4103.28	4101.41
19.0	1256.83	1254.44	2305.19	2302.95	3292.92	3290.85	4213.56	4211.63
20.0	1387.13	1384.63	2431.02	2428.68	3413.96	3411.73	4329.07	4327.02
21.0	1523.41	1520.68	2562.61	2560.14	3540.43	3538.06	4449.85	4447.57
22.0	1665.80	1663.05	2700.15	2697.57	3672.63	3670.15	4576.18	4572.92
23.0	1813.97	1811.21	2843.15	2840.42	3809.97	3807.35	4707.09	4703.81
24.0	1968.30	1965.25	2991.97	2989.16	3953.13	3950.14	4843.54	4839.64
25.0	2128.11	2125.08	3146.08	3143.20	4100.72	4098.27	4984.16	4980.08
26.0	2294.12	2290.58	3305.88	3302.95	4254.50	4252.38	5130.55	
27.0	2465.30	2462.03	3471.23	3468.18	4412.82	4409.90	5281.10	
28.0	2642.25	2638.88	3641.57	3638.50	4575.96	4573.90	5436.31	
29.0	2824.66	2821.29	3817.50	3814.52		4741.61		
30.0	3011.87	3008.62	3998.16	3994.94	4916.71	4914.22		
31.0								
32.0	3404.00	3400.86		4372.06				

continued...

TABLE III (cont.). (B) Term values (in cm^{-1}) for the A $^2\Pi$ state of ^{64}ZnD.

	v' = 0				v' = 1			
N	F_{1e}	F_{1f}	F_{2f}	F_{2e}	F_{1e}	F_{1f}	F_{2f}	F_{2e}
0.0	23224.32	23224.50				24544.45		
1.0	23235.41	23235.58			24555.15	24555.39		
2.0	23253.72	23254.21	23569.77	23569.76	24573.24	24573.77	24889.48	24889.52
3.0	23279.49	23280.06	23588.61	23588.67	24598.32	24598.84	24907.87	24907.70
4.0	23312.61	23313.31	23615.03	23615.06	24630.69	24631.47	24933.17	24933.33
5.0	23353.07	23354.01	23648.94	23648.99	24670.39	24671.21	24966.51	24966.74
6.0	23400.92	23401.94	23690.44	23690.38	24717.12	24718.16	25006.94	25007.10
7.0	23456.04	23457.33	23739.34	23739.30	24771.00	24772.11	25054.97	25054.95
8.0	23518.51	23519.79	23795.82	23795.73	24832.08	24833.31	25110.17	25110.08
9.0	23588.23	23589.75	23859.68	23859.71	24900.24	24901.61	25172.69	25172.60
10.0	23665.24	23666.86	23931.02	23930.98	24975.45	24976.90	25242.19	25242.12
11.0	23749.47	23751.15	24009.78	24009.65	25057.80	25059.29	25319.09	25318.92
12.0	23840.90	23842.75	24095.85	24095.80	25147.08	25148.87	25403.18	25403.13
13.0	23939.53	23941.53	24189.35	24189.17	25243.46	25245.22	25494.42	25494.37
14.0	24045.28	24047.41	24290.07	24289.89	25346.80	25348.62	25592.94	25592.72
15.0	24158.16	24160.34	24398.07	24397.95	25457.04	25458.97	25698.25	25698.28
16.0	24278.07	24280.41	24513.32	24513.13	25574.21	25576.25	25810.86	25810.58
17.0	24405.04	24407.49	24635.76	24635.61	25698.24	25700.39	25930.35	25930.28
18.0	24538.99	24541.54	24765.34	24765.11	25829.07	25831.34	26056.84	26056.65
19.0	24679.89	24682.45	24902.00	24901.70	25966.73	25968.94	26190.22	26190.01
20.0	24827.55	24830.31	25045.58	25045.36	26111.03	26113.43	26330.40	26330.24
21.0	24982.22	24984.93	25196.17	25195.78	26262.03	26264.36	26477.19	26477.03
22.0	25143.45	25146.48	25353.71	25353.40	26419.50	26422.10	26631.21	26630.99
23.0	25311.63	25314.35	25518.01	25517.54	26583.83	26586.10	26791.76	26791.15
24.0	25486.10	25489.32	25689.00	25688.71	26754.10	26756.87	26958.69	26958.30
25.0	25667.49	25670.47	25866.87	25866.39	26931.65	26933.31	27132.66	27131.79
26.0	25855.02	25857.94	26051.14	26050.80	27114.43	27117.20	27312.17	27312.64
27.0	26049.26	26052.50	26242.16	26241.83	27304.62	27306.66	27498.60	27498.14
28.0		26253.06	26439.88	26439.19	27500.66	27502.34	27691.32	27691.36
29.0	26456.66	26460.01	26643.75	26643.24	27700.83	27704.18	27889.81	
30.0		26672.46	26854.06	26852.74		27911.57	28095.59	
31.0			27070.16				28306.33	
32.0		27117.50		27292.34				
33.0			27522.20					
34.0				27757.21				
35.0			27999.65					

continued...

TABLE III. (B) (cont.)

N	v' = 2			
	F_{1e}	F_{1f}	F_{2f}	F_{1e}
0.0		25823.68		
1.0	25833.41	25834.23		
2.0	25851.29	25852.03	26168.18	26167.96
3.0	25876.34		26185.06	26186.04
4.0	25908.00	25908.58	26211.02	26211.24
5.0	25946.75	25947.38	26243.60	26243.43
6.0	25992.37	25993.28	26283.07	26283.25
7.0	26045.05	26045.88	26329.81	26329.59
8.0	26104.62	26105.58	26383.53	26383.44
9.0	26171.13	26172.27	26444.54	26444.43
10.0	26244.63	26245.78	26512.39	26512.39
11.0	26325.00	26326.24	26587.43	26587.40
12.0	26412.18	26413.57	26669.52	26669.56
13.0	26506.29	26507.58	26758.55	26758.37
14.0	26607.13	26608.64	26854.43	26854.51
15.0	26714.77	26716.20	26957.37	26957.39
16.0	26828.96	26830.79	27067.11	27067.01
17.0	26950.22	26951.66	27183.85	27183.56
18.0	27077.90	27079.55	27307.18	27306.84
19.0	27212.09	27213.94	27437.14	27436.95
20.0	27352.75	27354.67	27574.06	27573.81
21.0	27499.30	27501.96	27717.33	27717.17
22.0	27649.92	27655.85	27867.42	27867.12
23.0		27815.84	28023.73	28023.29
24.0		27982.23	28186.58	28186.41
25.0		28154.62	28355.53	28355.13
26.0		28333.51	28530.79	28530.65
27.0		28518.54	28712.40	28712.16
28.0		28708.91	28900.45	
29.0			29094.95	29093.14
30.0				29292.55

following combination differences from the appropriate spectral line positions:

$$\Delta_2 F_1''(N) = F_1''(N+1) - F_1''(N-1) \qquad \ldots(13a)$$

$$= R_1(N-1) - P_1(N+1) \qquad \ldots(13b)$$

$$\Delta_2 F_2''(N) = F_2''(N+1) - F_2''(N-1) \qquad \ldots(14a)$$

$$= R_2(N-1) - P_2(N+1). \qquad \ldots(14b)$$

The difference $R_i(N-1) - P_i(N+1)$ gives a specific term value separation in the $^2\Sigma^+$,v = v" state and does not depend on what vibrational level is involved in the $^2\Pi$ state. An average value can be taken of the $\Delta_2 F_i''$ values determined from all those bands having the same value of v" (e.g. average the $\Delta_2 F_1''(N)$ values from the 0-1, 1-1, and 2-1 bands). In the present work, the combination differences were obtained from the term values (Table III)--that is, equations (13a) and (14a) were used, rather than (13b) and (14b).

In the absence of spin - rotation splitting, the rotational constants would be determined from a single set of combination differences, $\Delta_2 F''(N) = B_v''(4N+2)$. With spin - rotation splitting present, $\Delta_2 F''(N)$ is the average of $\Delta_2 F_1''(N)$ and $\Delta_2 F_2''(N)$, since (from equation (1), ignoring D_v and higher order terms):

$$\Delta_2 F_1''(N) = B_v^*''(4N+2) + \gamma_v \qquad \ldots(15a)$$

$$\Delta_2 F_2''(N) = B_v^*''(4N+2) - \gamma_v. \qquad \ldots(15b)$$

$$\tfrac{1}{2}[\Delta_2 F_1''(N) + \Delta_2 F_2''(N)] = B_v^*''(4N+2) = \Delta_2 F''(N). \qquad \ldots(16)$$

With the inclusion of the term of the next higher order,

equation (16) becomes[3]

$$\Delta_2 F''(N) = (4B_v^{*}'' - 6D_v'')(N + \tfrac{1}{2}) - 8D_v''(N + \tfrac{1}{2})^3 . \qquad ...(17)$$

Still higher terms involving odd powers of (N + 1/2) can be included, but were not in the present work.

Upon rearrangement, equation (17) gives

$$\frac{\Delta_2 F''(N)}{4(N + \frac{1}{2})} = (B_v^{*}'' - \tfrac{3}{2}D_v'') - 2D_v''(N + \tfrac{1}{2})^2 . \qquad ...(18)$$

A plot of $\frac{\Delta_2 F''(N)}{4(N + \frac{1}{2})}$ against $(N + \frac{1}{2})^2$ provides a means of determining the rotational constants. The slope of the resulting straight - line graph gives D_v'', and the intercept gives B_v''.

The graphs were found to be linear over a wide range of N values.† A typical plot (for v" = 1) is shown in Fig. 13. The points tend to deviate from the straight line more at very low values of N than at moderate N values. This is to be expected because of the presence of N in the denominator of the left - hand - side of equation (18). Any error in $\Delta_2 F''(N)$ will also be divided by 4(N + 1/2), and as N increases, the error will become of decreasing importance.[69]

Of more significance is the deviation from the straight

---

† All straight lines on graphs in this work were fitted by the method of least squares. The range of N or J values used in determining the best straight lines are given in the tables in this thesis, as also are correlation coefficients.

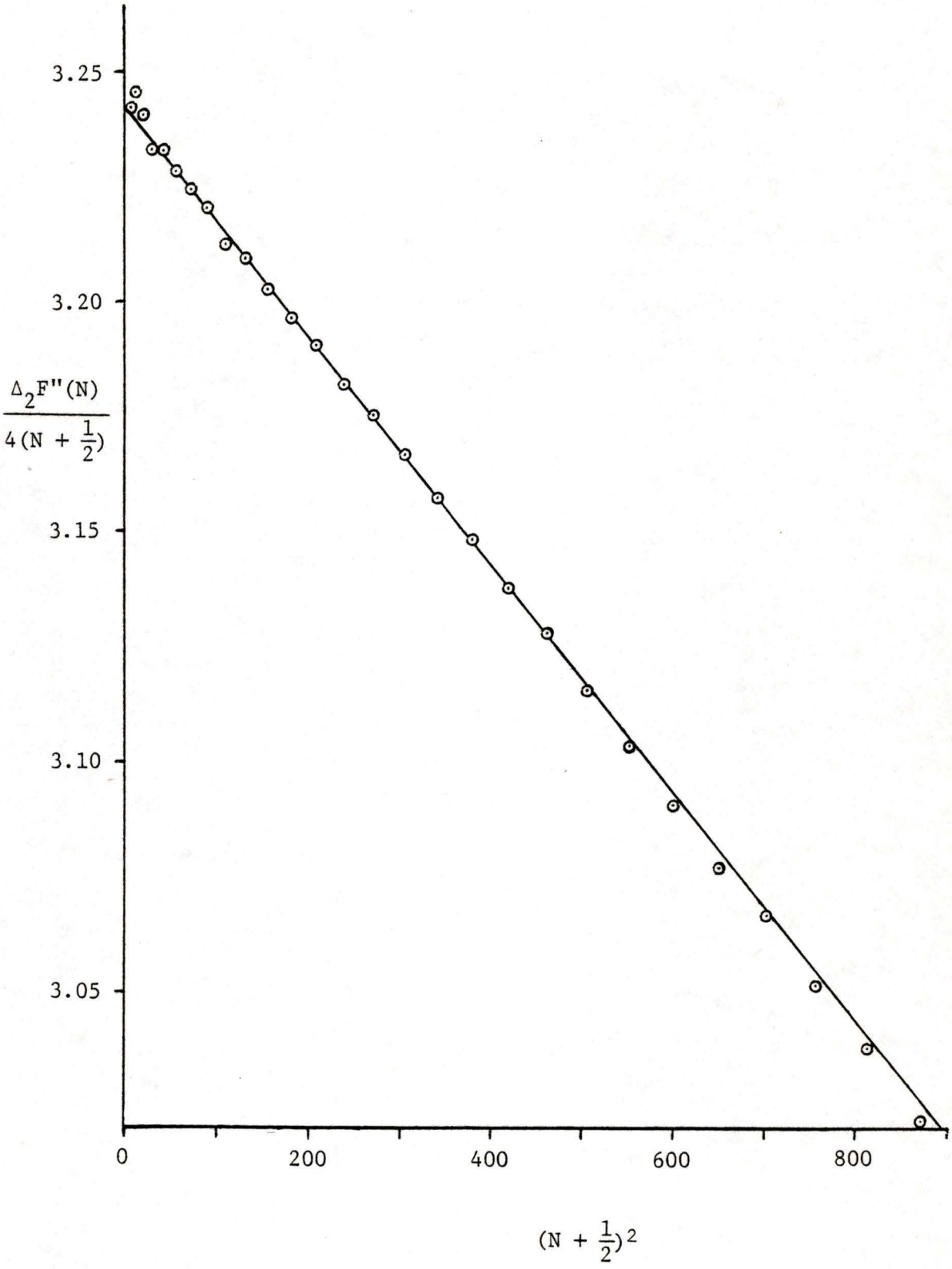

FIGURE 13. Determination of the rotational constants of the $X\ ^2\Sigma^+$, v" = 1 state. Slope = $-2D_v$". Intercept = B_v^*" - 3/2 D_v".

line at high N values. This is caused by the neglected terms of higher order than the D_v'' term.

The B_v^* and D_v constants of the X $^2\Sigma^+$ state are listed in Table IV. As mentioned earlier, the difference between B_v and B_v^* should be very small. Most workers ignore the difference, so the tabulated B_v^* values can be compared with literature values of B_v (which are really B_v^*). The constants for v" = 0 are compared with those of Fujioka and Tanaka in Table V: agreement is good, expecially for B_0^*.

TABLE IV. Rotational constants of the X $^2\Sigma^+$ state.[a]

v"	B_v^*	D_v	N used	Correlation coefficient[b]
0	3.349_8	$1.19_4 \times 10^{-4}$	6 - 22	-0.999 89
1	3.242_6	$1.24_3 \times 10^{-4}$	6 - 22	-0.999 77
2	3.127_6	$1.31_5 \times 10^{-4}$	6 - 26	-0.999 84
3	3.000_6	$1.38_5 \times 10^{-4}$	9 - 19	-0.998 86

(a) All values in this and the following tables are in cm^{-1}.

(b) for the least - squares straight line determined from the range of N values listed in the previous column.

TABLE V. Comparison of B_0^* and D_0 of the X $^2\Sigma^+$ state with the values of Fujioka and Tanaka.[43]

	B_0^*	D_0
This work	3.349_8	$1.19_4 \times 10^{-4}$
F & T	3.349_7	$1.24_0 \times 10^{-4}$

III.B.2. Rotational constants of the A $^2\Pi$ state

The combination differences appropriate for the determination of the rotational constants of the A $^2\Pi$ state are the following:

$$\Delta_2F_{1e}'(J) = F_{1e}'(J+1) - F_{1e}'(J-1) \quad ...(19a)$$

$$= R_1(J) - P_1(J) \quad ...(19b)$$

$$\Delta_2F_{1f}'(J) = F_{1f}'(J+1) - F_{1f}'(J-1) \quad ...(20a)$$

$$= {}^QR_{12}(J) - {}^OP_{12}(J) \quad ...(20b)$$

$$\Delta_2F_{2e}'(J) = F_{2e}'(J+1) - F_{2e}'(J-1) \quad ...(21a)$$

$$= {}^SR_{21}(J) - {}^QP_{21}(J) \quad ...(21b)$$

$$\Delta_2F_{2f}'(J) = F_{2f}'(J+1) - F_{2f}'(J-1) \quad ...(22a)$$

$$= R_2(J) - P_2(J)\,. \quad ...(22b)$$

Again, these were obtained from the term values, rather than directly from the spectral lines. The expressions corresponding to equations (17) and (18) are the following:[21]

$$\Delta_2F'(J) = 4(B_v' + \frac{q^*}{2} - D_v')(J + \tfrac{1}{2}) - 8D_v'(J + \tfrac{1}{2})^3 \quad ...(23)$$

$$\frac{\Delta_2F'(J)}{4(J + \frac{1}{2})} = (B_v' + \frac{q^*}{2} - D_v') - 2D_v'(J + \tfrac{1}{2})^2\,, \quad ...(24)$$

where $\Delta_2F'(J)$ is the average of $\Delta_2F_{1e}'(J)$, $\Delta_2F_{1f}'(J)$, $\Delta_2F_{2e}'(J)$, and $\Delta_2F_{2f}'(J)$. The term $-4D_v'(J + 1/2)$ is used instead of $-6D_v'(J + 1/2)$, as shown by Almy and Horsfall.[21] A plot of $\frac{\Delta_2F'(J)}{4(J + \frac{1}{2})}$ against $(J + \frac{1}{2})^2$ yields D_v' from the slope, but because of $^2\Sigma^+ - {}^2\Pi$ interaction, B_v^{*}', rather than B_v', is obtained from the intercept, where this

time

$$B_v^{*\prime} = B_v' + \frac{q^*}{2} \quad . \tag{25}$$

To obtain B_v', q^* has to be evaluated from the analysis of the Λ - doubling (section III.B.5).

As with the $X\ ^2\Sigma^+$ state, the graphs were linear over a good range of J values (Fig. 14), with increased deviations at low and high J values for the same reasons discussed previously.

The B_v^*, final B_v (cf. section III.B.5.a), and D_v constants of the $A\ ^2\Pi$ state are listed in Table VI, and a comparison of the B_v^* and D_v values for v' = 0 is made with those of Fujioka and Tanaka in Table VII (A). Again, agreement is good. In Table VII (B), the values of B_0 and D_0 are compared with those re-calculated by Veseth[22] from the data of Fujioka and Tanaka but now including correction terms† not used by Fujioka and Tanaka and not used in the present work. Because of these correction terms, the two sets of values in Table VII (B) cannot be compared directly; rather, the table is presented to show the small effect these corrections have, especially on B_v.

III.B.3. Spin doubling in the $X\ ^2\Sigma^+$ state

It follows from equations (1a) and (1b) that the spin

---

† These corrections are for centrifugal distortion (terms in H_v and F_v, in addition to D_v), spin - rotation interaction, and the dependence of A_v on the internuclear distance. The Mulliken and Christy formula (equation (6)) was also extended to include the terms derived by Dousmanis et al.[25]

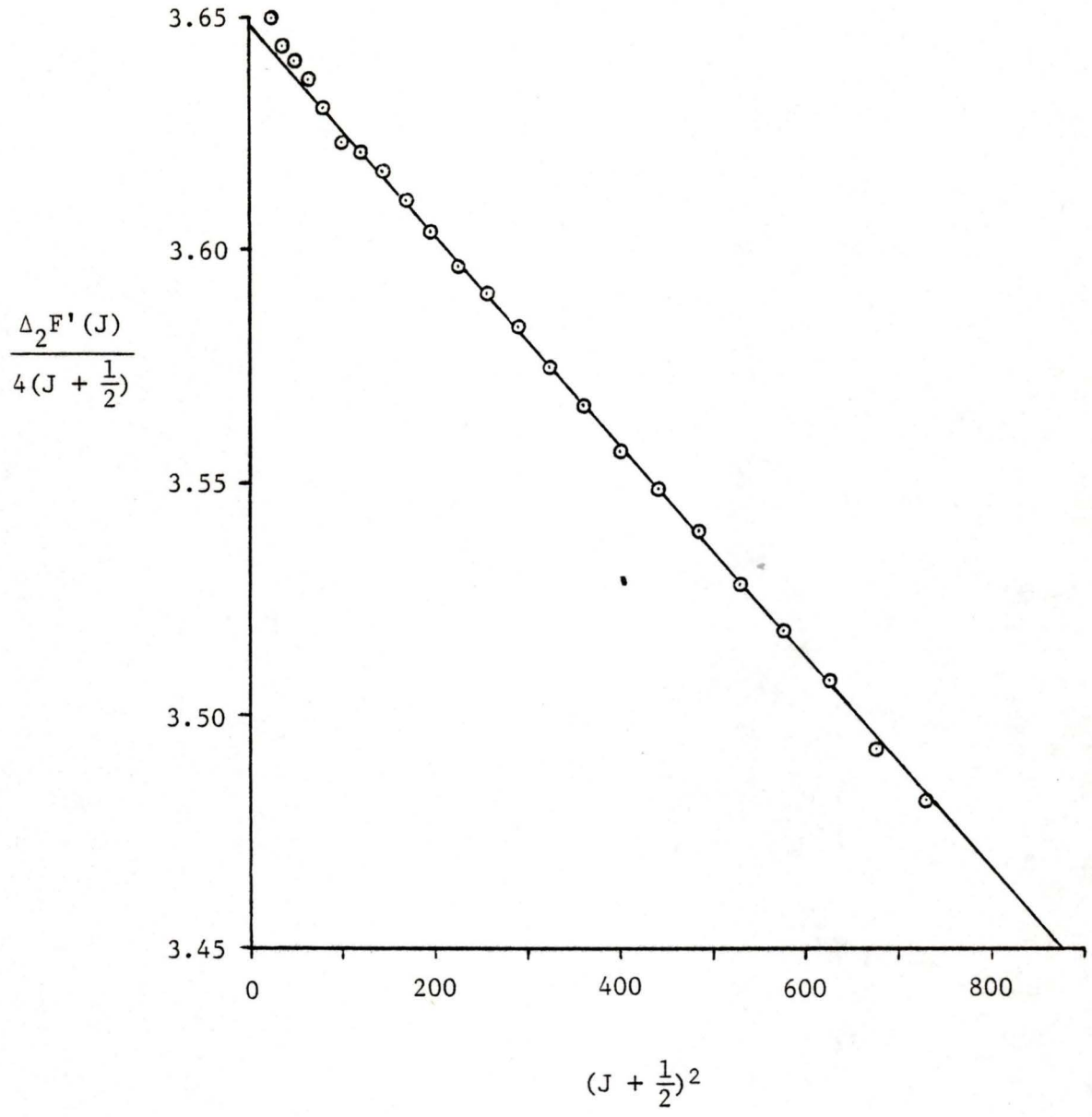

FIGURE 14. Determination of the rotational constants of the $A\ ^2\Pi$, $v' = 1$ state. Slope = $-2D_v'$. Intercept = $B_v^{*\prime} - D_v'$.

TABLE VI. Rotational constants of the A $^2\Pi$ state.

v'	B_v^*	B_v	D_v	J used	Correlation coefficient
0	3.734_5	3.733_8	$1.14_3 \times 10^{-4}$	4.5 - 23.5	-0.999 92
1	3.648_3	3.647_0	$1.13_2 \times 10^{-4}$	10.5 - 24.5	-0.999 87
2	3.561_7	3.560_3	$1.14_4 \times 10^{-4}$	7.5 - 19.5	-0.999 54

TABLE VII. (A) Comparison of B_0^* and D_0 of the A $^2\Pi$ state with the values of Fujioka and Tanaka.[43]

	B_0^*	D_0
This work	3.734_5	$1.14_3 \times 10^{-4}$
F & T	3.734_2	1.21×10^{-4} (a)

(a) In the original paper[43] this was written as 1.21×10^{-5}, but this must have been an error.

(B) Comparison of B_0 and D_0 of the A $^2\Pi$ state with the values of Veseth.[22]

	B_0	D_0	H_0
This work	3.733_8	$1.14_3 \times 10^{-4}$	—
Veseth	3.736	1.31×10^{-4}	1.6×10^{-8}

splitting is directly proportional to (N + 1/2), with γ_v, the spin - rotation coupling constant, as the constant of proportionality:

$$F_1''(N) - F_2''(N) = \gamma_v(N + \tfrac{1}{2}) \qquad ...(26)$$

The separation can be obtained from any of the following differences, or an average of them:

$$F_1''(N) - F_2''(N) = {}^{Q}R_{12}(N) - Q_1(N) \qquad ...(27a)$$

$$= {}^{P}Q_{12}(N) - P_1(N) \qquad ...(27b)$$

$$= R_2(N) - {}^{R}Q_{21}(N) \qquad ...(27c)$$

$$= Q_2(N) - {}^{Q}P_{21}(N), \qquad ...(27d)$$

but this, also, was determined from the term values in the present work.

To determine γ_v, a graph of $[F_1''(N) - F_2''(N)]$ versus (N + 1/2) can be plotted. A straight line should be obtained, with γ_v as the slope, and such is indeed the case (see Fig. 15 as an example). At high N values, such curves often deviate from a straight line, probably due to rotational stretching (centrifugal distortion) of the molecule.[59] Deviations were observed for large values of N, but the values of $[F_1''(N) - F_2''(N)]$ were too uncertain in this region to be able to attribute any of these deviations to centrifugal distortion. (The points with high N values on the graphs for v" = 0 and 2 are more obviously randomly distributed than the ones for v" = 1 shown in Fig. 15. A smooth deflection from the straight line would be expected if centrifugal distortion were the

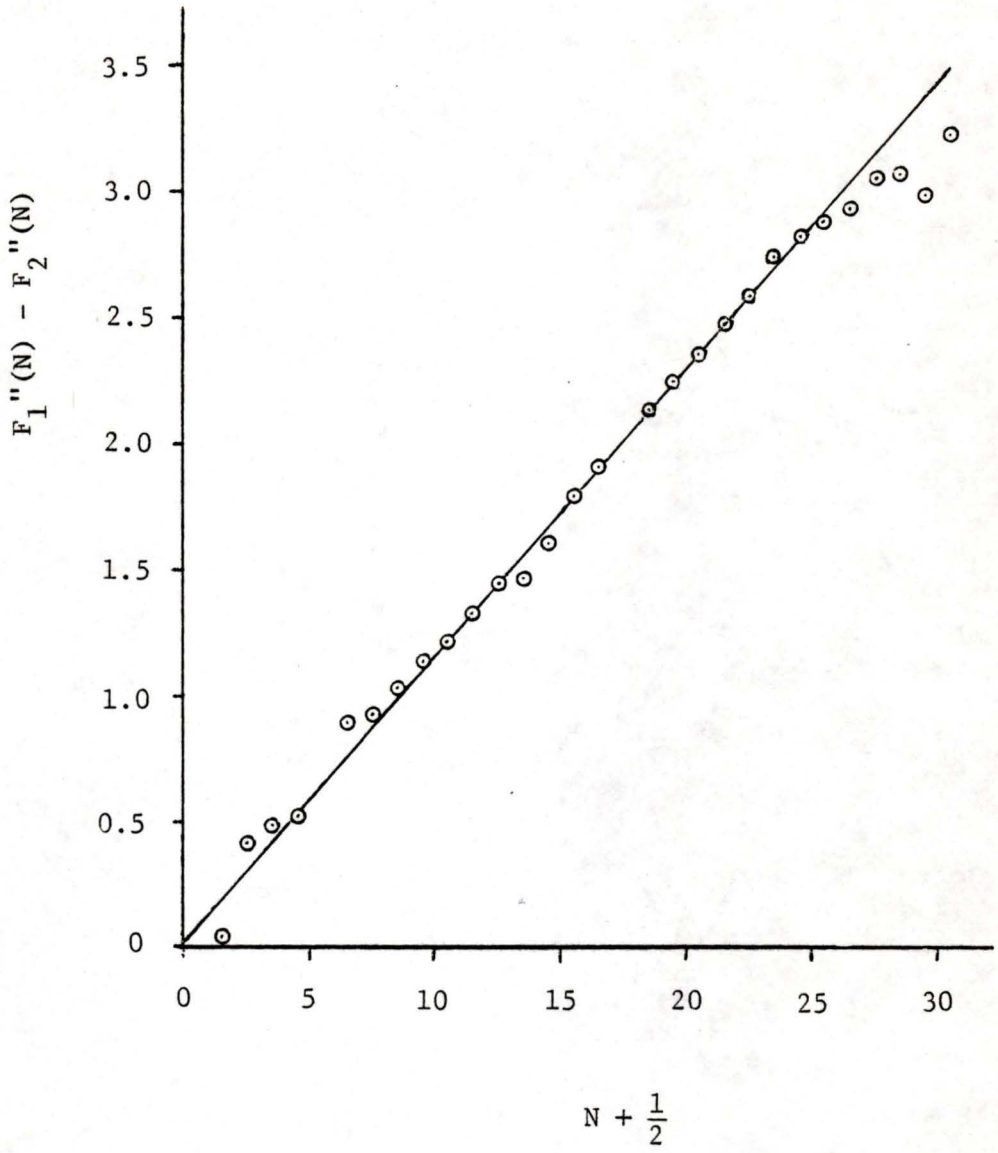

FIGURE 15. Determination of the spin - rotation coupling constant of the X $^2\Sigma^+$, v" = 1 state. Slope = γ_v. Intercept should be zero.

cause.)

As seen from equations (15a) and (15b)

$$\Delta_2 F_1''(N) - \Delta_2 F_2''(N) = 2\gamma_v . \qquad ...(28)$$

This also holds when D_v terms are included. Thus γ_v can also be obtained from the mean of these differences. Values obtained from the two methods are presented in Table VIII. The two sets are in agreement with each other to within experimental uncertainty.† It is believed that the graphical method gives the better values.

III.B.4. Spin doubling in the A $^2\Pi$ state

The splitting between the F_1 and F_2 components of $^2\Pi$ states which belong to coupling case (a) or to a case intermediate between (a) and (b) is due to spin - orbit coupling∫ and is represented by the spin - orbit coupling constant A_v.

The A $^2\Pi$ state of ZnD is a regular doublet--i.e. A_v is positive. It was not necessary to establish this in the present work, since ZnH and the v' = 0 level of ZnD have been studied previously. Otherwise, this could have been

---

† See Chapter IV regarding the experimental uncertainties in the values obtained from the graphical method. Standard deviations in the values obtained by the combination - differences method are given in Table VIII.

∫ The splitting due to spin - rotation coupling is small and has been ignored in this work.

TABLE VIII. Spin - rotation coupling constants of the X $^2\Sigma^+$ state.[a]

v"	Graphical method (equation (26))			Combination-differences method (equation (28))		Fujioka and Tanaka [43]
	γ_v	N used	Correlation coefficient	γ_v[b]	N used	γ_v
0	0.122_4	5 - 20	+0.999 1	0.121 (20)	6 - 19	0.131
1	0.112_8	7 - 24	+0.997 7	0.112 (29)	8 - 23	—
2	0.106_5	6 - 23	+0.997 9	0.111 (26)	7 - 22	—
3	0.098_7	9 - 20	+0.997 7	0.097 (18)	10 - 19	—

(a) The small, linear decrease in γ_v with increasing v is expected theoretically, since γ_v° should be proportional to B_v.[2] (The superscript on γ_v° denotes the J - independent part of γ_v, which is really what the values in the table are. The J - dependence only becomes important at high N values.)

(b) The figures in parentheses are standard deviations, with the decimal point located such that these two digits correspond to the last two digits in γ_v.

determined from the structure of the branches in the vicinity of the band origins or from the relative magnitudes of the Λ - doublet splittings in the two substates.

The effects of Λ - doubling (see next section) can be eliminated by taking the average of F_{1e} and F_{1f} and the average of F_{2e} and F_{2f}, since the Λ - type splitting is symmetrical. From equation (6), one obtains

$$F_1(J) = \frac{F_{1e}(J) + F_{1f}(J)}{2}$$

$$= B_v[(J + \tfrac{1}{2})^2 - 1 - \tfrac{1}{2}X_v] + \tfrac{1}{2}[o + \tfrac{1}{2}p^* + q^*(J + \tfrac{1}{2})^2]$$

$$- \frac{1}{2X_v}[(2 - Y_v)(o + \tfrac{1}{2}p^* + q^*) + (p^* + 2q^*)(J - \tfrac{1}{2})(J + \tfrac{3}{2})]$$

$$- D_v[J^2(J + 1)^2 - \tfrac{1}{2}J(J + 1) + \tfrac{13}{16}] + \ldots \qquad \ldots(29a)$$

$$F_2(J) = \frac{F_{2e}(J) + F_{2f}(J)}{2}$$

$$= B_v[(J + \tfrac{1}{2})^2 - 1 + \tfrac{1}{2}X_v] + \tfrac{1}{2}[o + \tfrac{1}{2}p^* + q^*(J + \tfrac{1}{2})^2]$$

$$+ \frac{1}{2X_v}[(2 - Y_v)(o + \tfrac{1}{2}p^* + q^*) + (p^* + 2q^*)(J - \tfrac{1}{2})(J + \tfrac{3}{2})]$$

$$- D_v[J^2(J + 1)^2 - \tfrac{1}{2}J(J + 1) + \tfrac{13}{16}] + \ldots . \qquad \ldots(29b)$$

J - doublets are then given by the expression

$$\Delta\nu_{21}(J) = F_2(J) - F_1(J)$$

$$= B_vX_v + \frac{1}{X_v}[(2 - Y_v)(o + \tfrac{1}{2}p^* + q^*)$$

$$+ (p^* + 2q^*)(J - \tfrac{1}{2})(J + \tfrac{3}{2})] + \ldots \qquad \ldots(30)$$

in which many of the terms, including the centrifugal distortion D_v terms, have cancelled out. Let the second

group of terms in equation (30) be represented by $Z_v(J)$. Then

$$\Delta\nu_{21}(J) - Z_v(J) = B_v[Y_v(Y_v - 4) + 4(J + \tfrac{1}{2})^2]^{1/2}, \qquad ...(31)$$

where X_v has been substituted for from equation (4). By squaring both sides, one obtains

$$[\Delta\nu_{21}(J) - Z_v(J)]^2 = B_v^2[Y_v(Y_v - 4) + 4(J + \tfrac{1}{2})^2] \qquad ...(32a)$$

$$= A_v(A_v - 4B_v) + 4B_v^2(J + \tfrac{1}{2})^2. \qquad ...(32b)$$

Most spectroscopists neglect the $Z_v(J)$ term:[†]

$$[\Delta\nu_{21}(J)]^2 \simeq A_v(A_v - 4B_v) + 4B_v^2(J + \tfrac{1}{2})^2. \qquad ...(33)$$

They plot $[\Delta\nu_{21}(J)]^2$ as a function of $(J + 1/2)^2$ and obtain an almost straight line, the intercept of which is $A_v(A_v - 4B_v)$. Since $Z_v(J)$ is small compared with $\Delta\nu_{21}(J)$ (<1% for ZnD A $^2\Pi$), this is reasonable as a first approximation. However, since in the present work, as discussed in section III.B.5.a, an iterative procedure was used to determine o, p*, q*, B_v, and A_v, it was easy enough to include the $Z_v(J)$ term as a correction on $\Delta\nu_{21}(J)$. $[\Delta\nu_{21}(J) - Z_v(J)]^2$ was plotted against $(J + 1/2)^2$ (Fig. 16), with $Z_v(J)$ calculated from the values of o, p*, q*, B_v, and A_v determined in the previous iteration.

The final values of A_v are given in Table IX. For $v' = 0$, the value of A_v that would have been obtained if $Z_v(J)$ had been ignored, was also calculated (Table X). This

---

[†] See, for example, ref. (3), p. 263, and ref. (70).

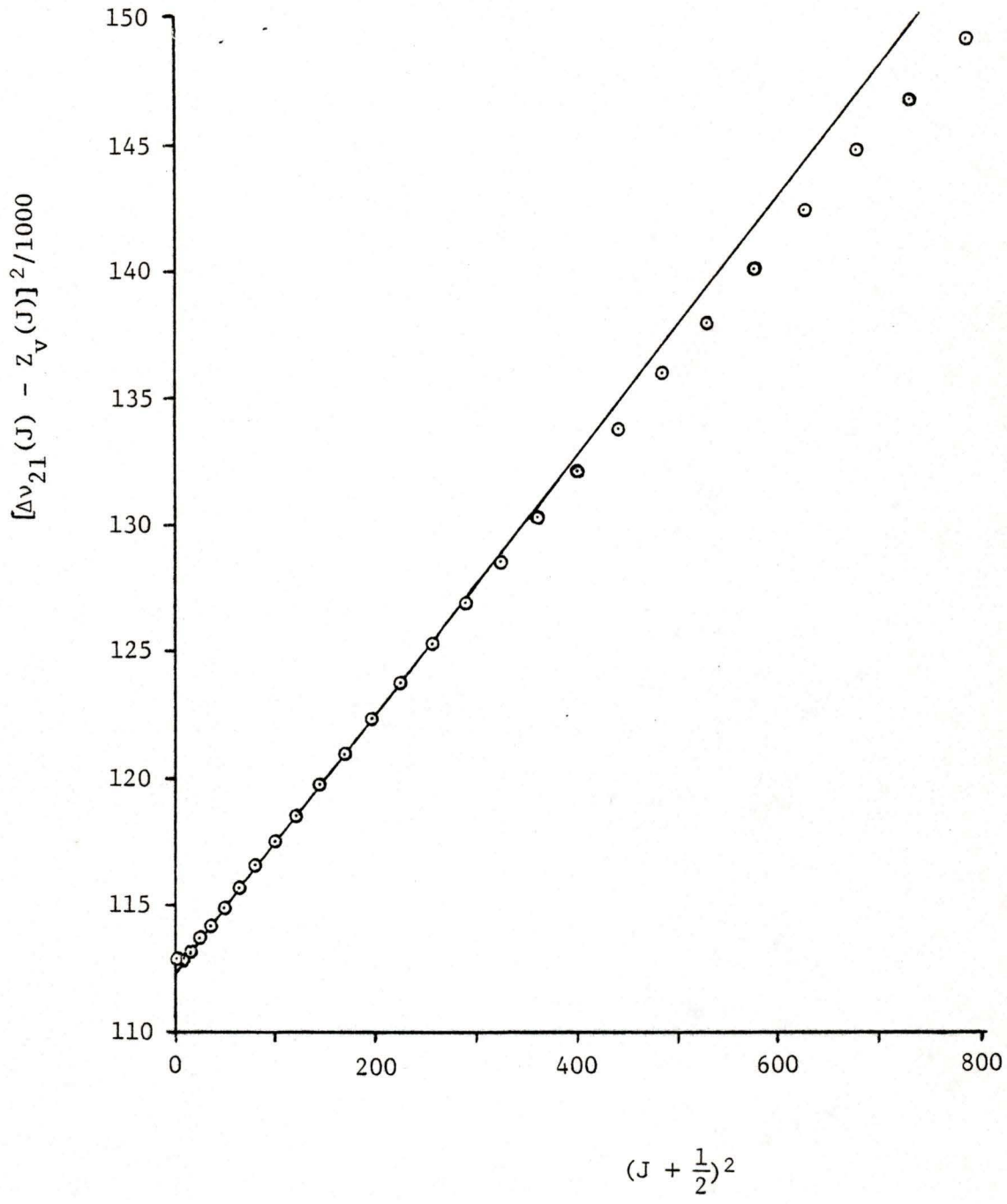

FIGURE 16. Determination of the spin - orbit coupling constant of the A $^2\Pi$, v' = 1 state. The graph is for the final iteration. Intercept = $A_v(A_v - 4B_v)$. Slope = $4B_v^2$.

TABLE IX. Spin - orbit coupling constants of the A $^2\Pi$ state.[a]

v'	A_v	J used	Correlation coefficient
0	343.28_6	1.5 - 11.5	+0.999 97
1	342.55_5	3.5 - 13.5	+0.999 85
2	342.03_5	4.5 - 16.5	+0.999 93

(a) Values are from the final iteration.

TABLE X. Comparison of the values of A_0 determined with and without including the term $Z_v(J)$, and comparison with the values of Fujioka and Tanaka[43] and Veseth.[22]

	A_o
This work ($Z_v(J)$ included)	343.28_6
This work ($Z_v(J)$ not included)	341.49_7
F & T ($Z_v(J)$ not included)	341.04
Veseth ($Z_v(J)$ included[a])	342.82

(a) The value of Veseth is not directly comparable with that obtained here (343.28_6 cm^{-1}) because of the additional corrections included by Veseth.

gives an indication of the magnitude of the error present in many of the literature values of A_v. It is often more than just the final "significant" figure which is affected by neglecting the $Z_v(J)$ term.

Also included in Table X are the values of A_0 obtained by Fujioka and Tanaka and by Veseth (recalculated from the data of Fujioka and Tanaka). Although Fujioka and Tanaka apparently used a different method to obtain A_0 than that used here, they did neglect the terms in $Z_v(J)$, so their value should be comparable with that obtained here when $Z_v(J)$ was neglected. The difference between the values is somewhat larger than expected, the reason for which is not known. It is believed that the value obtained here (at least with the $Z_v(J)$ term included) is better than that of Fujioka and Tanaka. The method devised by Veseth[22] has at least the potential to produce a better value yet than that obtained here, but the actual value given by Veseth may or may not be better since it was based on the data of Fujioka and Tanaka. (It was noted earlier that the line positions of Fujioka and Tanaka were in good agreement with the measurements obtained in the present study, except at very low J.) Veseth's value of A_0 cannot be directly compared with the present value because of the additional correction terms incorporated in the derivation by Veseth.†

---

† See footnote on page 74.

A bonus is obtained from the plot of $[\Delta\nu_{21}(J) - Z_v(J)]^2$ against $(J + 1/2)^2$: the slope is $4B_v^2$ (equation (32b)). This provides another method of obtaining the B_v constants of the A $^2\Pi$ state. However, this bonus is of doubtful merit. The values obtained by this method (which will here be called Method II) are considerably different from those obtained by the previous method (Method I—section III.B.2)—see Table XI. In every case, the value obtained by Method II is lower than that obtained by Method I and by an amount which is one or two orders of magnitude larger than the estimated experimental uncertainty. The reason for this was not ascertained. To check that the problem is one of theory and not of bad data (e.g. misassigned J numbers), Method II was applied to the data (line positions of the 0-0 band) given by Verma and Mulliken[70] for the A $^2\Delta$ - X $^2\Pi$ system of CCl.† With the $Z_v(J)$ terms ignored, the value of B_0 obtained for the X $^2\Pi$ state was 0.674 8 cm^{-1},

† Verma and Mulliken also used the graphical method involved in Method II, but only to obtain A_v values; they made no mention of using it to obtain B_v values. As a check. A_0 for the X $^2\Pi$ state of CCl was also determined by the author (neclecting $Z_v(J)$, as did Verma and Mulliken). A value of 134.99 cm^{-1} was obtained, which compares favorably with the value of 134.92 cm^{-1} reported by Verma and Mulliken—the slight difference, since the two values came from the same data, may have been due to the range of J values used (8.5 - 36.5 were used here; Verma and Mulliken did not specify) or to differences in the manner in which the line positions and $\Delta\nu_{21}(J)$ values were averaged.

TABLE XI. Comparison of the B_v values of the A $^2\Pi$ state obtained by the usual combination - diffences method (Method I) and from the graph of $[\Delta\nu_{21}(J) - Z_v(J)]^2$ versus $(J + 1/2)^2$ (Method II).

	Method I	Method II
B_0	3.733_8	3.653
B_1	3.647_0	3.57_4
B_2	3.560_3	3.45_5

which is considerably different (and again, lower) than the value obtained by Verma and Mulliken by Method I: $0.693\ 6_3$ cm^{-1}. The ratio of the Method II value to the Method I value appears to be approximately constant—97 - 98% for all the vibrational levels tested of the $^2\Pi$ states of the two molecules.

Negative deviations from linearity were observed on the graphs of $[\Delta\nu_{21}(J) - Z_v(J)]^2$ versus $(J + 1/2)^2$ as J increased. This J - dependence has been studied in other molecules by James,[71] who expressed it by the formula

$$A = A_v + 2A_J(J + \tfrac{1}{2}). \qquad \ldots(34)$$

Veseth[59] has obtained a formula for A_J in terms of other spectroscopic constants. The J - dependence was not studied in the present work, but its existence in ZnD is noted.

III.B.5. Λ - doubling in the A $^2\Pi$ state

The following expression for the Λ - type doublet separations, $\Delta\nu_{fe}$, can be obtained directly from the Mulliken and Christy formula (equation (6)):[2]

$$\Delta\nu_{fe}(J) = F_f(J) - F_e(J)$$

$$= \pm[(\tfrac{1}{2}p + q)(\pm 1 + \frac{2}{X_v} - \frac{Y_v}{X_v})$$

$$+ \frac{2q}{X_v}(J - \tfrac{1}{2})(J + \tfrac{3}{2})](J + \tfrac{1}{2}) + \ldots . \qquad \ldots(35)$$

The - sign in ± is for F_1 levels and the + sign is for F_2 levels. For Hund's coupling case (a), this reduces to[2]

$$^2\Pi_{1/2}: \quad \Delta\nu_{1fe}(J) = p(J + \tfrac{1}{2}) + \ldots \qquad (36a)$$

$$^2\Pi_{3/2}: \quad \Delta\nu_{2fe}(J) = \text{zero} + \ldots \qquad (36b)$$

In (36a) and in the following equations, the signs are appropriate for a regular doublet, such as the A $^2\Pi$ state of ZnD. The subscripts 1 and 2 on $\Delta\nu_{fe}$ indicate the F_1 and F_2 components, respectively (i.e. $^2\Pi_{1/2}$ and $^2\Pi_{3/2}$, respectively). Fujioka and Tanaka[43] have added the next smaller terms to that of equation (36a), as have Mulliken and Christy and Fujioka and Tanaka for equation (36b):

$$^2\Pi_{1/2}: \quad \Delta\nu_{1fe}(J) = (p + 2q)(J + \tfrac{1}{2}) - (\frac{p}{Y_v^2} + \frac{2q}{Y_v})(J + \tfrac{1}{2})^3 + \ldots \qquad \ldots(37a)$$

$$^2\Pi_{3/2}: \quad \Delta\nu_{2fe}(J) = (\frac{p}{Y_v^2} + \frac{2q}{Y_v})(J^2 - \tfrac{1}{4})(J + \tfrac{3}{2}) + \ldots . \qquad \ldots(37b)$$

This is equivalent to saying that they have allowed for some case (b) character—i.e. the situation is intermediate

between cases (a) and (b), but still fairly close to case (a). For a situation even farther from case (a), the general equation (35) has to be used. (For pure case (b), the Λ - type splitting is given by the formula

$$\Delta\nu_{fe}(N) = \mp qN(N+1), \qquad \ldots(38)$$

where the - sign is for F_1 levels and the + sign is for F_2 levels. However, this equation is not appropriate for ZnD, since Y_v is large.)

The Λ - type splittings cannot be obtained directly from the spectral line positions. Unless term values are first determined (see below), the best that can be done is to use the following relations:[30]

$$F_{1e}'(J+1) - F_{1f}'(J) = R_1(J) - Q_1(J) = {}^{P}Q_{12}(J+1) - {}^{O}P_{12}(J+1)$$

$$= \Delta_1 F_{1e}'(J+\tfrac{1}{2}) - \Delta\nu_{1fe}(J)$$

$$\text{or } \Delta_1 F_{1f}'(J+\tfrac{1}{2}) - \Delta\nu_{1fe}(J+1) \qquad \ldots(39a)$$

$$F_{1f}'(J+1) - F_{1e}'(J) = Q_1(J+1) - P_1(J+1) = {}^{Q}R_{12}(J) - {}^{P}Q_{12}(J)$$

$$= \Delta_1 F_{1e}'(J+\tfrac{1}{2}) + \Delta\nu_{1fe}(J+1)$$

$$\text{or } \Delta_1 F_{1f}'(J+\tfrac{1}{2}) + \Delta\nu_{1fe}(J) \qquad \ldots(39b)$$

$$F_{2f}'(J+1) - F_{2e}'(J) = R_2(J) - Q_2(J) = {}^{R}Q_{21}(J+1) - {}^{Q}P_{21}(J+1)$$

$$= \Delta_1 F_{2f}'(J+\tfrac{1}{2}) + \Delta\nu_{2fe}(J)$$

$$\text{or } \Delta_1 F_{2e}'(J+\tfrac{1}{2}) + \Delta\nu_{2fe}(J+1) \qquad \ldots(39c)$$

$$F_{2e}'(J+1) - F_{2f}'(J) = Q_2(J+1) - P_2(J+1) = {}^{S}R_{21}(J) - {}^{R}Q_{21}(J)$$

$$= \Delta_1 F_{2f}'(J + \tfrac{1}{2}) - \Delta\nu_{2fe}(J+1)$$

$$\text{or } \Delta_1 F_{2e}'(J + \tfrac{1}{2}) - \Delta\nu_{2fe}(J). \qquad \ldots(39d)$$

From the differences (39b - 39a) and (39c - 39d), the sum of the widths of two consecutive levels is obtained:

$$F_{1f}'(J+1) - F_{1e}'(J+1) + F_{1f}'(J) - F_{1e}'(J) = \Delta\nu_{1fe}(J+1) + \Delta\nu_{1fe}(J) \qquad \ldots(40a)$$

$$F_{2f}'(J+1) - F_{2e}'(J+1) + F_{2f}'(J) - F_{2e}'(J) = \Delta\nu_{2fe}(J+1) + \Delta\nu_{2fe}(J), \qquad \ldots(40b)$$

and these can be closely approximated by $\Delta\nu_{1fe}(J + 1/2)$ and $\Delta\nu_{2fe}(J + 1/2)$, since to the accuracy of equation (36a) a linear relationship exists between $\Delta\nu_{1fe}$ and J, and although $\Delta\nu_{2fe}$ and J are not directly linearly related, the magnitude of $\Delta\nu_{2fe}$ is small (at least for low and moderate J values) and the difference between adjacent values is small. Equations (36a), (37a), and (37b) can still be used with these fictitious $\Delta\nu_{fe}(J + 1/2)$ values if J is replaced by $J + 1/2$.

The Λ - type splittings were calculated in the present study from the term values:

$$\Delta\nu_{fe}(J) = F_f(J) - F_e(J). \qquad \ldots(41)$$

This approach had the potential advantage that no approximations were made (i.e. the $\Delta\nu_{fe}(J)$ splittings were obtained, rather than the approximate fictitious $\Delta\nu_{fe}(J + 1/2)$ values). However, it was found that the data points fell

on smoother curves if the fictitious $\Delta\nu_{fe}(J + 1/2)$ values (calculated by averaging $\Delta\nu_{fe}(J)$ and $\Delta\nu_{fe}(J+1)$) were used. This was because of the problem of the term values belonging to two non-interconnecting sets (see section III.A). The e and f levels from which each $\Delta\nu_{fe}(J)$ value was calculated were members of the opposing sets. Any errors in the location of the term value sets relative to each other would have led to large relative errors in the $\Delta\nu_{fe}(J)$ values, since these values were small in magnitude.†

For a $^2\Pi_{1/2}$ substate belonging to case (a), it follows from equation (36a) that a plot of $\Delta\nu_{1fe}(J)$ against J (or $\Delta\nu_{1fe}(J + 1/2)$ against $(J + 1/2)$) should yield a straight line of slope p. Such a plot is shown in Fig. 17 for the v' = 1 level of ZnD. Also shown is $\Delta\nu_{2fe}$ as a function of J, although a linear relation is not expected in this case. This latter plot was made to show the variation of $\Delta\nu_{2fe}$ with J and to compare $\Delta\nu_{2fe}$ with $\Delta\nu_{1fe}$ and was also found to be useful in choosing which $\Delta\nu_{2fe}(J)$ values to discard in subsequent plots because of random errors.

The $\Delta\nu_{2fe}$ values are much smaller than the $\Delta\nu_{1fe}$ values (a fact which can be used to distinguish between the $^2\Pi_{3/2}$

---

† The curves for $\Delta\nu_{fe}(J + 1/2)$ would also appear smoother than those for $\Delta\nu_{fe}(J)$ because random errors would be averaged over two adjacent points rather than concentrated in single points, though this probably would not improve the accuracy.

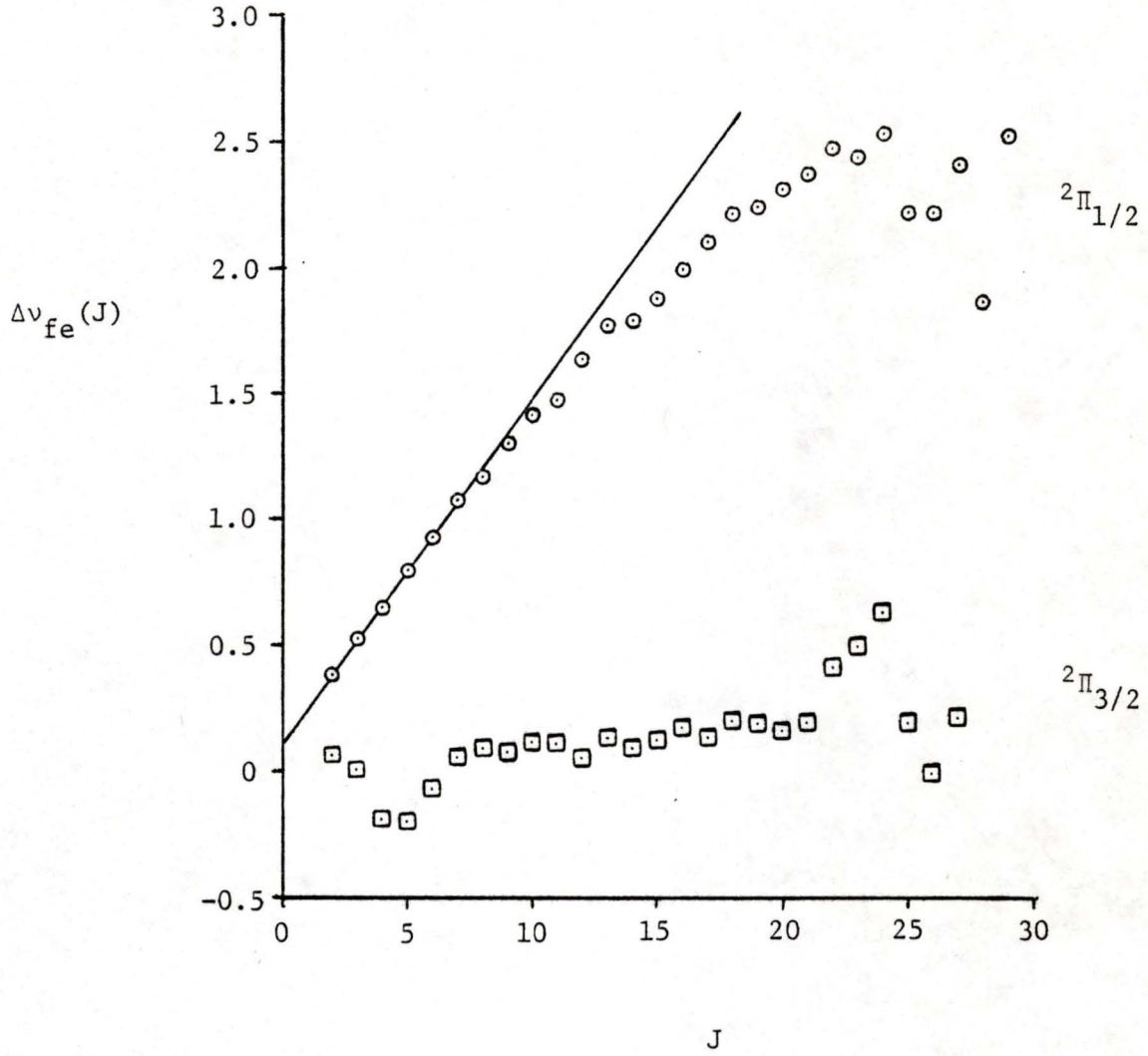

FIGURE 17. Λ - doubling in the A $^2\Pi$, v' = 1 state. The points are plotted for the fictitious $\Delta\nu_{fe}(J + 1/2)$ values. For the $^2\Pi_{1/2}$ substate, according to equation (36a): slope = p; intercept should equal 1/2 p.

and $^2\Pi_{1/2}$ substates and thus to determine whether the doublet is regular or inverted). Small negative values have been obtained for $\Delta\nu_{2fe}$ at low J for all three vibrational levels studied, but there is probably no significance to this. Watson and Parker[72] obtained negative values for low J values in BeH, but Mulliken and Christy[2] attributed this to experimental error.

Other than these first few points, $\Delta\nu_{fe}$ for $^2\Pi_{1/2}$ and that for $^2\Pi_{3/2}$ have the same signs, as is usual for case (a).[2] The curves for $\Delta\nu_{1fe}$ are linear only at low J (up to J + 1/2 = 10 or less). Beyond this range, each curve deviates towards the $\Delta\nu_{fe}$ = 0 axis. If it could be extended to much higher J values, it would bend around completely,† and $\Delta\nu_{1fe}$ would eventually become negative, so that as case (b) is approached $\Delta\nu_{1fe}$ and $\Delta\nu_{2fe}$ would have opposite signs[2] (cf. the ± sign in equation (38)).

There are at least two reasons why the plot of $\Delta\nu_{1fe}$ against J deviates from a straight line. First to be considered is the fact that ZnD does not belong to pure case (a) but only approximates this condition. For the A $^2\Pi$ state, Y (= A/B) ≃ 90 - 100, whereas even in HgH, for

---

† The curve for v' = 1 (Fig. 17) may even have reached and passed this maximum, but this cannot be stated with certainty in view of the large scatter in the points having large J values, the reason for which has not been determined (possibilities: incorrect line assignments; perturbations).

which Y ≃ 560 in the A $^2\Pi$ state, pure case (a) behavior is not achieved (at least with regard to spectral line intensity distributions).[73]

Graphs (Fig. 18) based on equation (37a), which allows for some departure from pure case (a), were found to be linear over a wider range of J values than the previous graphs. (The points in Fig. 18 appear much more widely scattered than those in Fig. 17, but this is mainly due to the large scale at which the equation (37a) graphs were drawn.) These graphs each consist of a plot of $\frac{\Delta\nu_{1fe}(J)}{J + \frac{1}{2}}$ as a function of $(J + 1/2)^2$. The result is a straight line with slope = $-(\frac{p}{Y_v^2} + \frac{2q}{Y_v})$ and intercept = $(p + 2q)$, from which p and q can be solved for simultaneously once Y_v has been determined.

For the $^2\Pi_{3/2}$ substate, according to equation (36b), there should be no Λ - doubling if the coupling scheme is pure case (a). This is clearly not the case, so allowance for some case (b) character has to be made—equation (37b).

According to equation (37b), a graph of $\Delta\nu_{2fe}(J)$ against $(J^2 - \frac{1}{4})(J + \frac{3}{2})$ should be a straight line, also with slope = $(\frac{p}{Y_v^2} + \frac{2q}{Y_v})$, this time with a + sign in front. According to Fujioka and Tanaka, this equation includes terms of the same order as does equation (37a). An example graph is shown in Fig. 19. It was found that the

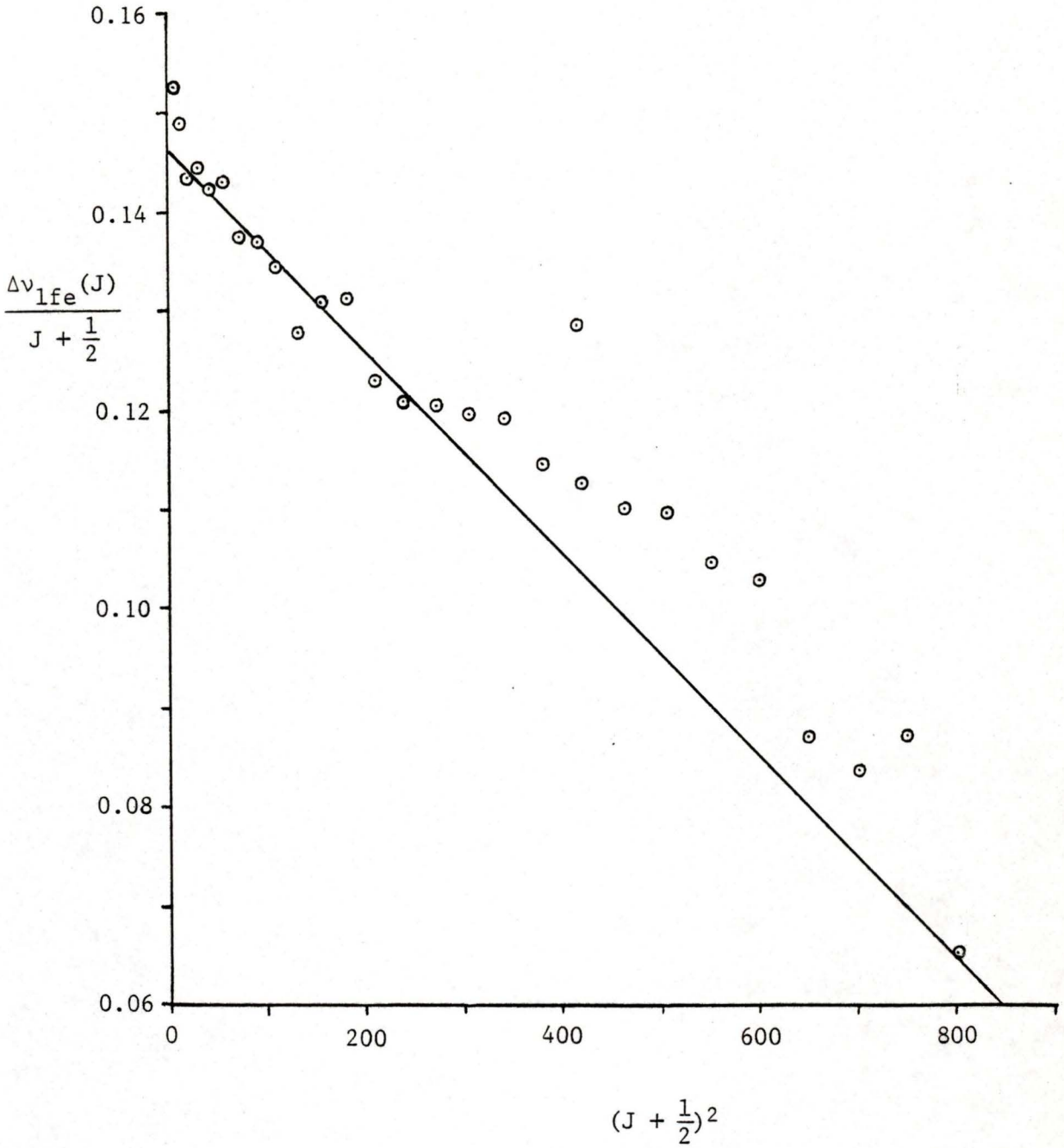

FIGURE 18. Determination of the Λ - doubling parameters by means of equation (37a). The graph is for the A $^2\Pi_{1/2}$, v' = 1 substate, with the points plotted for the fictitious J + 1/2 values. Slope = $-(\frac{p}{Y_v^2} + \frac{2q}{Y_v})$. Intercept = p + 2q.

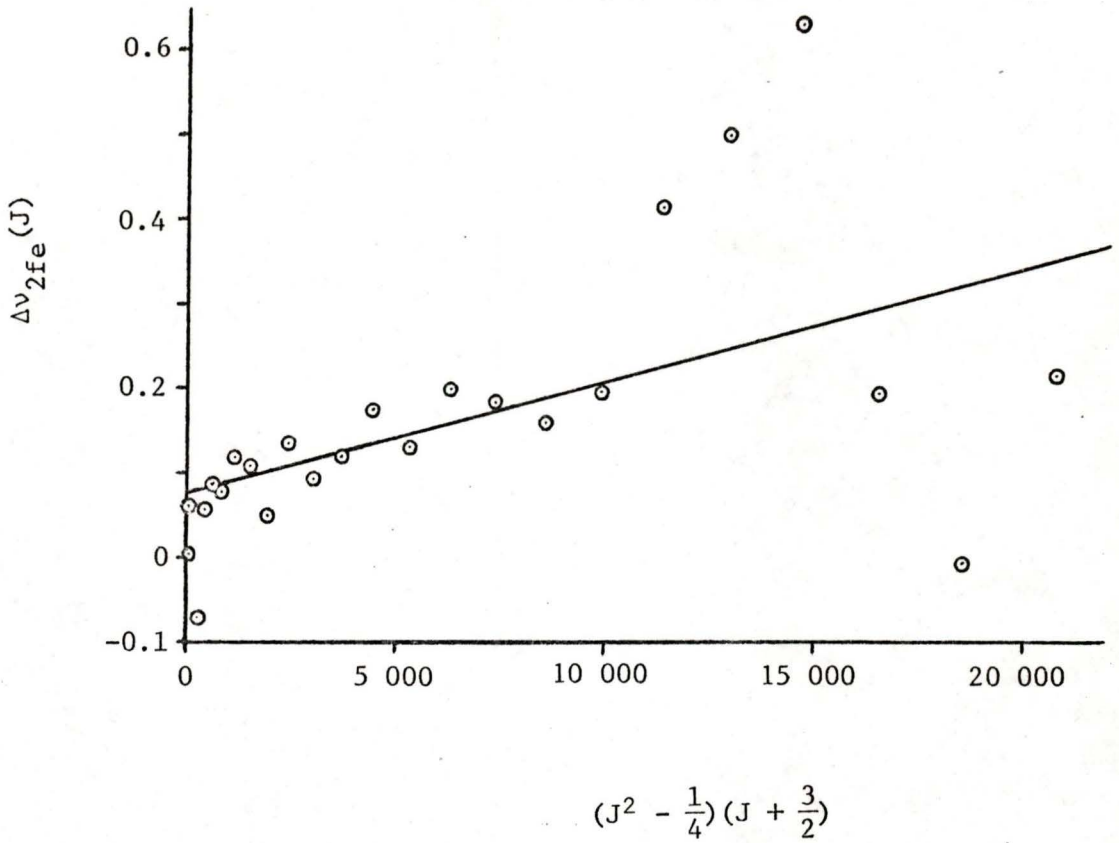

FIGURE 19. Determination of the Λ - doubling parameters by means of equation (37b). The graph is for the $A\ ^2\Pi_{3/2}$, v' = 1 substate, with the points plotted for the fictitious J + 1/2 values.

Slope = $(\frac{p}{Y_v^2} + \frac{2q}{Y_v})$. Intercept should be the origin.

values of $(\frac{p}{Y_v^2} + \frac{2q}{Y_v})$ obtained by this method (based on equation (37b)) differed considerably from those obtained by the previous method (based on equation (37a)). (For example, for v' = 0: this method, $(\frac{p}{Y_v^2} + \frac{2q}{Y_v}) = 3.2_8 \times 10^{-5}$; previous method, $5.4_2 \times 10^{-5}$; Fujioka and Tanaka obtained (also by the previous method), $(7.3 \pm 3.9) \times 10^{-5}$.) The values of p and q determined using $(\frac{p}{Y_v^2} + \frac{2q}{Y_v})$ obtained from the equation (37a) method were in better agreement with those determined from the method of equation (42b) (see below) than those determined using $(\frac{p}{Y_v^2} + \frac{2q}{Y_v})$ obtained from the equation (37b) method (see Table XII). A possible explanation is discussed later.

Equation (35), valid for any situation between cases (a) and (b) was also employed. The following relations can easily be obtained from equation (35):[2]

$$\Delta\nu_{2fe}(J) + \Delta\nu_{1fe}(J) = (p + 2q)(J + \tfrac{1}{2}) + \ldots \qquad \ldots(42a)$$

$$\Delta\nu_{2fe}(J) - \Delta\nu_{1fe}(J) = \frac{1}{X_v}[(p + 2q)(2 - Y_v) + 4q(J - \tfrac{1}{2})(J + \tfrac{3}{2})](J + \tfrac{1}{2}) + \ldots . \qquad \ldots(42b)$$

Straight lines were obtained from plots of $[\Delta\nu_{2fe}(J) + \Delta\nu_{1fe}(J)]$ against $(J + \frac{1}{2})$ (Fig. 20) and

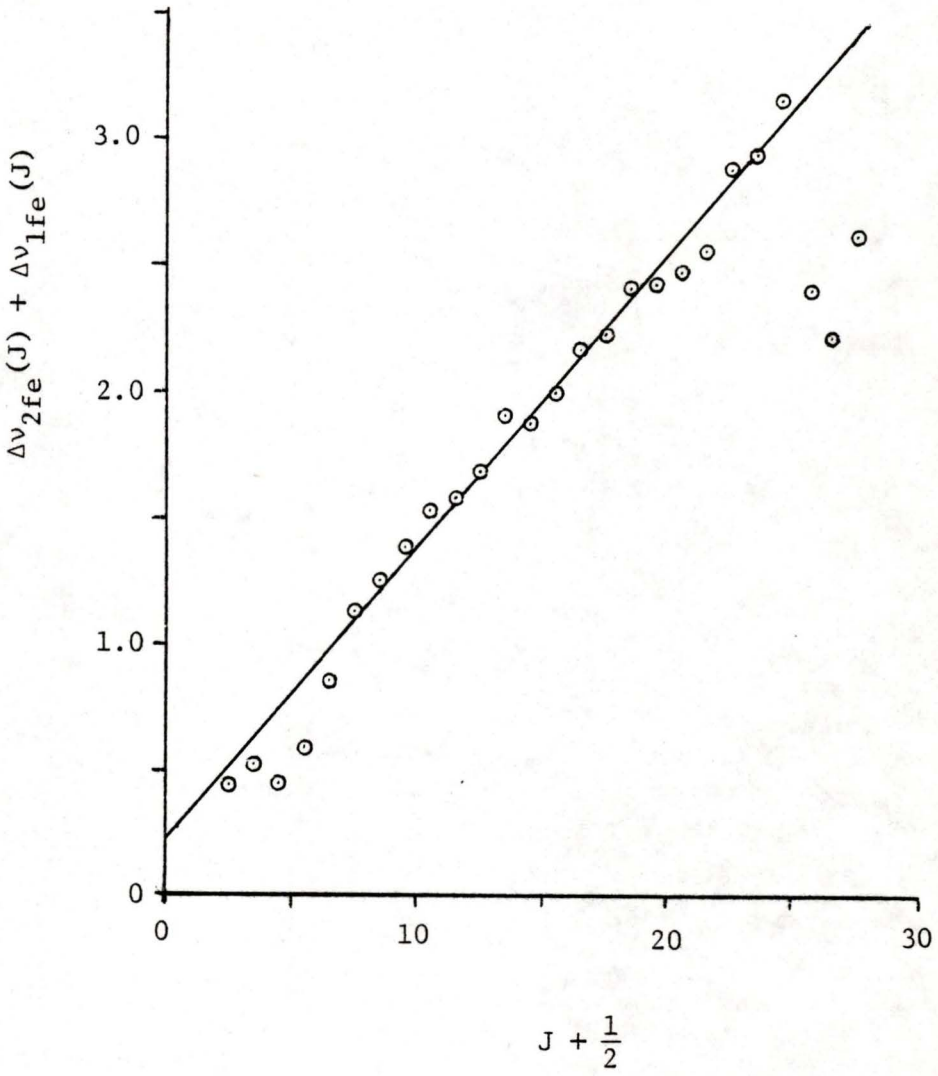

FIGURE 20. Determination of the Λ - doubling parameters by means of equation (42a). The graph is for the v' = 1 level of the A $^2\Pi$ state, with the points plotted for the fictitious J + 1/2 values. Slope = (p + 2q). Intercept should be the origin.

$\frac{[\Delta\nu_{2fe}(J) - \Delta\nu_{1fe}(J)]\cdot X_v}{J + \frac{1}{2}}$ against $(J - \frac{1}{2})(J + \frac{3}{2})$ (Fig. 21).

The ranges of the J values over which the graphs were linear were roughly comparable with those for the graphs based on equations (37a) and (37b), although for v = 0, deviation from linearity occurred at lower J values than with equation (37a). The values of p and q were obtained from the quantities 4q (the slope of the line based on equation (42b)) and (p + 2q), with the latter obtained either from (1) the slope of the line corresponding to equation (42a) or from (2) the intercept of the line based on equation (42b) after dividing by $(2 - Y_v)$. It was found that method (2) always gave a value for p in better agreement with that from the Fujioka and Tanaka method (equation (37a)) than did method (1), so the former values were used in calculating the final average values (Table XII), since there was expected to be little difference between the results obtained by the two methods.

A second reason for the deviation from a straight line of the plot of $\Delta\nu_{1fe}$ against J and also a reason for the curvature at high J values in the other Λ - doubling graphs (though in the latter cases this is often masked by random errors at high J values) is the fact that p and q are known to vary with J, due to stretching of the molecule. This centrifugal distortion effect has been discussed by Mulliken and Christy[2] and by Veseth.[59] Mulliken and Christy have expressed the J - dependence (written in terms of N) by the formulas

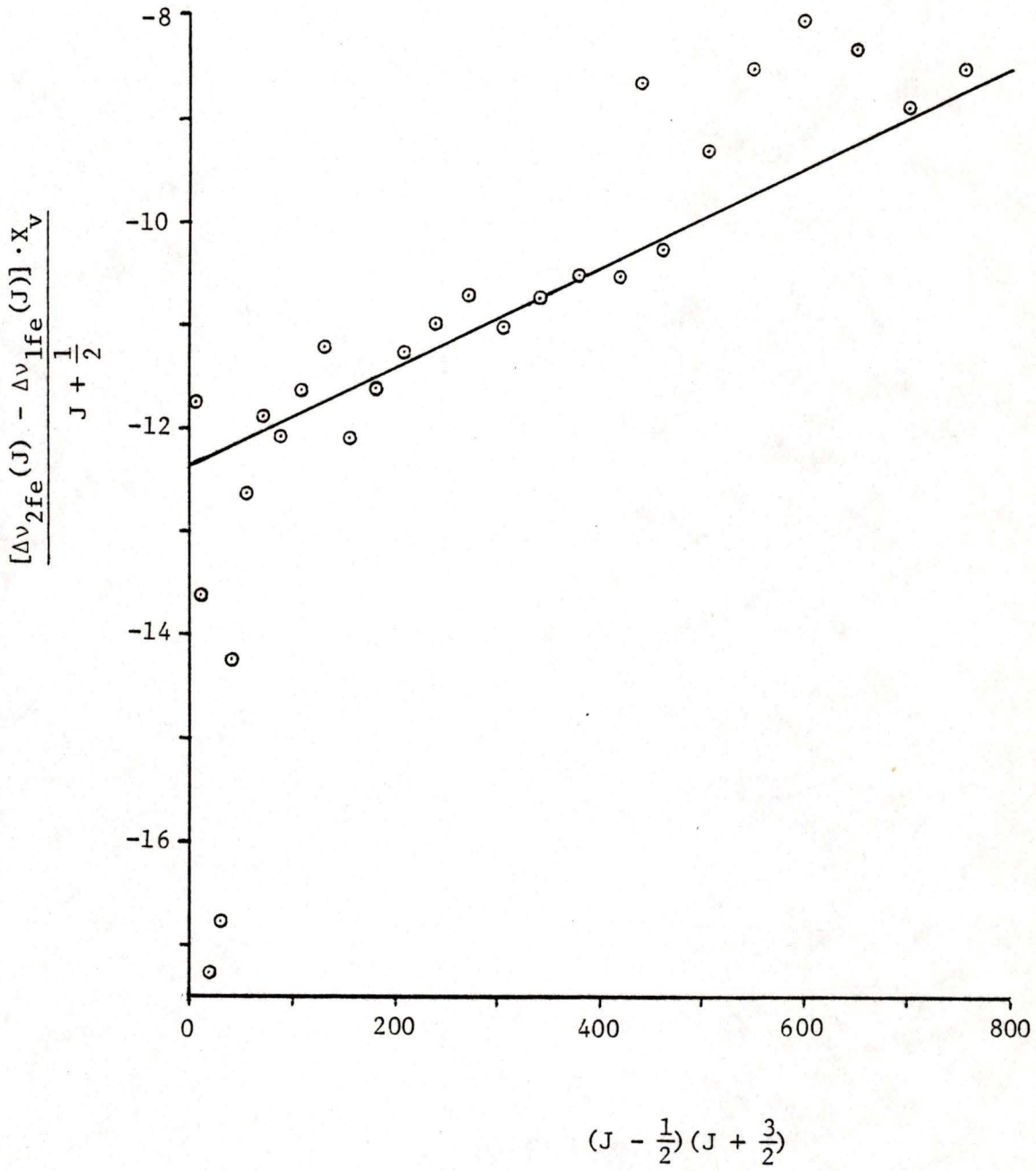

FIGURE 21. Determination of the Λ - doubling parameters by means of equation (42b). The graph is for the final iteration for the v' = 1 level of the A $^2\Pi$ state, with the points plotted for the fictitious J + 1/2 values. Slope = 4q. Intercept = $(p + 2q)(2 - Y_v)$.

TABLE XII. Λ - doubling parameters of the A $^2\Pi$ state. The quantities shown are the final values obtained from the iterative procedure described in the text.

(A) Values of p:

v'	Method					"Best" values (average of (d) & (g))	Literature values		Calculated values for pure precession
	(a)	(c)	(d)	(f)	(g)		Fujioka and Tanaka[43]	Dufayard and Nedelec[26]	
0	0.155_6	0.151_6	0.149_6	0.15_{57}	0.148_4	0.149_0	0.17	0.146 ± 0.002	0.22
1	0.138_0	0.146_7	0.138_3	0.113_0	0.132_3	0.135	—	—	0.22
2	0.102_2	0.116_2	0.109_3	0.088_1	0.111_4	0.110_4	—	—	0.22

(B) Values of q:

v '	Method				"Best" values (average of (d) & (e))	Literature value: Dufayard and Nedelec[26]	Calculated values for pure precession
	(b)	(c)	(d)	(e)			
0	$0.000\ 73_9$	$0.000\ 68_5$	$0.001\ 6_8$	$0.001\ 3_8$	$0.001\ 5_3$	0.001 12 ± 0.000 02	0.0024
1	$-0.000\ 1_2$	$-0.000\ 16_7$	$0.004\ 0_4$	$0.001\ 2_0$	$0.002\ 6$	—	0.0023
2	$0.000\ 76_1$	$0.000\ 6_9$	$0.004\ 1$	$0.001\ 7$	$0.002\ 9$	—	0.0023

continued on next page...

TABLE XII (cont.)

p and q were evaluated from the following quantities:

(a) Equation (36a): slope

(b) Equation (36a): slope and Equation (37b): slope

(c) Equation (37a): intercept and Equation (37b): slope

(d) Equation (37a): slope and intercept

(e) Equation (42b): slope

(f) Equation (42a): slope and Equation (42b): slope

(g) Equation (42b): slope and intercept

(C) Statistical information about the data used to determine the least - squares straight lines.

v'	Equation	J used	Correlation coefficient
0	36a	1 - 10	-0.998 7
	37a	3 - 27	+0.985 8
	37b	6 - 22	+0.984 7
	42a	2 - 14	+0.997 0
	42b	4 - 21	+0.955 4
1	36a	2 - 7	-0.999 7
	37a	4 - 16	+0.968 1
	37b	7 - 21	+0.827 8
	42a	2 - 24[(i)]	+0.995 0
	42b	7 - 21	+0.911 3
2	36a	5 - 9	-0.977 6
	37a	5 - 15	+0.866 2
	37b	2 - 23[(ii)]	+0.938 1
	42a	5 - 20	+0.979 0
	42b	5 - 20[(iii)]	+0.963 9

J values omitted:

(i) 4, 5, 6

(ii) 3, 7, 8, 14, 17

(iii) 7, 8, 10, 14, 17, 18

$$p = p_0 / [1 + u^2N(N + 1)] \simeq p_0[1 + 2u^2N(N + 1) + \ldots] \quad \ldots(43a)$$

$$q = q_0 / [1 + u^2N(N + 1)] \simeq q_0[1 - 4u^2N(N + 1) + \ldots], \quad \ldots(43b)$$

where

$$u^2 = \frac{4B_e^2}{\omega_e^2} = \frac{D_e}{B_e} . \quad \ldots(44)$$

Veseth has obtained the formulas

$$p' = p + p_J J(J + 1) \quad \ldots(45a)$$

$$q' = q + q_J J(J + 1) \quad \ldots(45b)$$

and has given expressions for p_J and q_J. Dufayard and Nedelec[26] have used the latter formulas, with the dependence on J expressed in the form $[1 + xJ(J + 1)]$, where x is an adjustable parameter. For ZnH, they have found that the Λ - doublet splitting of the $^2\Pi_{3/2}$ substate is reduced by centrifugal distortion by 10 - 20% over the J - range 2.5 - 21.5.

Although Dufayard and Nedelec did not explicitly study this effect on the $^2\Pi_{1/2}$ substate, they state that it is much smaller than the effect on the $^2\Pi_{3/2}$ substate. This provides a clue as to why different results were obtained from the different methods of determining the Λ - doubling parameters (cf. Table XII). Although this has not been tested, the following explanation is tentatively put forth. Equation (37b) involves exclusively $\Delta\nu_{2fe}$ (which is for the $^2\Pi_{3/2}$ substate), and based on the work of Dufayard and Nedelec, $\Delta\nu_{2fe}$ is not expected to be accurate, due to the effects of centrifugal distortion. Equation (37a), on the other hand, involves exclusively

$\Delta\nu_{1fe}$, which should be relatively unaffected by centrifugal distortion according to Dufayard and Nedelec—hence the difference between the results obtained from these two equations. The values of p and q obtained exclusively from equation (37a) (by simultaneous solution of the expressions for the slope and intercept—method (d) in Table XII) should be the more accurate values. Equation (42a) and (42b) involve both $\Delta\nu_{1fe}$ and $\Delta\nu_{2fe}$; however, the magnitude of $\Delta\nu_{1fe}$ is greater than that of $\Delta\nu_{2fe}$, so the centrifugal distortion effect should be small in these equations. Thus, it is not surprising that equation (42b) yields results in reasonable agreement with those of equation (37a). What is surprising is that the results of equation (42a) are not in as good agreement with either of these, and the reason for this is not known.

The small differences between the results of equations (37a) and (42b) can be tentatively attributed to the small centrifugal distortion effect (especially in (42b)) and also to the neglect of smaller terms (i.e. allowance for more case (b) interaction) in (37a). Since without further study it is not known which of these two factors is the more important, the final "best" values of p and q given in Table XII were taken as an average of the two sets.

These "best" values are in reasonable agreement with the values obtained by Dufayard and Nedelec for the v' = 0 level (Table XII). The values of Dufayard and Nedelec are

probably more accurate, because they not only corrected for the centrifugal distortion effect on the $^2\Pi_{3/2}$ substate but also took into account the second order terms of Dousmanis et al.

If the $^2\Pi$ state and a $^2\Sigma$ state stand to each other in the relation of pure precession, values for p and q can be calculated from the following expressions:

$$p = \pm \frac{2A_v B_v L(L+1)}{\nu_{\Pi,\Sigma}} \qquad \ldots(46a)$$

$$q = \pm \frac{2B_v^2 L(L+1)}{\nu_{\Pi,\Sigma}}, \qquad \ldots(46b)$$

where $\nu_{\Pi,\Sigma}$ has been defined previously,† and is positive (negative) if the Π level is above (below) the Σ level, and the $\pm$ sign is + for a $^2\Sigma^+$ state and - for a $^2\Sigma^-$ state. The fact that p and q have been found to be positive for the A $^2\Pi$ state of ZnD, means that if a pure precession relation with a $^2\Sigma^+$ state exists for this state, the other state involved must lie below the A $^2\Pi$ state in energy. (The possibility of a low - lying $^2\Sigma^-$ state above the A $^2\Pi$ state is unlikely.ʃ) The only known state of lower energy than the A $^2\Pi$ state is the X $^2\Sigma^+$ state. Using values of $\nu_{\Pi,\Sigma}$ obtained for these two states from the RKR potential energy curves (section III.D.4), using the values of B_v

---

† See page 15, especially the second footnote to the page.

ʃ See the first footnote on page 15.

for the $^2\Pi$ state,[†] and with L = 1 (predicted from the united atom), the pure precession values of p and q listed in Table XII are predicted. The experimental values of p are lower than the calculated ones. This is as expected, because the case of pure precession represents the maximum interaction between a Σ and a Π state.(2) The fact that the experimental values are lower indicates that the X $^2\Sigma^+$ and A $^2\Pi$ states of ZnD are not related to each other in the manner of the absolute limiting case of pure precession. But since the calculated values are at least of the correct order of magnitude, these states <u>may</u> still be partly related in this manner, with the relation not being completely good due to other influences (such as the unobserved B $^2\Sigma^+$ state).

The experimental q values would also be expected to be lower than the calculated ones. Comparison with the "best" values shows this to be true only for the v' = 0 level. The larger experimental values for the other two levels can most likely be attributed to the large relative uncertainty in the experimental values. (If the q values obtained from method (e) in Table XII, rather than the "best" values, are used in the comparison, the experimental values <u>are</u> lower than the values calculated for pure

---

[†] In the ideal case of pure precession, the B_v values would be the same for the two states. Otherwise, B_v for the $^2\Pi$ state should be used, according to the instructions of Mulliken and Christy.(2)

precession for all the levels. It may be that the method (e) values alone should really have been used as the "best" values.)

The values of γ_v (Table VIII) are similar, but not exactly equal to those of p (Table XII). In the case of pure precession, they would be exactly equal.(2)

III.B.5.a. Iterative procedure

In order to evaluate q by any of the methods employed, one has to have previously determined A_v. But in order to obtain A_v, one has to know B_v (and, for utmost accuracy, also p*, q*, and o), and B_v comes from B^*, which contains a term involving q* (= q), and this is what we wanted to find in the first place. Thus, an iterative procedure was used to obtain B_v, A_v, p (= p*), q (= q*), and o. Since q* is small relative to B_v, it was easy to obtain an initial value of B_v that was close to the true value. Convergence was achieved for all the parameters in two to three iterations. This procedure was applied to each vibrational level.

III.B.6. Effect of vibration on the rotational constants

The dependence of B_v on the vibrational state can be conveniently expressed as a power series:

$$B_v = B_e - \alpha_e(v + \tfrac{1}{2}) + \gamma_e(v + \tfrac{1}{2})^2 + \ldots , \qquad \ldots(47)$$

where B_e is the B value that would be obtained in the absence of vibration—that is, the value at the bottom of

the potential well, corresponding to the equilibrium position. The parameters α_e, γ_e, ... are the vibration - rotation interaction constants, which define the dependence of B_v on v. This variation of B_v with v is due mainly to the effect of anharmonicity.

The B_v^*" values of the X $^2\Sigma^+$ state were fitted to equation (47) by the method of least squares. The difference between B_v^* and B_v was ignored, and terms of higher order than the γ_e term were neglected. The values of B_e", α_e", and γ_e" thus determined are listed in Table XIII. For the A $^2\Pi$ state, the three B_v' values were used to form three equations based on (47), which were solved simultaneously to obtain B_e', α_e', and γ_e'. It turned out that γ_e' was negligible.

The centrifugal distortion constant, D_v, can also be fitted to a power series:

$$D_v = D_e + \beta_e(v + \tfrac{1}{2}) + \ldots . \qquad \ldots(48)$$

For the $^2\Sigma^+$ state, this was done by the method of least squares, and the values of D_e" and β_e" obtained are listed in Table XIII. For the three analyzed vibrational levels of the $^2\Pi$ state, the variation of D_v' with v' was negligible, so a fit to equation (48) was not done.

Both γ_v of the $^2\Sigma^+$ state and A_v of the $^2\Pi$ state have been observed to vary with v. These v - dependences can be expressed by empirical relations of the type of equation (47)—e.g. for A_v, the relation

TABLE XIII. Equilibrium rotational constants and vibration - rotation interaction constants.

(A) Constants

State	B_e	α_e	γ_e	D_e	β_e
$X\ ^2\Sigma^+$	3.399_0	$0.096\ 3_7$	$-0.004\ 97_1$	$1.15_6 \times 10^{-4}$	$0.006\ 4_4 \times 10^{-4}$
$A\ ^2\Pi$	3.777_2	0.086_8	—	—	—

(B) Comparison of the B_v and D_v values calculated from the constants in (A) with the experimental values.

	v			
	0	1	2	3
B_v^{*}'' (experimental)	3.349_8	3.242_6	3.127_6	3.000_6
B_v^{*}'' (calculated)	3.349_6	3.243_3	3.127_0	3.000_8
B_v' (experimental)	3.733_8	3.647_0	3.560_3	—
B_v' (calculated)	3.733_8	3.647_0	3.560_2	—
D_v (experimental)	$1.19_4 \times 10^{-4}$	$1.24_3 \times 10^{-4}$	$1.31_5 \times 10^{-4}$	$1.38_5 \times 10^{-4}$
D_v (calculated)	$1.18_8 \times 10^{-4}$	$1.25_3 \times 10^{-4}$	$1.31_7 \times 10^{-4}$	$1.38_1 \times 10^{-4}$

$$A_v = A_e - \alpha_A(v + \tfrac{1}{2}) \qquad \ldots(49)$$

has been used by a number of workers.[74],[75],[59] In view of the low number of analyzed vibrational levels for ZnD, it was not considered worthwhile to study the variation of A_v with v in any more detail than to note its

existence. The variation of γ_v has been mentioned in footnote (a) of Table VIII.

III.B.7. Effective rotational constants of the A $^2\Pi$ state

If $^2\Pi$ states have their angular momenta coupled in a manner approaching that of Hund's coupling case (a), the Hill and Van Vleck term $B_v[(J + 1/2) - 1 \pm 1/2\ X_v]$ (cf. equation (3) or (6)) can be replaced by

$$B_{v,eff}J(J + 1)\,, \qquad \ldots(50)$$

where the effective rotational constant differs for the two doublet components. According to Mulliken,[1] for doublet states

$$B_{v,eff} = B_v\left(1 \pm \frac{B_v}{A_v\Lambda} + \ldots\right)\,, \qquad \ldots(51)$$

where the + sign refers to the substate with $\Sigma = +1/2$ (i.e. $^2\Pi_{3/2}$ for $^2\Pi$ states) and the - sign refers to the substate with $\Sigma = -1/2$ (i.e. $^2\Pi_{1/2}$). For Π states, $\Lambda = 1$.

Often spectroscopists study the substates individually and obtain the $B_{v,eff}$ values directly. In order to obtain the true B_v values, they then average the $B_{v,eff}$ values. In the present study, the true B_v values were obtained directly, since it was felt that this method was more accurate. However, effective values were required to calculate the RKR potential curves (section III.D.4). These effective values were calculated from equation (51), with higher order terms neglected, and are given in Table XIV.

TABLE XIV. Calculated effective rotational constants for the A $^2\Pi$ state. The true B_v values are included for comparison.

v'	B_v	$B_{v,eff}$ ($^2\Pi_{1/2}$)	$B_{v,eff}$ ($^2\Pi_{3/2}$)
0	3.733_8	3.722_9	3.744_7
1	3.647_0	3.636_4	3.657_6
2	3.460_3	3.549_9	3.570_7

III.C. Vibrational Analysis

III.C.1. Band origins

The origin, ν_o, of a band is defined as follows. If T" and T' are the total term values of the ground state (X $^2\Sigma^+$) and excited state (A $^2\Pi$), respectively, then the wavenumber of the spectral line corresponding to a transition between them is given by

$$\nu = T' - T''$$

$$= [T_e' + G_v' + F_v'(J')] - [T_e'' + G_v'' + F_v''(N'')], \quad ...(52)$$

where the electronic (T_e), vibrational (G_v), and rotational (F_v) energies (in cm^{-1}) have been assumed to be completely independent of each other (Born - Oppenheimer approximation). Rearranging,

$$\nu = [T_e' - T_e''] + [G_v' - G_v''] + [F_v'(J') - F_v''(N'')]$$

$$= \nu_e + \nu_v + [F_v'(J') - F_v''(N'')]$$

$$= \nu_o + [F_v'(J') - F_v''(N'')], \quad ...(53)$$

where

$$\nu_o = \nu_e + \nu_v$$

$$= [T_e' - T_e''] + [G_v' - G_v''] . \qquad ...(54)$$

The particular ν_o for the 0-0 band is called ν_{oo}.

For the $^2\Pi$ state, the single mean rotational term can be obtained from equation (29):

$$F_v(J) = \frac{F_1(J) + F_2(J)}{2}$$

$$= B_v[(J + \tfrac{1}{2})^2 - 1] + \tfrac{1}{2}[o + \tfrac{1}{2}p^* + q^*(J + \tfrac{1}{2})^2]$$

$$- D_v[J^2(J + 1)^2 + \tfrac{1}{2}J(J + 1) + \tfrac{13}{16}] + \ldots . \qquad ...(55)$$

Similarly, for the $^2\Sigma^+$ state, from equation (1),

$$F_v(N) = \frac{F_1(N) + F_2(N)}{2}$$

$$= B_v^*N(N + 1) - \tfrac{1}{2}\gamma_v + 0 - D_vN^2(N + 1)^2 + \ldots . \qquad ...(56)$$

Then, for $N'' = J' - \frac{1}{2}$:

$$[F_v'(J') - F_v''(N'')] = [F_v'(J') - F_v''(J' - \tfrac{1}{2})]$$

$$= (B_v' - B_v^{*''})(J^2 - \tfrac{1}{4}) + B_v'(J - \tfrac{1}{2}) + \tfrac{1}{2}\gamma_v$$

$$+ \tfrac{1}{2}[o + \tfrac{1}{2}p^* + q^*(J + \tfrac{1}{2})^2] - 0$$

$$+ (D_v'' - D_v')(J - \tfrac{1}{2})^2(J + \tfrac{1}{2})^2$$

$$- D_v'(J + \tfrac{1}{2})(2J^2 - \tfrac{1}{2}) - D_v' , \qquad ...(57)$$

where the prime on J has been dropped. Upon substitution into equation (53), ν_o is given by

$$\nu_o^* = \nu - \{(B_v' - B_v^{*\prime\prime})(J^2 - \tfrac{1}{4}) + B_v'(J - \tfrac{1}{2}) + \tfrac{1}{2}\gamma_v''$$

$$+ \tfrac{1}{2}[o + \tfrac{1}{2}p^* + q^*(J + \tfrac{1}{2})^2] - O + (D_v'' - D_v')(J - \tfrac{1}{2})^2(J + \tfrac{1}{2})^2$$

$$- D_v'(J + \tfrac{1}{2})(2J^2 - \tfrac{1}{2}) - D_v' + \ldots . \qquad \ldots(58)$$

(The reason for the asterisk on ν_o^* will be discussed shortly.)

At this stage, a problem is encountered. The author is not aware of any method for evaluating O (other than in the case of pure precession, where[2] $O = -o$). The effects of interaction between states is often ignored when evaluating ν_o—that is, the $1/2[o + 1/2\ p^* + q^*(J + 1/2)^2] - O$ terms are neglected. Because O was unknown, this practice was followed here also, and this was done by defining a ν_o^{**} as

$$\nu_o^{**} = \nu_o^* + \tfrac{1}{2}[o + \tfrac{1}{2}p^* + q^*(J + \tfrac{1}{2})^2] - O . \qquad \ldots(59)$$

The quantity ν_o^* in equations (58) and (59) is still not the true ν_o as defined by equation (54), however, because a term which really belongs to the rotational part of the energy, but which is independent of J and which is not determinable from the spectrum, has been included with the vibronic energy.† This term (often represented by the symbol $B_v\langle\vec{L}_\perp^2\rangle$) has therefore not been included in any of the rotational energy expressions given in this text (for either the $^2\Sigma^+$ or $^2\Pi$ states).

---

† See references (1) and (76), for example.

Since most spectroscopists do not consider the $1/2\,[o + 1/2\,p^* + q^*(J + 1/2)\,] - O$ or $B_v\langle\vec{L}_\perp^2\rangle$ terms when evaluating band origins, the quantity that has here been called ν_o^{**} corresponds to what is normally called simply ν_o.

The terms $1/2\,[\ldots] - O$ consist of a J - dependent part and a J - independent part. In view of the inclusion of the $B_v\langle\vec{L}_\perp^2\rangle$ terms in with the vibronic energy, and therefore in ν_o^* and ν_o^{**}, the inclusion of the J - independent part of $1/2\,[\ldots] - O$ in ν_o^{**} is logical.

The J - dependence of $1/2\,[o + 1/2\,p^* + q^*(J + 1/2)^2] - O$, and hence of ν_o^{**}, consists of both the explicitly stated $(J + 1/2)^2$ factor and the hidden J - dependences of p^* and q^* (cf. equation (43)) and possibly also of o and O. To obtain the J - independent value of ν_o^{**}, ν_o^{**} has to be extrapolated to $J = 1/2$ (the lowest possible J value). The ν_o^{**}'s so determined correspond to the energy separation between the $J' = 1/2$ level of an $A\ ^2\Pi$ vibronic state and the $N'' = 0$ level of an $X\ ^2\Sigma^+$ vibronic state, where the $J' = 1/2$ level of the $A\ ^2\Pi$ state is the average of $F_1(1/2)$ and the hypothetical $F_2(1/2)$. Note that the ν_o^{**}'s are not exactly equal to this energy separation, due to the J - independent terms, $1/2\ \gamma_v^\circ$ and D_v':

$$\nu_o^{**\circ} = \nu_{J' = 1/2,\ N'' = 0} - [\tfrac{1}{2}\gamma_v^\circ - D_v'] , \qquad \ldots(60)$$

where the superscript zeroes are used to denote the J - independent part of γ_v and ν_o^{**}. The value of ν_{oo} for

ZnH given by Huber and Herzberg[4] is for essentially this same energy separation, so the values of ν_{oo} for ZnH and $\nu_{oo}^{**\circ}$ for ZnD can be compared (see section III.E.1). However, Huber and Herzberg apparently have included the $[1/2\ \gamma_v^\circ - D_v']$ term in with the vibronic energy—that is, $\nu_o^{**\circ} = \nu_{J' = 1/2,\ N'' = 0}$ for Huber and Herzberg's ZnH value.

The values of ν for the transitions between the J' levels of the $^2\Pi$ state and the N" = J' - 1/2 levels of the $^2\Sigma^+$ state were calculated from the term values, and, using the experimental values of B_v', B_v'', D_v', and γ_v,† ν_o^{**} was calculated for each J value. Graphs of ν_o^{**} as a function of J were then plotted. It was expected that the curves would asymptotically approach the J - independent $\nu_o^{**\circ}$ values with decreasing J, but in general this was not the case, as shown in Fig. 22. This resulted in some uncertainty in the manner in which the ν_o^{**} curves should be extrapolated to J = 1/2. The $\nu_o^{**\circ}$ values listed in the form of a Deslandres table in Table XV were determined by following the experimental points to as low J values as possible, then extrapolating, even though the behavior at low J was not asymptotic. Another possibility was to ignore the low - J points and extrapolate from the

---

† Actually γ_v° in the nomenclature of equation (60), which is a modification of that of Mulliken and Christy.[2]

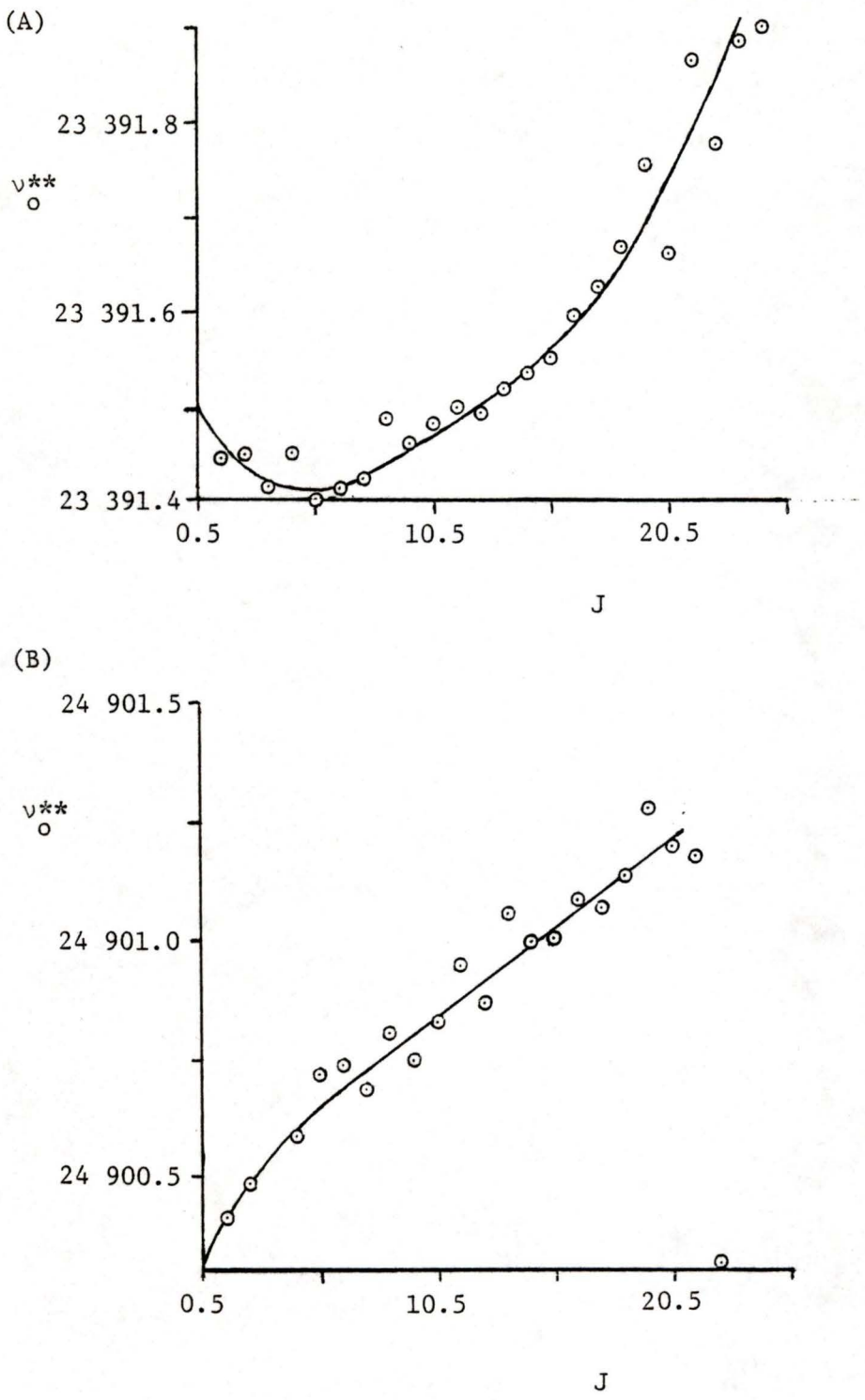

FIGURE 22. Determination of the J - independent value of ν_o^{**} — that is, $\nu_o^{**\circ}$. This is the value of ν_o^{**} at J = 0.5. Two types of behavior as the curve approaches J = 0.5 are shown. (A) 0-0 band. (B) 2-1 band.

TABLE XV. Deslandres table of band origins, $\nu_0^{**\circ}$, of the A $^2\Pi$ - X $^2\Sigma^+$ system. The horizontal and vertical differences are included (small type).

v' \ v''	0		1		2		3
0	23 391.50 ± 0.15	1089.79	22 301.71 ± 0.3	1032.58	21 269.13 ± 0.3	969.6_3	20 299.5 ± 0.5
	1320.08		1320.01		1320.02		1320.0
1	24 711.58 ± 0.4	1089.86	23 621.72 ± 0.5	1032.57	22 589.15 ± 0.3	969.6_5	21 619.5 ± 0.4
	1278.58		1278.60		1278.55		1278.7_5
2	25 990.16 ± 0.3	1089.84	24 900.32 ± 0.2	1032.62	23 867.70 ± 0.4	969.4_5	22 898.2_5 ± 0.4

moderate - and high - J points and possibly introduce a bend in the curve to achieve an asymptotic approach. The large uncertainties listed in Table XV allow for this second possibility. It is felt that the former method is probably the correct method to use, so the ν_o values in the table are probably better than would be indicated by the accompanying uncertainties. The constancy of the $\Delta G_{v + 1/2}$ values (see next section) lends support to this statement.

III.C.2. Vibrational constants

The vibrational quanta, $\Delta G_{v + 1/2}$, were calculated from the band origins:

$$\Delta G^{**}_{v' + 1/2} = G^{**}(v'+1) - G^{**}(v')$$

$$= \nu^{**\circ}_{o}(v'+1,v'') - \nu^{**\circ}_{o}(v',v'') \qquad \ldots(61a)$$

$$\Delta G^{**}_{v'' + 1/2} = G^{**}(v''+1) - G^{**}(v'')$$

$$= \nu^{**\circ}_{o}(v',v''+1) - \nu^{**\circ}_{o}(v',v'') \, . \qquad \ldots(61b)$$

These are included in Table XV, written in small type. The various possible values for each vibrational quantum, listed along horizontal or vertical rows, are in good agreement with each other. The averages[†] of these were used to calculate the vibrational constants in the (usual[3]) manner described below.

But first, the $\Delta G^{**}_{v' + 1/2}$ values (for the $^2\Pi$ state)

[†] The values involving v" = 3 were not included in the averages for $\Delta G^{**}_{v' + 1/2}$, since they were of lower accuracy than the others.

were corrected for the term $1/2\ (o + 1/2\ p^* + q^*(J + 1/2)^2]$ neglected in the ν_o^{**} determination. They could not be corrected for the neglected $B_v\langle\vec{L}_\perp^2\rangle$ term, however. Thus the $\Delta G_{v' + 1/2}^{**}$ values were converted into $\Delta G_{v' + 1/2}^{*}$ values. This was done by means of the equation[†]

$$\Delta G_{v' + 1/2}^{*} = \Delta G_{v' + 1/2}^{**} - \frac{1}{2}[o + \frac{1}{2}p^* + q^*]_{v'+1} + \frac{1}{2}[o + \frac{1}{2}p^* + q^*]_{v'} \ . \qquad ...(62)$$

The corrected and uncorrected values are given in Table XVI. The correction for the neglected O term could not be made for the $^2\Sigma^+$ state.

TABLE XVI. Vibrational quanta for the X $^2\Sigma^+$ and A $^2\Pi$ states.

$v + 1/2$	$\Delta G_{v'' + 1/2}^{**}$	$\Delta G_{v' + 1/2}^{**}$	$\Delta G_{v' + 1/2}^{*}$
1/2	1089.83_0	1320.03_7	1320.10_1
3/2	1032.59_0	1278.57_7	1278.71_5
5/2	969.5_{77}	—	—

In the following discussion, the asterisks have been dropped for simplicity. To be consistent with the nomenclature used in this thesis, a single asterisk should be added mentally to all the following G and ΔG values for the $^2\Pi$ state and a double asterisk for the $^2\Sigma^+$ state.

[†] J has been set to 1/2.

The second and third differences are defined as

$$\Delta^2 G_{v+1} = \Delta G_{v+3/2} - \Delta G_{v+1/2} \qquad \ldots(63)$$

$$\Delta^3 G_{v+3/2} = \Delta^2 G_{v+2} - \Delta^2 G_{v+1} . \qquad \ldots(64)$$

In terms of the vibrational constants, the term values of the anharmonic oscillator and the above $\Delta^i G$ values (i = 1 to 3) are given by the following expressions:

$$G(v) = \left[\frac{B_e}{4} + \frac{\alpha_e \omega_e}{12 B_e} + \frac{\alpha_e^2 \omega_e^2}{144\, B_e^2} - \frac{\omega_e x_e}{4}\right] + \omega_e(v+\tfrac{1}{2}) - \omega_e x_e (v+\tfrac{1}{2})^2 + \omega_e y_e (v+\tfrac{1}{2})^3 + \ldots \qquad \ldots(65)$$

$$\Delta G_{v+1/2} = (\omega_e - \omega_e x_e + \omega_e y_e) - (2\omega_e x_e - 3\omega_e y_e)(v+\tfrac{1}{2}) + 3\omega_e y_e (v+\tfrac{1}{2})^2 \qquad \ldots(66)$$

$$\Delta^2 G_{v+1} = -(2\omega_e x_e - 6\omega_e y_e) + 6\omega_e y_e (v+1/2) \qquad \ldots(67)$$

$$\Delta^3 G_{v+3/2} = 6\omega_e y_e , \qquad \ldots(68)$$

where higher order terms have been neglected. The term in square brackets in equation (65) is an approximate expression for Y_{oo} of the Dunham formula (equation (8)).† This constant term, which is a result of anharmonicity,(77) is often not included, but it does, in fact, contribute to the zero point energy.

Equations (66) - (68) yielded the values of ω_e'', $\omega_e x_e''$, and $\omega_e y_e''$ for the $X\ ^2\Sigma^+$ state listed in Table XVII. For

---

† As pointed out by Bunker,(78) the expression for Y_{oo} given by Herzberg (ref. (3), p. 109) contains a misprint.

TABLE XVII. Vibrational constants. The values in the column labelled "Corrected" were determined from the $\Delta G^{*}_{v + 1/2}$ values (Table XVI); those in the "Uncorrected" column, from the $\Delta G^{**}_{v + 1/2}$ values.

	Uncorrected	Corrected
ω_e''	1141.5_4	—
$\omega_e x_e''$	24.2_9	—
$\omega_e y_e''$	-0.96_2	—
ω_e'	1361.49_7	1361.48_7
$\omega_e x_e'$	20.73_0	20.69_3

the A $^2\Pi$ state, data were available for only three vibrational levels, so only two vibrational constants, ω_e', and $\omega_e x_e'$, could be obtained (Table XVII). This was accomplished by setting $\omega_e y_e$ to zero in equations (66) and (67).

The values of ω_e, $\omega_e x_e$, and $\omega_e y_e$ in Table XVII may have small errors in them, the magnitude of which is not known, due to the neglect of $B_v\langle\vec{L}_\perp^2\rangle$ and O (if O depends on v).

The origin of the band system ν_e (that is, the electronic energy separation of the two states) can now be evaluated (equations (54) and (65)) using the vibrational constants evaluated above and the previously determined $\nu_o^{**\circ}$ values. An average was taken over the nine bands having the smallest experimental uncertainties (v' = 0 - 2, v" = 0 - 2), yielding $\nu_e = 23\ 279.9_9\ cm^{-1}$. If the

Dunham Y_{oo} term is omitted from equation (65) (i.e. if Y_{oo} is considered to belong to the electronic energy, rather than the vibrational energy), the value obtained is $\nu_e^{**\circ} = 23\ 280.54_7\ cm^{-1}$. The latter type of value is the one which is usually reported.

The $\nu_o^{**\circ}$ values were re-calculated from this average $\nu_e^{**\circ}$ value (the latter one) and the vibrational constants, and the differences between the experimental and calculated $\nu_o^{**\circ}$ values were obtained. These differences were small ($\leq 0.03\ cm^{-1}$) for the bands in v' = 0 - 2, v" = 0 - 2; and $\leq 0.11\ cm^{-1}$ for the remaining three bands, v' = 0 - 2, v" = 3) and appeared to be random, so no further adjustments of the vibrational constants were made.

III.C.3. Vibrational terms, effective terms, and effective constants

Vibrational term values G(v) were required for the determination of the RKR potential curves (section III.D.4). These were determined in the following manner. Asterisks have again been omitted from the G and ΔG values and are to be added mentally: one for the $^2\Pi$ state and two for the $^2\Sigma^+$ state.

G(0) is simply the zero point energy and was calculated from the formula

$$G(0) = \frac{1}{2}\omega_e - \frac{1}{4}\omega_e x_e + \frac{1}{8}\omega_e y_e + \ldots . \qquad \ldots(69)$$

The Y_{oo} term was not used (cf. equation (65)); the G(v)

values determined here can easily be converted to those that would be obtained if Y_{oo} were included by adding the constant terms $+0.1_8$ and -0.38_6 cm^{-1} for the A $^2\Pi$ and X $^2\Sigma^+$ states, respectively (obtained from the term in square brackets in equation (65)). The $\omega_e y_e$ term was not used for the $^2\Pi$ state.

Each of the remaining G(v) values was then determined by summing the $\Delta G_{v + 1/2}$ values up to the appropriate vibrational level and adding this sum to the zero point value. The values are listed in Table XVIII.

TABLE XVIII. Vibrational terms of the X $^2\Sigma^+$ and A $^2\Pi$ states. The term Y_{oo} has not been included.

v	$G^{**}{}''(v)$	$G^{*}{}'(v)$	$G^{*}_{eff,^2\Pi 1/2}(v)$	$G^{*}_{eff,^2\Pi 3/2}(v)$
0	564.57_9	675.566_0	675.74_2	675.39_0
1	1654.40_9	1995.66_7	1996.0_0	1995.2_1
2	2686.99_9	3274.38_2	3274.6_1	3273.7_5
3	3656.5_{76}	—	—	—

For the $^2\Pi$ state, G values were required for the individual substates. These effective values were calculated from the true values by means of the equation

$$(G'_{eff}(v))_{prelim} = G'(v) \pm \tfrac{1}{2}B_v'X_v + \tfrac{1}{2}[o + \tfrac{1}{2}p^* + q^*]$$

$$\pm \frac{1}{2X_v}(2 - Y_v)(o + \tfrac{1}{2}p^* + q^*) - D_v', \qquad ...(70)$$

where the + sign in ± refers to the F_2 substate and the

- sign refers to the F_1 substate. This equation is obtained by means of equation (29) by setting J' = 1/2. That is, the effective G'(v) values are defined as corresponding to the lowest possible rotational level of each vibrational level (again, this is a fictional level for the F_2 substate). These effective values are labelled as preliminary, because the final values will have to be referred to the bottom of the potential wells, and the zero point energies (which will differ for the two substates), at this stage have not been evaluated. The differences between adjacent $(G'_{eff}(v))_{prelim}$ values gave $\Delta G'_{v + 1/2,\ eff}$ values, from which effective vibrational constants ($\omega_e'_{,\ eff}$, $\omega_e x_e'_{,\ eff}$) were calculated for each substate in the same manner as described previously. From these vibrational constants (Table XIX), effective zero point energies were calculated (equation (69)), and finally the remaining $G'_{eff}(v)$ values were determined relative to the bottoms of the potential wells of the two substates in the same manner as before. These are given in Table XVIII.

TABLE XIX. True and effective vibrational constants for the A $^2\Pi$ state.

	True constants	Effective constants	
		$^2\Pi_{1/2}$	$^2\Pi_{3/2}$
ω_e'	1361.48_7	1361.8_9	1361.1_0
$\omega_e x_e'$	20.69_3	20.8_2	20.6_4

III.D. Derived Quantities

Before deriving quantities from the spectroscopic constants, the magnitude of the terms neglected, according to Dunham,[27] in expressions such as (71) below will be considered. The neglected terms involve the ratio B_e^2/ω_e^2. For ZnD, this ratio has the value 8.866×10^{-6} for the $X\ ^2\Sigma^+$ state and 7.697×10^{-6} for the $A\ ^2\Pi$ state. ZnD is sufficiently heavy to make these values quite small. It has therefore been assumed that the higher terms can be safely neglected, at least in the expressions for B_e, and ω_e.[†] They may be of more importance in the expressions for α_e, D_e, and β_e,[3] but these were not of primary concern here.

III.D.1. Bond lengths

The rotational constant B_e is related to the equilibrium internuclear distance r_e according to the well - known expression

$$B_e = \frac{h}{8\pi^2 c I_e} \qquad \ldots(71)$$

$$I_e = \mu r_e^2 \ . \qquad \ldots(72)$$

[†] By way of comparison, B_e^2/ω_e^2 approaches 10^{-3} for H_2 and here the extra terms become of importance. Values of 10^{-6} are usually too small to be detected. Calculations have not been performed to check this in ZnD.

I_e is the moment of inertia in the equilibrium position, μ is the reduced mass, h is Planck's constant, and c is the velocity of light in vacuum.

The internuclear distance or "bond length' can also be defined for the vibrational state v by analogy with the equilibrium value, as follows:(3)

$$B_v = \frac{h}{8\pi^2 c\mu} \overline{\left[\frac{1}{r^2}\right]}_v \quad , \qquad \ldots(73)$$

where $\overline{[1/r^2]}_v$ is the mean value of $1/r^2$ during the vibration. The internuclear distance is then defined as

$$r_v = \overline{\left[\frac{1}{r^2}\right]}_v^{-1/2} \quad . \qquad \ldots(74)$$

Values of I_e, r_e, and r_v are given in Table XX. The value of r_e is slightly smaller in the A $^2\Pi$ state than in the X $^2\Sigma^+$ state, and both values depict a fairly long bond. Within each state, r_v increases with v due to the effect of anharmonicity.

III.D.2. Force constants

The force constant k measures the force required to stretch a bond by a given distance and is thus related to the strength of the bond and to the shape of the potential curve. The value of the force constant at the bottom of the potential well, k_e (i.e. the value for infinitesimal vibrational amplitudes), can be obtained from the vibrational constant ω_e by means of the well -

TABLE XX. Moments of inertia and bond lengths of ^{64}ZnD.(a)

(A) Equilibrium values:

	I_e(kg m^2)	r_e(nm)
X $^2\Sigma^+$	$8.235_8 \times 10^{-47}$	$0.159\ 3_7$
A $^2\Pi$	$7.411_1 \times 10^{-47}$	$0.151\ 1_9$

(B) Effective vibrational values:

v	X $^2\Sigma^+$		A $^2\Pi$	
	I_v(kg m^2)	r_v(nm)	I_v(kg m^2)	r_v(nm)
0	$8.356_8 \times 10^{-47}$	$0.160\ 5_4$	$7.497_3 \times 10^{-47}$	$0.152\ 0_6$
1	$8.633_0 \times 10^{-47}$	$0.163\ 1_7$	$7.675_6 \times 10^{-47}$	$0.153\ 8_6$
2	$8.950_3 \times 10^{-47}$	$0.166\ 1_4$	$7.862_6 \times 10^{-47}$	$0.155\ 7_2$
3	$9.329_3 \times 10^{-47}$	$0.169\ 6_3$	—	—

(a) The following quantities were used to calculate the above values from the B_e and B_v values:(79) $h = 6.626\ 176 \times 10^{-34}$ J·s, $c = 2.997\ 924\ 58 \times 10^8$ m·s^{-1}. The reduced mass of ^{64}ZnD is given in Table XXIV.

known formula(3)

$$\omega_e = \frac{1}{2\pi c}\sqrt{\frac{k_e}{\mu}} \quad . \qquad \ldots(76)$$

The values given in Table XXI for ZnD are typical of fairly weak bonds. (For comparison, the very strong bond in $N \equiv N$ has a force constant of 2295 $N \cdot m^{-1}$ in the ground state.[4]) The force constant is greater in the A $^2\Pi$ state than in the X $^2\Sigma^+$ state, and this is related to the shorter bond length already noted in the A $^2\Pi$ state.

TABLE XXI. Force constants.

	k_e ($N.m^{-1}$)
X $^2\Sigma^+$	149.91_7
A $^2\Pi$	213.25_3

III.D.3. Dissociation energies

If the vibrational levels can be represented accurately by[†]

$$G(v) = \omega_e(v + \tfrac{1}{2}) - \omega_e x_e(v + \tfrac{1}{2})^2 \qquad \ldots(76)$$

with higher powers of (v + 1/2) being negligible, then the dissociation energy measured with respect to the bottom of the potential well, D_e, or measured with respect

[†] As shown below, this method of determining the dissociation energy yields only approximate results, so Y_{oo} can be ignored.

to the zero point energy level, D_o, can be calculated from the well - known Birge - Sponer equations:†

$$D_e = \frac{\omega_e^2}{4\omega_e x_e} \qquad \ldots(77a)$$

$$D_o = \frac{\omega_o^2}{4\omega_o x_o} \; . \qquad \ldots(77b)$$

These equations are obtained by finding v_{max}, the value of v at which G(v) (or $G_o(v)$ when referred to the zero point energy) no longer increases with increasing v —i.e. the derivative dG/dv (or dG_o/dv) is set equal to zero. The value obtained is:

$$v_{max} = \frac{\omega_e}{2\omega_e x_e} - \frac{1}{2} \qquad \ldots(78a)$$

$$v_{max} = \frac{\omega_o}{2\omega_o x_o} \; . \qquad \ldots(78b)$$

The value of G(v) (or $G_o(v)$) at which this occurs is the dissociation energy. Substitution of the expressions for v_{max} into equation (76) then yields equations (77a) and (77b)—$G(v_{max}) = D_e$; $G_o(v_{max}) = D_o$. The relationship between D_e and D_o is

$$D_e = D_o + G(0) \; . \qquad \ldots(79)$$

(This derivation has been repeated here, because it has

---

† The relationships between the vibrational constants used when energies are expressed relative to G(0), the zero point energy (ω_o, $\omega_o x_o$, ...), and those when referring to the bottom of the potential well (ω_e, $\omega_e x_e$, ...) are given by Herzberg.(3)

been extended to include the next higher power of $(v + 1/2)$ (see below)—a method which is not as common.)

Dissociation energies obtained by this method are often in error by a considerable amount (usually high, often by as much as 40% or more).

An alternative approach is to plot $\Delta G_{v + 1/2}$ against v. The area under this curve is the dissociation energy D_o, since[†]

$$D_e = G(v_{max}) = \sum_{v = -\frac{1}{2}}^{v_{max}} \Delta G_v \qquad \ldots(80a)$$

$$D_o = G_o(v_{max}) = \sum_{v = 0}^{v_{max}} \Delta G_{v + 1/2} \, . \qquad \ldots(80b)$$

If equation (76) describes the situation exactly, then the curve will be linear and the area will give the same value of D_o as equation (77b). Otherwise, this method gives better values than equation (77b).

For the $X\ ^2\Sigma^+$ state of ZnD, equation (76) is not exact; a value of $\omega_e y_e$, corresponding to the next higher power of $(v + 1/2)$, has been obtained. Still higher terms are probably needed to describe the situation exactly, but these are not available. A plot of $\Delta G_{v + 1/2}$ against v is not linear in this case (Fig. 23). As an aid in extrapolating the plot, the value of v_{max} can be calculated:

$$v_{max} = \frac{2\omega_e x_e - 3\omega_e y_e \pm 2\sqrt{(\omega_e x_e)^2 - 3\omega_e(\omega_e y_e)}}{6\omega_e y_e} \qquad \ldots(81a)$$

[†] ΔG_v is the value intermediate between $\Delta G_{v + 1/2}$ and $\Delta G_{v - 1/2}$.

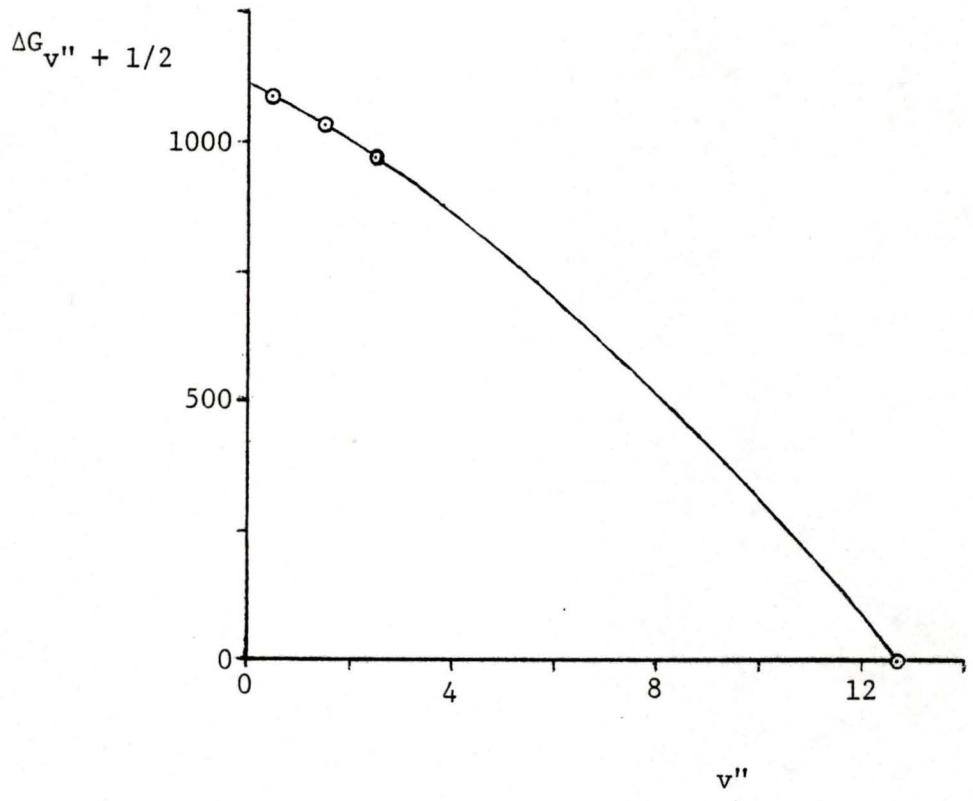

FIGURE 23. Determination of the dissociation energy of the $X\ ^2\Sigma^+$ state of ZnD. The dissociation energy D_o equals the area under the curve.

$$v_{max} = \frac{\omega_o x_o \pm \sqrt{(\omega_o x_o)^2 - 3\omega_o(\omega_o y_o)}}{3\omega_o y_o} \quad \ldots(81b)$$

These equations were obtained in the same manner as equations (78a) and (78b). The + or - sign is chosen (according as $\omega_o y_o$ is positive or negative, respectively) so that the value of v_{max} is positive. For the $X\ ^2\Sigma^+$ state of ZnD, from equation (81), $v_{max} = 12._7$.

The dissociation energy can be obtained by determining the area under the curve, or it can be calculated. The latter method avoids the problem of accurately interpolating the graph in the region between the experimental points and the calculated point at v_{max}. It can be done either by substituting the numerical value of v_{max} into the expression for G to obtain $G(v_{max})$ or $G_o(v_{max})$ (= D_e or D_o) or by substituting the algebraic expression for v_{max} into the expression for G to obtain a general expression for D_e or D_o (analogous to equations (77a) and (77b)). The expression for D_o is:

$$D_o = \frac{3\omega_o(\omega_o x_o) \pm 2\omega_o\sqrt{(\omega_o x_o)^2 - 3\omega_o(\omega_o y_o)}}{9\omega_o y_o}$$

$$- \frac{2(\omega_o x_o)^3 \pm 2(\omega_o x_o)^2\sqrt{(\omega_o x_o)^2 - 3\omega_o(\omega_o y_o)}}{27(\omega_o y_o)} \quad \ldots(82)$$

This is a considerably more complex expression than equation (77), undoubtedly the reason why it is not normally used. If still higher power terms of (v + 1/2) beyond the $\omega_e y_e$ term are required to fit the observed

vibrational levels, analogous equations could be derived but would be too complex to be of much practical use. Even equation (82) is of doubtful value.

An easier method would then be to calculate successive values of $G(v)$ or $G_o(v)$ from equations like (76) but with higher power terms included. The maximum value of G is the dissociation energy.

For the $X\ ^2\Sigma^+$ state of ZnD, equation (82) yields a value of $8._{06} \times 10^3\ cm^{-1}$ for D_o^o.† From equation (79), the equilibrium value is $D_e = 8._{62} \times 10^3\ cm^{-1}$. If the $\omega_e y_e$ term is omitted, a linear Birge - Sponer extrapolation (equation (77)) yields $D_o^o = 12.1_1 \times 10^3\ cm^{-1}$—considerably different from the above value, which should be the better value. The inclusion of the $\omega_e z_e$ term (if available) or the graphical equivalent (more $\Delta G_{v + 1/2}$ values to plot against a wider range of v) would probably further refine the $8._{06} \times 10^3\ cm^{-1}$ value.

For the $A\ ^2\Pi$ state, only the vibrational constants ω_e and $\omega_e x_e$ are known. By the above methods, the best that can be done is to use equation (77) to obtain a value of $D_o = 2.172 \times 10^4\ cm^{-1}$ and $D_e = 2.239 \times 10^4\ cm^{-1}$.

An alternative method is available for determining

---

† The superscript on D_o^o indicates that this is the energy required to dissociate the molecule from the lowest rotational and vibrational level of the ground electronic state to the normal atoms.

the dissociation energy of the A $^2\Pi$ state. As can be seen from Fig. 1,

$$D_e(A\ ^2\Pi) = D_e(X\ ^2\Sigma^+) + \nu_{^3P - {}^1S} - \nu_{e\ ^2\Pi - {}^2\Sigma^+}\ , \qquad ...(83)$$

where $\nu_{e\ ^2\Pi - {}^2\Sigma^+}$ is the electronic energy separation of the two molecular states ($\simeq \nu_e^{**\circ} = 23\ 280\ cm^{-1}$) and $\nu_{^3P - {}^1S}$ is the energy separation of the first excited state (^3P) and ground state (^1S) of atomic Zn (32 567 cm^{-1}).† The value obtained is $D_e(A\ ^2\Pi) = 1.7_9 \times 10^4\ cm^{-1}$.

The dissociation energies quoted above are not expected to be very accurate. In addition to the neglect of higher power (v + 1/2) terms, at least one, and possibly two, factors have not been allowed for which can cause considerable errors. First, as already discussed with reference to Fig. 1, the X $^2\Sigma^+$ state is most likely involved in an avoided crossing between two $^2\Sigma^+$ states. Since only the lowest vibrational levels have been observed and since this region of the potential curve is little perturbed by the other $^2\Sigma^+$ state, the experimental dissociation energy might actually be closer to that of the fictitious unperturbed state than to that of the actual state. Thus, the value obtained is expected to be greater than the true dissociation energy.

---

† An average of the three values given by Moore[80] for the three components of the triplet atomic state is given, since it is not known to which component the $^2\Pi$ state correlates.

Second, for states which have ionic character, the opposite effect has been observed to occur in a number of molecules—i.e. dissociation energies obtained by the above methods are smaller than the true values. This may have some effect in ZnD; the possibility of some ionic character has been discussed previously (section I.A).

Stenvinkel[16] has obtained a value of $D_o^\circ = 6.8_6 \times 10^3$ cm^{-1} for the X $^2\Sigma^+$ state of ZnH. Since there is very little isotope effect on electronic energies (see section III.E.1), the values for ZnH and ZnD should be almost identical. The difference is due to the fact that Stenvinkel had data available on more vibrational levels for ZnH than are presently available for ZnD. Using data from levels closer to the dissociation limit allows a more realistic $\Delta G_{v + 1/2}$ versus v curve to be plotted—i.e. the factors discussed above which affect the dissociation energy determination are more likely to be better taken into account. Thus, the value $D_o^\circ = 6.8_6 \times 10^3$ cm^{-1} is probably closer to the true dissociation energy of the X $^2\Sigma^+$ state of ZnH or ZnD than the value $8._{06} \times 10^3$ cm^{-1} determined here.

III.D.4. RKR potential energy curves and Franck - Condon factors

The Rydberg - Klein - Rees procedure is the most practical method for determining a potential energy function directly from the experimental vibrational and rotational

spectroscopic constants. RKR curves for the X $^2\Sigma^+$ and A $^2\Pi$ states of ZnD have been calculated by means of a computer program by Zare.[81] For the $^2\Pi$ state, effective curves for the two substates were calculated. The classical turning points are given in Table XXII, and the curves are shown in Fig. 24.

TABLE XXII. Potential energy curves for the X $^2\Sigma^+$ and A $^2\Pi$ states of ZnD calculated by the RKR method. The true or effective $G_o(v)$ and B_v values used to calculate the curves are given, along with the classical turning points.

	v	$G_o(v)$	B_v	r_{min}(nm)	r_{max}(nm)
X $^2\Sigma^+$	0	0	3.349_8	$0.148\ 2_0$	$0.173\ 0_3$
	1	1090	3.242_6	$0.141\ 3_9$	$0.185\ 2_7$
	2	2122	3.127_6	$0.137\ 2_7$	$0.195\ 2_7$
	3	3092	3.000_6	$0.134\ 2_9$	$0.204\ 7_8$
A $^2\Pi_{1/2}$	0	0	3.722_9	$0.141\ 0_8$	$0.163\ 7_5$
	1	1320	3.636_4	$0.134\ 5_8$	$0.174\ 3_6$
	2	2599	3.549_9	$0.128\ 2_7$	$0.185\ 0_7$
A $^2\Pi_{3/2}$	0	0	3.744_7	$0.140\ 6_4$	$0.163\ 3_1$
	1	1320	3.657_6	$0.134\ 1_4$	$0.173\ 9_2$
	2	2598	3.570_7	$0.127\ 8_2$	$0.184\ 6_1$

The intensity of a band is proportional to its Franck - Condon factor (the square of the overlap integral for the two states involved in the transition). The proportionality constant includes a factor for the population of the initial state. Franck - Condon factors

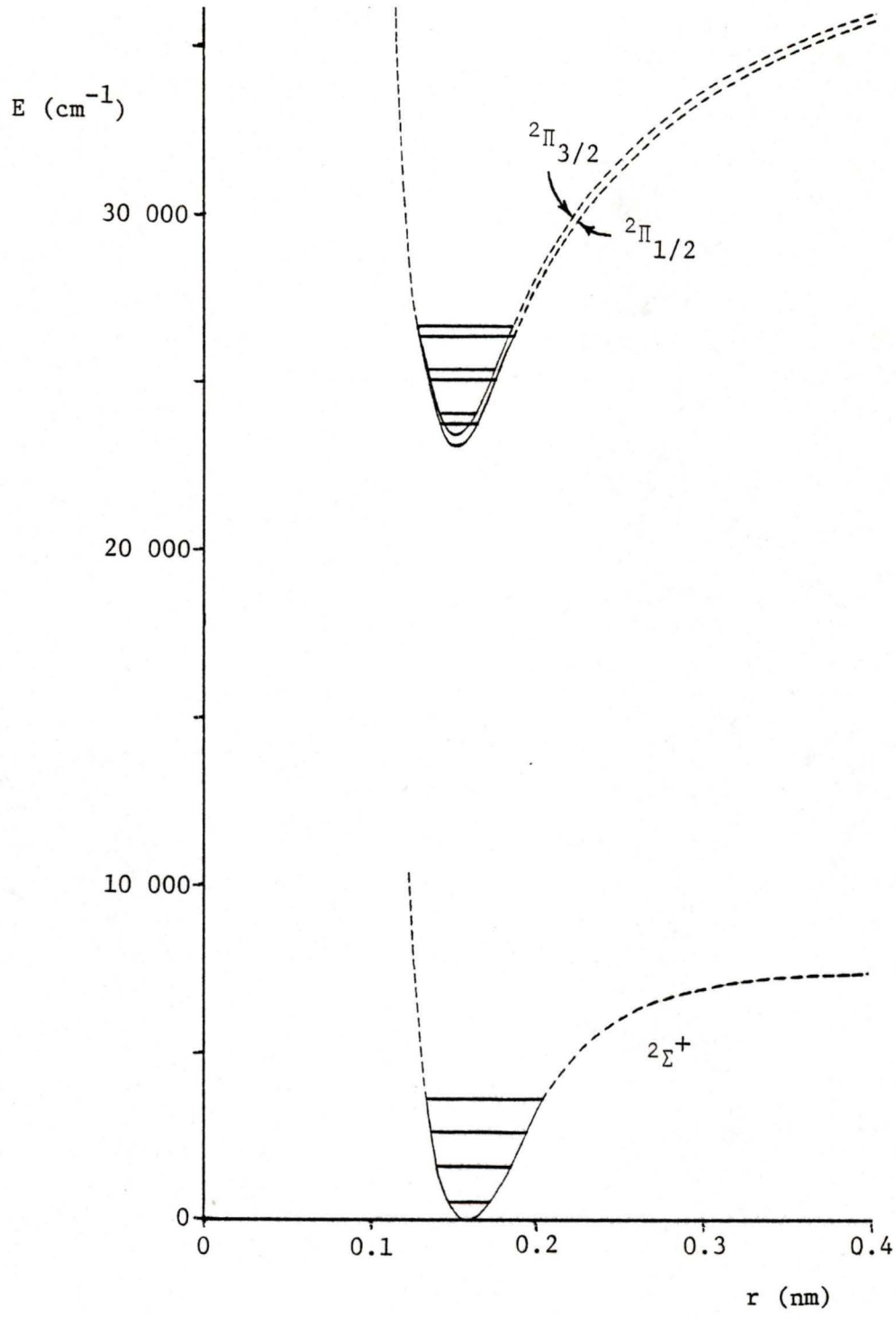

FIGURE 24. RKR potential energy curves for the X $^2\Sigma^+$ and A $^2\Pi$ states of ZnD.

have been calculated with another program by Zare.[81] These are given in Table XXIII.

TABLE XXIII. Franck - Condon factors for the A $^2\Pi$ - X $^2\Sigma^+$ system of ZnD.

	v' \ v"	0	1	2	3
$^2\Pi_{1/2}$	0	0.779 0	0.181 1	0.032 8	0.005 5
	1	0.203 0	0.425 4	0.252 2	0.084 7
	2	0.017 8	0.351 8	0.206 2	0.210 4
$^2\Pi_{3/2}$	0	0.758 4	0.193 5	0.038 6	0.007 2
	1	0.220 2	0.385 4	0.256 8	0.094 2
	2	0.021 0	0.371 6	0.168 4	0.202 6

The Franck - Condon factors are in good qualitative agreement with the intensities of the bands observed in the spectrum. The 0-0 band is the most intense band. The 0-1 and 1-0 bands have similar intensities to each other and are of lesser intensity than the 0-0 band.

III.E. Isotope Effect

The effect on the spectrum of isotopic substitution is discussed both for the hydrogen isotopes and for the three most abundant zinc isotopes. Since the change in the reduced mass of the molecule is much greater upon

exchange of deuterium for hydrogen than for interchange of the zinc isotopes, the isotope effect on the spectrum is much larger in the former case than in the latter. Very accurate reduced masses obtained from mass spectrographic data are given in Table XXIV.

TABLE XXIV. Reduced masses[(a)]

	amu	kg
^{64}ZnH	0.992 183 5	$1.647\ 586 \times 10^{-27}$
^{66}ZnH	0.992 650 2	$1.648\ 361 \times 10^{-27}$
^{68}ZnH	0.993 090 2	$1.649\ 091 \times 10^{-27}$
^{64}ZnD	1.952 585	$3.242\ 396 \times 10^{-27}$
^{66}ZnD	1.954 394	$3.245\ 398 \times 10^{-27}$
^{68}ZnD	1.956 100	$3.248\ 232 \times 10^{-27}$

(a) $\mu = \dfrac{m_{Zn} m_{H \text{ or } D}}{m_{Zn} + m_{H \text{ or } D}}$. Calculated from the masses listed in ref. (82).

III.E.1. ZnH versus ZnD

The total displacement between corresponding band lines of two isotopic molecules is the sum of electronic, vibrational, and rotational parts:

$$\Delta\nu = \Delta\nu_e + \Delta\nu_v + \Delta\nu_r \qquad \ldots(84)$$

The potential energy curve of a given electronic state is generally assumed to be invariant to isotopic substitution —i.e. $\Delta\nu_e$ is assumed to be zero. However, due to partial breakdown of the Born - Oppenheimer approximation, a small isotopic shift is often observed, especially for the lighter hydrides. Bunker[78] has given an approximate expression for this shift:

$$\Delta\nu_e = \nu_e(\mathrm{ZnH}) - \nu_e(\mathrm{ZnD})$$

$$= 0.000\ 068\ [\nu_e]$$

$$+ [B_c'(\mathrm{ZnH}) - B_e'(\mathrm{ZnD})][\langle\vec{L}'^2\rangle - \Lambda'^2 + S'(S'+1) - \Sigma'^2 - \Omega'^2]$$

$$- [B_e''(\mathrm{ZnH}) - B_e''(\mathrm{ZnD})][\langle\vec{L}''^2\rangle - \Lambda''^2 + S''(S''+1) - \Sigma''^2 - \Omega''^2]. \quad \ldots(85)$$

An average value of ν_e for ZnH and ZnD can be used in this expression. Theory has not yet been developed for the evaluation of the term $\langle\vec{L}^2\rangle$; Bunker suggests using the very approximate separated atom value:

$$\langle\vec{L}^2\rangle \simeq [L_H(L_H+1) + L_{Zn}(L_{Zn}+1)]\ , \quad \ldots(86)$$

where $L_H' = L_H'' = L_{Zn}'' = 0$, $L_{Zn}' = 1$. The approximate value of $\Delta\nu_e$ predicted by this method is, when the $^2\Pi_{1/2}$ substate is involved, 3.6_9 cm^{-1}, and for the $^2\Pi_{3/2}$ substate, -3.6_2 cm^{-1}. Interestingly, the shifts for the two substates are in opposite directions but of similar magnitudes.† These shifts were not compared directly with experimental values, since the ν_e value ($\nu_e^{**\circ}$) determined

† Footnote on next page.

here for ZnD and that given by Huber and Herzberg[4] for ZnH involve the $^2\Pi$ state that would exist in the absence of spin - orbit splitting, rather than effective values for the two substates. An average of the two predicted values of $\Delta\nu$ is +0.04 cm^{-1}, and this can be easily checked with the observed value: -6.8 cm^{-1}.[ʃ] Agreement is not good, which is not surprising considering the approximations involved in the derivation of equation (85) and especially in view of the approximation involved in using equation (86) and also especially in view of the fact that the $B\langle\vec{L}_\perp^2\rangle$ terms were neglected when determining the "observed" shift. The approximate formula used to calculate the Y_{oo} terms may also have contributed to the discrepancy. The conclusion of the author is that until better methods are available for determining $\langle\vec{L}^2\rangle$ and $\langle\vec{L}_\perp^2\rangle$, electronic isotope shifts are difficult to study.

The vibrational isotope shift is of considerably larger magnitude and the theory is better developed.

[†] Note that this does not mean that the A $^2\Pi$ substates themselves shift by about equal magnitudes in opposite directions energywise. The X $^2\Sigma^+$ states are also involved and the shift in these is the same regardless of whether the other state is $^2\Pi_{1/2}$ or $^2\Pi_{3/2}$.

[ʃ] In calculating this shift, the ν_e value given by Huber and Herzberg (23 276.9 cm^{-1}) was corrected for the $[1/2\ \gamma_e^\circ - D_e]$ term (see the discussion below equation (60)) (23 276.8 cm^{-1})—Y_{oo} was properly included as a vibrational term here. The final value (23 273.2 cm^{-1}) is now defined in the same manner as $\nu_e^{**\circ}$ (= 23 279.9_9 cm^{-1}) defined earlier in this thesis for ZnD.

To a good approximation, the shift is given by the equation[73]

$$\Delta\nu_v = \nu_v - \nu_v^{\,i} = (1 - \rho)[\omega_e'(v' + \tfrac{1}{2}) - \omega_e''(v'' + \tfrac{1}{2})]$$

$$- (1 - \rho^2)[\omega_e x_e'(v' + \tfrac{1}{2})^2 - \omega_e x_e''(v'' + \tfrac{1}{2})^2] , \qquad ...(87)$$

where the superscript i denotes the isotopic molecule and will be used here to refer to the heavier isotope. The ω_e and $\omega_e x_e$ values are those of the lighter molecule. The constant ρ is defined as

$$\rho = \left[\frac{\mu}{\mu^i}\right]^{1/2} , \qquad ...(88)$$

where μ and μ^i are the reduced masses.

It follows from equation (87) that the band system of the heavier molecule will be contracted relative to that of the lighter molecule, since ρ, as here defined, is less than one. With one exception, the ν_v values were not compared quantitatively, since the ν_o values given by Stenvinkel[16] for ZnH were defined in a different manner from those obtained here for ZnD. Qualitatively, the contraction of the ZnD bands relative to the ZnH bands was observed. It was possible to quantitatively compare the ν_v values for one set—the $v' = 0 \rightarrow v'' = 0$ transition—since the value of ν_{oo} given by Huber and Herzberg[4] for ZnH did correspond in definition with the value calculated here (and called ν_{oo}^{**o}) for ZnD, after making the small correction for the $[1/2\ \gamma_v^o - D_v']$ term (see the discussion

under equation (60)):

$$\Delta\nu_{v=0} = 47.0 \quad \text{(observed)}$$

$$\Delta\nu_{v=0} = 45.21 \quad \text{(calculated from equation (87)).}$$

Agreement is reasonable. It is not intended to discuss here the reasons for the small difference. One obvious possible source of error will be mentioned: the approximate formula used to evaluate Y_{oo} (the terms in the square bracket in equation (65)). Other sources of error have been discussed in the references cited by Johnson (ref. 73, p. 181).

A good approximation to the rotational isotope shift is given by the formula[3]

$$\begin{aligned}\Delta\nu_r &= \nu_r - \nu_r^i \\ &= (1-\rho^2)\{B_e'J'(J'+1) - B_e''N''(N''+1)\} \\ &\quad - (1-\rho^3)\{\alpha_e'(v'+\tfrac{1}{2})J'(J'+1) - \alpha_e''(v''+\tfrac{1}{2})N''(N''+1)\} \\ &\quad - (1-\rho^4)\{D_e'[J'^2(J'+1)^2 - \tfrac{1}{2}J'(J'+1) + \tfrac{13}{16}] \\ &\qquad - D_e''N''^2(N''+1)^2\} \\ &\quad - (1-\rho^5)\{\beta_e'[(v'+\tfrac{1}{2})J'^2(J'+1)^2 - \tfrac{1}{2}J'(J'+1) + \tfrac{13}{16}] \\ &\qquad - \beta_e''(v''+\tfrac{1}{2})N''^2(N''+1)^2, \qquad \ldots(89)\end{aligned}$$

where the Almy and Horsfall centrifugal distortion expression has been used for the $^2\Pi$ state, though equation (91) below may not be valid for these. The $^2\Pi$ state complicates the use of equation (89). $\Delta\nu_r$ values

could be calculated for each substate by means of the formula as written, using effective values of B_e', α_e'', D_e', and β_e', if the $^2\Sigma - {}^2\Pi$ interaction (Λ - doubling, etc.) is ignored. Alternatively, the formula could be modified by substituting the Hill and Van Vleck expression (equation (3)) for $B_e'J'(J' + 1)$; then the true B_e', α_e', D_e', and β_e' values would be used. However, the relations obtained from equation (91) below may not be valid in this case (but see below). Also, the $^2\Sigma - {}^2\Pi$ interaction has again been ignored. This neglect of the $^2\Sigma - {}^2\Pi$ interaction would mean that the $\Delta\nu_r$ values would be expected to be even poorer than those normally obtained from expressions like equation (89), since the $\Sigma - \Pi$ interaction parameters (p, q, etc.) would be altered by isotopic substitution. In view of these complications, and since $\Delta\nu_r$ would be small compared with $\Delta\nu_v$, equation (89) has not been tested directly here (but the isotope effect on the individual rotational constants has been tested—see the following paragraphs).

The isotope effect can also be expressed in terms of the individual vibrational and rotational constants. Kemble and Van Vleck[83] have shown that if the potential curves of the isotopic molecules are regarded as identical, and if the vibrational - rotational term values are written in the form of equation (8), then the vibrational and rotational constants for the different isotopes can be related as follows:

$$\frac{Y_{\ell m}{}^{i}}{Y_{\ell m}} = \rho^{(\ell + 2m)} \quad . \qquad \ldots(90)$$

That is (cf. equation (9)):

$$\omega_e{}^{i} = \rho\omega_e \qquad \ldots(91a)$$

$$\omega_e x_e{}^{i} = \rho^2 \omega_e x_e \qquad \ldots(91b)$$

$$\omega_e y_e{}^{i} = \rho^3 \omega_e y_e \qquad \ldots(91c)$$

$$B_e{}^{i} = \rho^2 B_e \qquad \ldots(91d)$$

$$\alpha_e{}^{i} = \rho^3 \alpha_e \qquad \ldots(91e)$$

$$D_e{}^{i} = \rho^4 D_e \qquad \ldots(91f)$$

$$\beta_e{}^{i} = \rho^5 \beta_e \quad . \qquad \ldots(92g)$$

These relations have been assumed in the expressions given earlier for $\Delta\nu_v$ and $\Delta\nu_r$.

To test these relations for ZnD versus ZnH, values of ρ were calculated from them. These are given in Table XXV. Comparison with the very accurate mass spectrometry value shows good agreement, particularly for the values obtained from ω_e', $\omega_e x_e'$, and B_e'. The especially good agreement in the latter case is somewhat surprising, since the rotational terms of the $^2\Pi$ state were not expressed in the form of equation (8). The agreement becomes increasingly poorer as ℓ or m increases, a result which can probably be attributed to the fact that the usual, mechanical expressions for $Y_{\ell m}$ become increasingly

TABLE XXV. Comparison of the values of ρ obtained from the spectral constants[3] with each other and with the mass spectrometry value—for ^{64}ZnD versus ^{64}ZnH.

	ρ
Mass spec. value	0.712 838 3
$\frac{\omega_e''^{i}}{\omega_e''}$	$0.710\ 09_0$
$\left[\frac{\omega_e x_e''^{i}}{\omega_e x_e''}\right]^{1/2}$	0.663_7
$\left[\frac{\omega_e y_e''^{i}}{\omega_e y_e''}\right]^{1/3}$	-1.3_4
$\frac{\omega_e'^{,i}}{\omega_e'}$	$0.712\ 74_6$
$\left[\frac{\omega_e x_e'^{,i}}{\omega_e x_e'}\right]^{1/2}$	0.712_2
$\left[\frac{B_e''^{i}}{B_e''}\right]^{1/2}$	$0.713\ 3_6$
$\left[\frac{\alpha_e''^{i}}{\alpha_e''}\right]^{1/3}$	0.727_8
$\left[\frac{\gamma_e''^{i}}{\gamma_e''}\right]^{1/4}$	0.602_8
$\left[\frac{B_e'^{,i}}{B_e'}\right]^{1/2}$	$0.712\ 8_5$
$\left[\frac{\alpha_e'^{,i}}{\alpha_e'}\right]^{1/3}$	$0.71_4\ 0$

poorer approximations to $Y_{\ell m}$ as ℓ or m increase, due to the increasing importance of higher order terms. This effect has been discussed by Crawford and Jorgensen,[84] who give more accurate expressions to account for it. The only particularly bad value of ρ (even the wrong sign) is that obtained from $\omega_e y_e$". This is probably because the $\omega_e y_e$ value was calculated in the absence of an $\omega_e z_e$ term for ZnD but with an $\omega_e z_e$ term for ZnH. $\omega_e z_e$ is actually larger in absolute value than $\omega_e y_e$ for ZnH.[4] The two $\omega_e y_e$ values are therefore not comparable. Other possible reasons for the discrepancies in the other ρ values are discussed in the references cited by Johnson (ref. 73, p. 181).

III.E.2. Zinc isotope effect

The reduced mass changes by only a small amount upon changing the isotopes of zinc (cf. Table XXIV). Therefore, the isotopic splitting is very small. The three most abundant isotopes of zinc, followed by their natural abundances (%) are ^{64}Zn, ^{66}Zn, and ^{68}Zn; 48.63, 27.90, and 18.75.[85] Lines due to these three isotopes have been clearly resolved in the spectra (Fig. 25). The relative intensities are visually in agreement with the above natural abundances—exact intensities were not measured.

The measured splittings of the lines of the $^{O}P_{12}$ branch of the 0-1 band are given in Table XXVI. The

FIGURE 25. Zinc isotopic splitting in the $^{O}P_{12}$ branch of the 0-1 band of the A $^{2}\Pi$ - X $^{2}\Sigma$ system of ZnD. Frequencies of the lines are given on the left hand side (in cm^{-1}). In order of increasing frequency: ^{64}Zn, ^{66}Zn, ^{68}Zn.

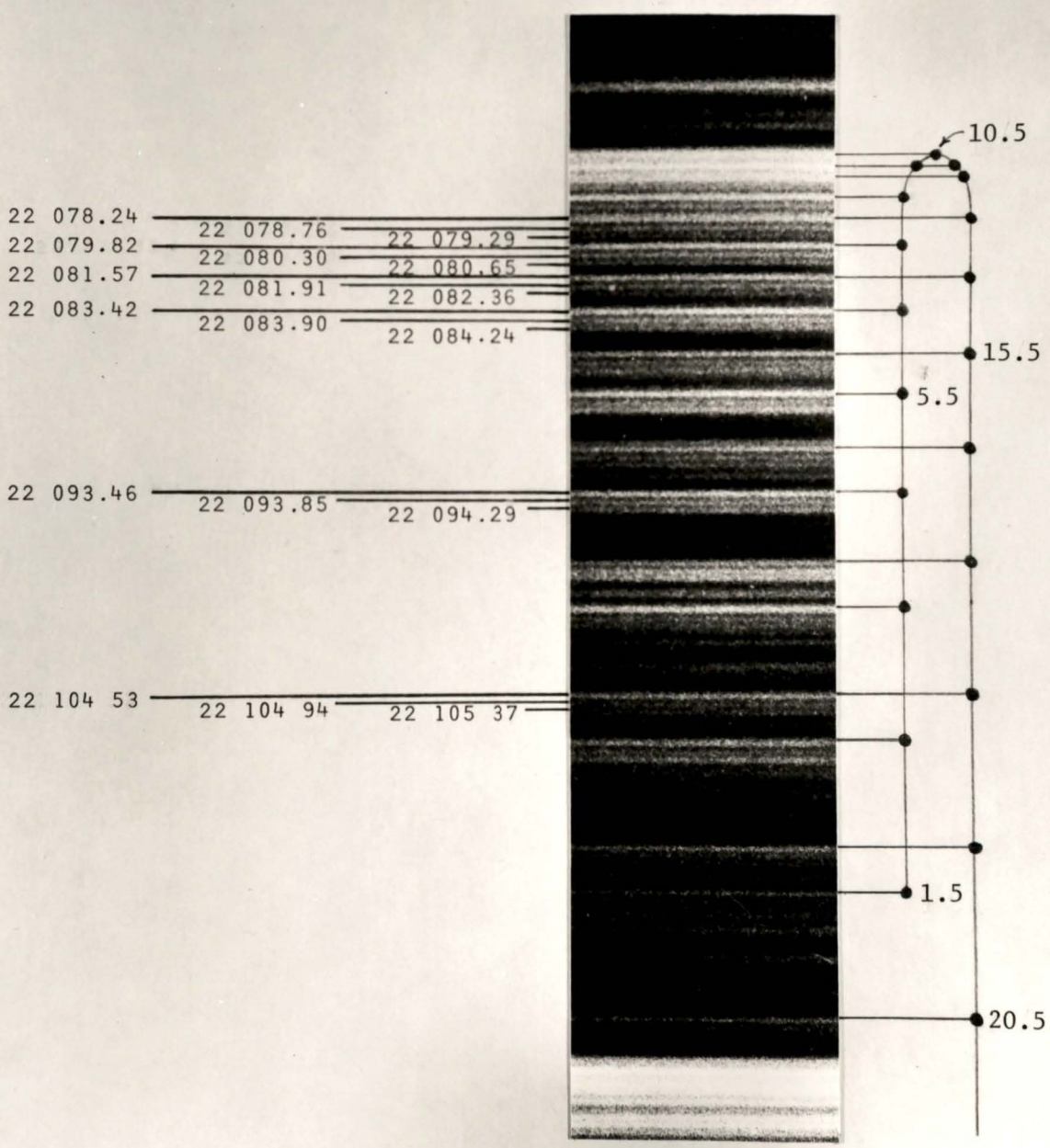

TABLE XXVI. Zinc isotopic splitting in the A $^2\Pi$ - X $^2\Sigma^+$ 0-1 band, $^OP_{12}$ branch. The observed values of $\Delta\nu$ are tabulated.

J"	^{64}ZnD - ^{66}ZnD	^{64}ZnD - ^{68}ZnD
4.5	-0.39	-0.83
6.5	-0.48	-0.82
7.5	-0.48	-0.83
13.5	-0.52	-1.05
14.5	-0.34	-0.79
18.5	-0.41	-0.84
average	-0.44	-0.86

electronic and rotational isotope effects are expected to be very small and the observed splittings are expected to be predominantly due to the vibrational isotope effect. Although there is an increase in $\Delta\nu$ as J increases for J between 4.5 and 13.5 in the tabulated values, possibly due to a rotational effect, the irregularities with J greater than 13.5 leave this interpretation in doubt. The splittings in a greater number of lines would have to be measured to obtain statistically valid evidence for or against. This was not pursued further. It was, however, observed that in some branches where the isotope splitting was too small to be resolved at low J values, it was often large enough to be resolved at high J values. Thus a rotational effect was at least qualitatively observed. Stenvinkel[16] has studied the

rotational zinc isotope effect quantitatively in ZnH.

In view of the discussion in the preceding paragraph, the splittings listed in Table XXVI were averaged. From equation (87), the vibrational isotope splittings were calculated to be -0.432 and - 0.838 cm^{-1}, respectively, for the ^{64}ZnD - ^{66}ZnD and ^{64}ZnD - ^{68}ZnD splittings. These values are very close to the observed average <u>total</u> isotopic splittings, -0.44 and -0.86 cm^{-1}, thus confirming the expectation that the vibrational isotope effect makes the largest contribution.

Mrozowski[49] has observed a very small nuclear isotope shift in ZnH. No attempt has been made to look for this in ZnD.

The magnitude of the zinc isotopic splittings varied from band to band (vibrational effect) and with J values within the bands (rotational effect). The splittings were often not large enough to be resolved. Thus, when measuring the spectrum, the accuracy was often limited by the blending of these lines.

CHAPTER IV

CONCLUSION

Although methods of analysis have been chosen so as to attempt to achieve the utmost accuracy wherever possible, this goal has had to be tempered to achieve results within reasonable time limits. Hence, certain approximations have had to be made, involving the neglect of higher order terms, as has been mentioned at the appropriate places in this thesis.

The molecular constants of ZnD have been evaluated primarily by the traditional, graphical method. The combination differences (and other differences not specifically called "combination" differences) that were used in these graphs were obtained from the term values, rather than directly from the spectral line positions. Some of the advantages and disadvantages of using a term value approach have been mentioned, and this has been further discussed by Albritton et al.[66] While the graphical method is conceptually simple and provides the spectroscopist with a good "feel" for the data, it is recognized that this approach has limitations. It is not particularly useful for determining higher order terms—at least, not without becoming complex.

Since the effects of the higher order terms (which result in non-linearities in the graphs) usually become more pronounced at high J values, the parameters have

been obtained from the data in the low and moderate J range—the particular values of J (or N) used in evaluating the parameters have been given in the appropriate tables. No attempt has been made to model the system over the entire J range. Thus, in this sense, the present work can be considered to be a preliminary analysis of the spectrum of ZnD.

Another disadvantage of the graphical method is that it is difficult to estimate the experimental uncertainties in the molecular constants obtained. Albritton et al.[66] have pointed out that the estimated experimental uncertainties are, in fact, often unduly optimistic. In view of this problem, error limits have generally not been explicitly stated in this thesis. The expected accuracy of the derived parameters is indicated by the number of significant figures—except were the method of evaluation itself is only approximate (in particular, the Birge - Sponer method for dissociation energies), in which case the number of significant figures stated for the calculated results are based on the assumption that the method is exact. Because of the difficulty in estimating the experimental uncertainties, the meaning of the last significant figure has to be interpreted more loosely than the usual definition: the error limits may in some cases be somewhat more than ±1 in the last decimal position, but should be less than ±9. Where last digits have been given as subscripts, the uncertainty

exceeds ±10 units of these digits and the above interpretation (≤ ±9) still applies to the last figure preceding the subscript.

Spectroscopists are increasingly using statistical (rather than graphical) methods to evaluate the molecular parameters, the most common method being that of least squares.† This more readily allows for the determination of higher order parameters (e.g. by the methods of Veseth[22]), and thus the data can be fitted over a wider range of J values. These methods are also better for estimating the experimental uncertainties.

One such statistical method has been devised by Aslund[68] and incorporated into a new computer program which evaluates the molecular constants and term values simultaneously. (The earlier method of evaluating the term values, then subsequently using these to obtain the molecular constants has been criticized.[66]) This program has now been obtained by this laboratory and, although not available in time for the work presented in this thesis, is intended to be used to further refine our knowledge of ZnD.

Despite the increasing use of statistical methods in spectroscopic analysis, the traditional methods are still of considerable value for the preliminary analysis of a spectrum—hence this thesis.

---

† "An introduction to the least - squares fitting of spectroscopic data" is provided in a chapter by that name in ref. (86).

REFERENCES

(1) R. S. Mulliken. *Rev. Mod. Phys.* 1930, 2, 60; 1931, 3, 89; 1932, 4, 1.

(2) R. S. Mulliken and A. Christy. *Phys. Rev.* 1931, 38, 87.

(3) G. Herzberg. *Molecular Spectra and Molecular Structure: I. Spectra of Diatomic Molecules*, 2nd ed. (Van Nostrand Reinhold: New York, N.Y.). 1950.

(4) K. P. Huber and G. Herzberg. *Molecular Spectra and Molecular Structure: IV. Constants of Diatomic Molecules.* (Van Nostrand Reinhold: New York, N.Y.). 1979.

(5) R. Colin. Private communication, 1980.

(6) W. J. Balfour and H. M. Cartwright. *Chem. Phys. Lett.* 1975, 32, 82.

(7) L. - E. Berg and L. Klynning. *Phys. Scr.* 1974, 10, 331.

(8) I. Kopp, M. Kronekvist, and A. Guntsch. *Arkiv Fysik* 1966, 32 371.

(9) L. Veseth. *Mol. Phys.* 1973, 25, 333.

(10) E. Bengtsson and E. Hulthén. *Trans. Far. Soc.* 1929, 25, 751.

(11) L. B. Knight and W. Weltner. *J. Chem. Phys.* 1971, 54, 3875.

(12) L. Klynning and H. Martin. *Phys. Scr.* 1979, 20, 594.

(13) L. B. Knight and W. Weltner. *J. Chem. Phys.* 1971, 55, 2061.

(14) J. H. Van Vleck. *Phys. Rev.* 1929, 33, 467.

(15) W. J. Balfour and B. Lindgren. *Can. J. Phys.* 1978, 56, 767.

(16) G. Stenvinkel. *Diss.* (Stockholm). 1936.

(17) J. M. Brown, et al. *J. Mol. Spectrosc.* 1975, 55, 500.

(18) G. W. King. *Spectroscopy and Molecular Structure*, pp. 201 - 211. (Holt, Rinehart and Winston: New York, N.Y.). 1964.

(19) C. H. Townes and A. L. Schawlow. *Microwave Spectroscopy*, pp. 174 - 185. (Dover: New York, N.Y.). 1975. [(McGraw - Hill). 1955].

(20) E. Hill and J. Van Vleck. *Phys. Rev.* 1928, 32, 250.

(21) G. M. Almy and R. B. Horsfall. *Phys. Rev.* 1937, 51, 491.

(22) L. Veseth. *J. Mol. Spectrosc.* 1971, 38, 228.

(23) I. Kovács. *Opt. Spectrosc.* 1962, 12, 8. Cited by Veseth (ref. (22)).

(24) M. Mizushima. *The Theory of Rotating Diatomic Molecules*, p. 280. (John Wiley & Sons (Wiley - Interscience): New York. N.Y.). 1975.

(25) G. C. Dousmanis, T. M. Sanders, and C. H. Townes. *Phys. Rev.* 1955, 100, 1735.

(26) J. Dufayard and O. Nedelec. *J. Physique* 1977, 38, 449.

(27) J. L. Dunham. *Phys. Rev.* 1932, 41, 721.

(28) R. S. Mulliken. *Phys. Rev.* 1927, 30, 138; 1927, 30, 785. Cited by Jevons (ref. (30)).

(29) L. T. Earls. *Phys. Rev.* 1935, 48, 423.

(30) W. Jevons. *Report on Band - Spectra of Diatomic Molecules.* (The Physical Society: London). 1932.

(31) E. Howson. *Astrophys. J.* 1912, 36, 292. Cited by Stenvinkel (ref. 16).

(32) H. Hagenbach and H. Schumacher. *ZS. f. Wiss. Phot.* 1919, 19, 142. Cited by Stenvinkel (ref. 16).

(33) E. Hulthén. *Compt. Rend.* 1921, 173, 524; *Z. Physik* 1922, 11, 284; *Nature* 1925, 116, 642.

(34) E. Hulthén. *Diss.* (University of Lund). 1923.

(35) A. Kratzer. *Ann. Physik* 1923, 71, 72. (*C.A.* 1923, 17, 3135.)

(36) R. S. Mulliken. *Proc. Nat. Acad. Sci.* 1926, 12, 144.

(37) H. Volkringer. *Compt. Rend.* 1929, 189, 1264.

(38) E Hulthén. *Arkiv Mat. Astron. Fysik* 1929, 21B, 1.

(39) M. Fukuda. *Sci. Papers Inst. Phys. Chem. Res.* 1931, 15, 227.

(40) R. S. Mulliken. *Phys. Rev.* 1928, 32, 388.

(41) G. Stenvinkel and E. Svensson. *Nature* 1935, 135, 955.

(42) G. Stenvinkel, E. Svensson, and E. Olsson. *Arkiv Mat. Astron. Fysik* 1938, 26A, 1.

(43) Y. Fujioka and Y. Tanaka. *Sci. Papers Inst. Phys. Chem. Res.* 1937, 32, 143.

(44) M. A. Khan. *Proc. Phys. Soc.* 1962, 80, 599.

(45) M. Rafi et al. *J. Sci. (Karachi)* 1976, 4, 85.

(46) W. W. Watson and B. Perkins. *Phys. Rev.* 1927, 30, 592.

(47) W. W. Watson. *Phys. Rev.* 1930, 36, 1134.

(48) P. Bender. *Phys. Rev.* 1930, 36, 1543.

(49) S. Mrozowski. *Phys. Rev.* 1940, 58, 597.

(50) A. Egerton and S. Rudrakanchana. *Proc. Roy. Soc., A* 1954, 225, 427.

(51) H. U. Lee and R. N. Zare. *Combust. Flame* 1975, 24, 27.

(52) H. M. Hulbert and J. O. Hirschfelder. *J. Chem. Phys.* 1941, 9, 61.

(53) E. R. Lippincott, D. Steele, and P. Caldwell. *J. Chem. Phys.* 1961, 35, 123.

(54) L. Wojtczak. *Acta Phys. Polon.* 1965, 2, 233.

(55) S. M. Mirajkar. *Indian J. Phys.* 1970, 44, 521.

(56) P. Politzer. *J. Phys. Chem.* 1966, 70, 4041.

(57) E. Ishiguro and M. Kobori. *J. Phys. Soc. Japan* 1967, 22, 263.

(58) G. Simons and R. G. Parr. *J. Chem. Phys.* 1971, 55, 4197.

(59) L. Veseth. *J. Phys. B: Atom. Molec. Phys.* 1970, 3, 1677.

(60) A. N. Pandey et al. *Indian J. Pure Appl. Phys.* 1973, 11, 69.

(61) *Revision of Rowland's preliminary table of solar spectrum wave-lengths.* (Washington, D.C.). 1928. Cited by Stenvinkel, Svensson, and Olsson (ref. (42)).

(62) R. S. Wojslaw and B. F. Peery. *Astrophys. J. Suppl. Ser.* 1976, 31, 75.

(63) H. M. Cartwright. *J. Phys. E* 1976, 9, 92.

(64) H. M. Crosswhite. *J. Res. Natl. Bur. Stand., Sect. A* 1975, 79, 17.

(65) N. Aslund. *Arkiv Fysik* 1965, 30, 377.

(66) D. L. Albritton et al. *J. Mol Spectrosc.* 1973, 46, 67.

(67) G. Edvinsson, L. - E. Selin, and N. Aslund, *Arkiv Fysik* 1965, 30, 283; N. Aslund. *Arkiv Fysik* 1965, 30, 377. Cited by Albritton et al. (ref. (66)).

(68) N. Aslund. *J. Mol. Spectrosc.* 1974, 50, 424.

(69) W. J. Balfour. Private communication, 1980.

(70) R. D. Verma and R. S. Mulliken. *J. Mol. Spectrosc.* 1961, 6, 419.

(71) T. C. James. *J. Chem. Phys.* 1964, 41, 631.

(72) W. W. Watson and A. E. Parker. *Phys. Rev.* 1931, 37, 167.

(73) R. C. Johnson. *An Introduction to Molecular Spectra.* (Methuen & Co.: London). 1949.

(74) M. D. Olman, M. D. McNelis, and C. D. Hause. *J. Mol. Spectrosc.* 1964, 14, 62.

(75) J. L. Griggs and K. N. Rao. *J. Mol. Spectrosc.* 1967, 22, 383.

(76) J. T. Hougen. *The Calculation of Rotational Energy Levels and Rotational Line Intensities in Diatomic Molecules*, p. 11. (U.S. National Bureau of Standards Monograph 115: Washington, D.C.). 1970.

(77) I. N. Levine. *Molecular Spectroscopy*, pp. 155 - 158. (John Wiley & Sons: New York, N.Y.). 1975.

(78) P. R. Bunker. *J. Mol. Spectrosc.* 1968, 28, 422.

(79) R. C. Weast, ed. *CRC Handbook of Chemistry and Physics*, 59th ed., p. F-250. (CRC Press: West Palm Beach, Florida). 1978.

(80) C. E. Moore. *Atomic Energy Levels*, vol. II, p. 125. (U.S. National Bureau of Standards, NSRDS-NBS 35: Washington, D.C.). 1952 (reissued 1971).

(81) R. N. Zare. *Programs for Calculating Relative Intensities in the Vibrational Structure of Electronic Band Systems.* (University of California Radiation Laboratory Report UCRL-10925: Berkeley, Calif.). 1963; *J. Chem. Phys.* 1969, 51, 1667.

(82) J. A. Dean, ed. *Lange's Handbook of Chemistry*, 11th ed., pp. 3-13 and 3-23. (McGraw - Hill: New York, N.Y.). 1973.

(83) E. C. Kemble and J. H. Van Vleck. *Phys. Rev.* 1923, 21, 653. Cited by T. H. Crawford and T. Jorgensen, *Phys. Rev.* 1935, 47, 932.

(84) T. H. Crawford and T. Jorgensen. *Phys. Rev.* 1935, 47, 932; 1936, 49, 745.

(85) I.U.P.A.C. Commission on Atomic Weights. *Pure & Appl. Chem.* 1979, 51, 405.

(86) D. L. Albritton, A. L. Schmeltekopf, and R. N. Zare. "An Introduction to the Least - Squares Fitting of Spectroscopic Data." In K. N. Rao, ed. *Molecular Spectroscopy Modern Research*, vol. II, pp. 1 - 67. (Academic Press: New York, N.Y.). 1976.

(87) R. S. Mulliken. *J. Phys. Chem.* 1937, 41, 5.

(88) A. G. Gaydon. *Dissociation Energies and Spectra of Diatomic Molecules*, 3rd ed., p. 62. (Chapman and Hall: London). 1968.

(89) A. Schadee. *Astron. and Astrophys.* 1975, 41, 203.

VITA

Surname: TAYLOR Given Names: ALAN WILLIAM

Place of Birth: VICTORIA, B.C. Date of Birth: JUNE 21, 1956

Educational Institutions Attended, with Dates of Entering and Leaving:

UNIVERSITY OF VICTORIA, B.C. 1974 to 1978

UNIVERSITY OF VICTORIA, B.C. 1978 to 1980

Degrees, Diplomas, Etc., Awarded, with Dates and Names of Institutions:

B.Sc. (Honors) 1978 UNIVERSITY OF VICTORIA, B.C.

Honors and Awards:

UNIVERSITY OF VICTORIA PRESIDENT'S ENTRANCE SCHOLARSHIP, 1974/75

UNIVERSITY OF VICTORIA PRESIDENT'S SCHOLARSHIPS, 1975/76 and 1976/77

LEONARD FOUNDATION SCHOLARSHIPS, 1975/76, 1976/77, and 1977/78

CHEMICAL RUBBER COMPANY FRESHMAN CHEMISTRY ACHIEVEMENT AWARD, 1975/76

OCEAN CONSTRUCTION SUPPLIES LIMITED SCHOLARSHIP, 1975/76

INCO PARTICIPATING SCHOLARSHIPS, 1976/77 and 1977/78

BAPCO PAINT LIMITED SCHOLARSHIP, 1976/77

THE WOODS TRUST SCHOLARSHIP, 1976/77

NRC/NSERC POSTGRADUATE SCHOLARSHIPS, 1978/79 and 1979/80

PARTIAL COPYRIGHT LICENSE

I hereby grant the right to lend my thesis or dissertation (the title of which is shown below) to users of the University of Victoria Library, and to make *single copies only* for such users or in response to a request from the library of any other university, or similar institution, on its behalf or for one of its users. I further agree that permission for extensive copying of this thesis for scholarly purposes may be granted by me or a member of the University designated by me. It is understood that copying or publication of this thesis for financial gain shall not be allowed without my written permission.

Title of Thesis/Dissertation

THE A $^2\Pi$ - X $^2\Sigma^+$ ELECTRONIC SPECTRUM OF ZnD

Author [redacted]
Signature

ALAN W. TAYLOR
Name

NOVEMBER 21, 1980
Date